PONTIFICIA UNIVERSIDAD CATÓLICA DE CHILE

Facultad de Ciencias Biológicas

Programa de Doctorado en Ciecias Biológicas

Mención Biología Celular y Molecular

ROLE OF WDR44 IN VESICULAR PROTEIN TRANSPORT

Tesis entregada a la Pontificia Universidad Católica de Chile en cumplimiento parcial de los requisitos para optar al grado de Doctor en Ciencias con mención en Biología Molecular y Celular.

Por: BEATRIZ GENOVEVA VÁSQUEZ SOTO

Director de Tesis: Dr. Alfonso González de la Rosa

Octubre 2021

Dedicated to my parents for supporting all my decisions throughout life, to my granny María for being an example of working woman, to Silvia Sanhueza for her unconditional love and to Gabriela Gutiérrez and José Pincu for being the most loving adoptive parents. To Juan, the love of my life, and my daughter Julieta, the best result of this thesis.

Dedicado a mis padres por apoyar cada una de mis deciciones a lo largo de la vida, a mi abuelita María por ser un ejemplo de mujer trabajadora, a Silvia Sanhueza por su amor incondicional y a Gabriela Gutiérrez y José Pincu por ser los más amorosos padres adoptivos.

A Juan, el amor de mi vida, y a mi hija Julieta, el mejor resultado de esta tesis.

ACKNOWLEDGMENTS

I would like to thank Dr. Alfonso Gonzalez for giving me the opportunity to work with him despite I came from a plant biology laboratory, and for being an intellectual and emotional support throughout these years. I would also thank to all the members from his laboratory for being a kindly group of people keeping a friendly and trusting work environment, always available for talking about scientific issues and also about the daily and personal life. Specially to Claudia Metz for teaching me to handle cell culture and most of the cellular biology techniques, to Claudio Retamal for teaching me microscopy image acquisition and analysis, to Claudia Oyanedel and Carmen Espinoza, for their advice in biotinylating and co-immunoprecipitation assays and their sincerely friendship and strong support specially the first months of my pregnancy, to Jaime Venegas for doing analysis of WDR44 and EGFR localization and inverted invasion assay, to Mariana Labarca for working in produce recombinant WDR44 fragments and for being the best Lab partner of weekends, to Francisca Barake for patiently reading and correcting much of this Thesis and her tremendous friendship, to Andrea Soza for her constant intellectual support and friendship, to Patricia Gajardo for continuing testing of mycoplasma, to Javier Venegas for his invaluable technical help and the most enthusiastic conversations starting the workday and to Irma Castillo for her great managing and personal help. I am also thankful to Evelyn Pardo, Fabián Segovia, Fabián Montecinos, Lisette Sandoval, Marcela Bravo, Jonathan Barra, Milena Mimica, Dr. Loreto Masardo, Tomás Jimenez and Cristian Herrera for their friendship and support throughout these years.

I would also greatly thank to Dr. David Sabatini, who discovered the WDR44 and facilitated several tools and unpublished information for studying the function of WDR44. I am also thankful to Dr. Mindong Ren and Dr. Milton Adesnik for kindly meeting me at New York University (NYU) and discussing the results of my thesis.

I would also thank to Stephanie Miserey-Lenkei from Institut Curie by performing the WDR44-EGFP and Rab11a-EGFP GFP-trap and for managing the mass spectrometry sequencing, at the Université Paris Diderot, Sorbonne Paris Cité, Proteomics/Mass spectrometry core facility, Institut Jacques Monod, Paris, French. I am also thankful to Dr. José Ignacio Valenzuela for facilitating cDNA encoding to EGFP-tagged Rabs.

I also greatly thank to Jorge Cancino for facilitating HeLa cells stably expressing the KDELR-EGFP and KDELR(D193N)-EGFP and for his tremendous support in FLIP assays.

I am thankful to Bernardita Medel for the qRT-PCR experiments and her friendship, to Dr. Patricia Burgos and Omar Cortés for kindly facilitating ATG9KO HeLa cells, to Cristóbal Cerda from Patricia Burgos laboratory, for agreeing to silence Rab1a and Rab1b in HeLa for exploratory experiments and to Juan Burgueño for plotting gene ontology enrichment analysis.

This thesis was financed by CONICYT National Doctoral studies fellowship Chile (21120650), VRI International Fellowship (PUC) Chile, Chilean Society of Cell Biology, Programa de Apoyo a Centros con Financiamiento Basal AFB170005 to the Center for Aging and Regeneration (CARE), AFB170004 to Fundación Ciencia & Vida, FONDECYT 1181907.

INDEX

FIGURE INDEX

TABLE INDEX

ABBREVIATIONS

AP-1	Adaptor protein complex 1
AP-2	Adaptor protein complex 2
AP-3	Adaptor protein complex 3
B2AR	Beta-2 adrenergic receptor
BFA	Brefeldin A
CI-M6PR	Cation-independent mannose 6-phosphate receptor
CtBP/BARS	C-terminal-binding protein/brefeldin A ADP-ribosylated substrate
DLIC-2	Dynein light intermediate chain 2 subunit
DMEM	Dulbecco's Modified Eagle Medium
DMSO	Dimethyl sulfoxide
EEA1	Early endosome antigen 1
EGFR	Epidermal growth factor receptor
eIF2a	Eukaryotic translation initiation factor 2A
ER	Endoplasmic reticulum
ERGIC	Endoplasmic reticulum-Golgi intermediate compartment
FACS	Fluorescence-activated cell sorting
FBS	Fetal bovine serum
GAP	GTPase activating protein
GDI	Guanine nucleotide dissociation inhibitor
GDP	Guanosine diphosphate
GEF	Guanine nucleotide exchange factor
GFP	Green fluorescent protein
GLUT4	Glucose transporter type 4
GTP	Guanosine-5'-triphosphate
KD	Knock-down
KDELR	KDEL receptor
Ns	Non-significant
ON	Over night
P/S	Penicilin/Streptamicin
PA	Phosphatidic acid
PBS	Phosphate buffered saline
PCR	Polimerase chain reaction
PDI	Protein disulfide isomerase
PERK	PKR-like endoplasmic reticulum kinase
PFA	Paraformaldehyde
PKA	Protein kinase A
PRD	Proline rich domain
qRT-PCR	Quantitative Reverse transcriptase PCR

Rab11-FIP	Rab11-Family interacting proteins
RBD	Rab binding domain
RT	Room temperature
RT-PCR	Reverse transcriptase PCR
SEM	Standard error of the mean
SNARE	SNAP (Soluble NSF Attachment Protein) Receptor
TfR	Transferrin receptor
TGN	Trans-Golgi network
TN	Tunicamycin
UPR	Unfolded protein response
VAPA	VAMP-Associated Protein A
VAPB	VAMP-Associated Protein B
WIPI2	WD repeat domain phosphoinositide-interacting protein 2
WT	Wild type

RESUMEN

El tráfico vesicular de proteínas incluye las rutas secretora y endocítica, las cuales regulan la composición de la membrana plasmática y de los organelos intracelulares. La ruta biosintética (secreción) transporta proteínas neosintetizadas desde el retículo endoplásmico (RE) al complejo de Golgi con dirección a la membrana plasmática, mientras que la ruta endocítica internaliza proteínas de la superficie celular y las distribuye ya sea hacia el reciclaje o a degradación. Los pasos fundamentales en el proceso de tráfico vesicular incluye la selección de la carga durante la formación de la vesícula, seguido por el movimiento y fusión del vehículo vesicular con un compartimento blanco específico.

RabGTPasas (Rabs) son los principales reguladores del tráfico de proteínas. Estas proteínas ciclan entre un estado inactivo y citosólico asociado a GDP y un estado activo unido a membrana asociado a GTP, en el cual interactúa con variadas proteínas efectoras. Los efectores de las Rabs incluyen proteínas adaptadoras, complejos de envoltura, motores moleculares, factores de acoplamiento y proteínas de fusión. Rab11 es una RabGTPasa que principalmente se localiza en los endosomas de reciclaje perinuclear y regula la ruta lenta de reciclaje endocítico. La función de Rab11 se ha involucrado con la composición de la membrana plasmática y el establecimiento de polaridad celular, incluyendo ciliogénesis y migración celular.

Los efectores de Rab11 son funcionalmente diversos e incluyen motores moleculares, factores intercambiadores de nucleótido de guanina (GEFs) de Rabs, reguladores del citoesqueleto de actina, la familia de proteínas de interacción con Rab11 (Rab11-FIPs) y WDR44. Rab11FIPs comprende 5 proteínas de andamio (FIP1-FIP5) que han sido

ampliamente caracterizadas. En contraste, WDR44 ha sido pobremente estudiada, aun cuando fue el primer efector identificado de Rab11.

WDR44 se une a la Rab11 asociada a GTP por medio de su dominio de unión a Rab (RBD) y además tiene un dominio similar a FFAT, un dominio rico en prolina y siete repetidos WD40. La versión truncada de WDR44 que incluye el RBD, inhibe el reciclaje del receptor de transferrina (TfR), lo cual involucra a la Rab11 en la ruta de reciclaje. Sin embargo, la función de WDR44 en el reciclaje endocítico permanece desconocida. WDR44 también interactúa, por medio de su dominio similar a FFAT, con las proteínas de transmembrana del RE asociadas a VAMP A y B (VAPA y VAPB), las que reclutan a la WDR44 al RE. VAPA/B son proteínas de acoplamiento que median el contacto del RE con varios organelos y han sido involucradas en el transporte de proteínas entre el RE y el complejo de Golgi. Todavía no ha sido explorado si WDR44 está involucrada en el transporte de proteínas en la interfaz RE-Golgi.

Nosotros proponemos **la hipótesis** que *"WDR44 funciona en reciclaje endocítico y en el tráfico de proteínas entre retículo endoplásmico y el complejo de Golgi".*

Nosotros caracterizamos el interactoma de WDR44 unido a EGFP por medio de un GFP-trap y análisis de espectrometría de masas y lo comparamos con el interactoma de Rab11a-EGFP. Nuestro interactoma de WDR44 muestra un enriquecimiento de proteínas involucradas en el transporte de proteínas desde los endosomas tempranos hacia los endosomas tardíos y en el tráfico desde el RE al Golgi, así como desde el Golgi al RE. En cambio, el interactoma de Rab11a está enriquecido en proteínas de la maquinaria de endocitosis y exocitosis. Potenciales proteínas que interactúan con WDR44 incluye las subunidades del complejo de envoltura COPI, Rab1 y Rab6, involucradas en el transporte desde Golgi al RE, así como también Rab4 de la ruta endocítica. Nuestros experimentos de co-immunoprecipitación validaron las interacciones con Rab1a, Rab1b, Rab6A, Rab4a y Rab4b. Análisis de inmunofluorescencia reveló colocalización de WDR44 con Rab11a, Rab4a

y Rab4b en endosomas de reciclaje perinuclear, parcialmente en endosomas tempranos y no en el complejo de Golgi. Nosotros no encontramos colocalización con Rab1a, Rab1b or RAB6A. Consistentemente, GTPγS disminuye la interacción de WDR44 con Rab1b, suggiriendo que WDR44 preferentemente une a la Rab1 unida a GDP en el citoplasma.

Para estudiar el rol de WDR44 nosotros realizamos experimentos de silenciamiento de WDR44 con shRNA así como de Rab11a. Nosotros no detectamos efectos del silenciamiento de WDR44 ni de Rab11a en el reciclaje endocítico del TfR. Sin embargo, observamos una disminución del reciclaje a la superficie celular del receptor del factor de crecimiento epidermal (EGFR), previamente acumulado en los endosomas de reciclaje perinucleares donde Rab11 está unido a GTP. Así, WDR44 pareciera ser funcional en el reciclaje endocítico desde el endosoma de reciclaje perinuclear y muy probablemente, no afecta el reciclaje del TfR desde los endosomas tempranos. Las células con niveles disminuidos de WDR44 también mostraron menores niveles de migración e invasión, similar a las células silenciadas de Rab11, lo que podría reflejar un proceso regulado en común.

Nosotros también observamos que el silenciamiento de WDR44 induce la fragmentación del complejo de Golgi, el cual es un fenotipo asociado a problemas en el transporte entre RE y Golgi. WDR44 se localiza en RE y su silenciamiento disminuyó el transporte retrógrado desde Golgi al RE del receptor de KDEL (KDELR). El KDELR cicla entre el RE y el complejo de Golgi, devolviendo al RE las chaperonas con motivo KDEL. Consistentemente, las células silenciadas de WDR44 muestran un aumento en la membrana plasmática de la chaperona con motivo KDEL, PDI, lo que sugiere una saturación del KDELR con chaperonas-KDEL en el Golgi, debido a su deficiente transporte hacia el RE.

El silenciamiento de WDR44 indujo la respuesta a proteínas mal plegadas (UPR), aumentando los niveles de PERK, revelando un sostenido estrés de retículo. Si bien el silenciamiento de WDR44 induce la expresión de mRNA de genes asociados al UPR, éste

disminuyó los niveles chaperonas de retículo. Particularmente intrigante es la notable disminución de los niveles de calnexina, una chaperona de transmembrana de RE normalmente abundante, lo cual también se observó al silenciar Rab1a y Rab1b, sugiriendo un tipo de deterioro de la homeostasis de RE no descrito previamente.

Durante el desarrollo de esta tesis, se publicó evidencia de que WDR44 está involucrada en el transporte vesicular con dirección al endosoma de reciclaje y en la regulación de ciliogenénesis. Nuestros descubrimientos suman un rol de WDR44 en el reciclaje desde el compartimento de reciclaje perinuclear y en el transporte retrógrado desde el complejo de Golgi hacia el RE.

ABSTRACT

The vesicular protein trafficking includes secretion and endocytic pathways that regulate the composition of the plasma membrane and intracellular organelles. The biosynthetic (secretion) route transports newly synthesized proteins from the endoplasmic reticulum (ER) to Golgi complex en route to the plasma membrane, while the endocytic route internalize cell surface proteins and sort them to either recycling or degradation pathways. Fundamental steps in the vesicular trafficking process include cargo selection during vesicle formation followed by movement and fusion of the vesicular vehicles with a specific target compartment.

RabGTPases are the main regulators of protein trafficking. These proteins cycle between an inactive cytosolic GDP-bound state and an activated GTP-bound state that associates with membranes and interact with a variety of effector proteins. Rabs effectors include cargo adaptors, vesicular coat complex, molecular motors, tethering factors and fusion proteins. Rab11 is a RabGTPase that mostly localizes to the perinuclear recycling endosomes and regulates a slow endocytic recycling route. The function of Rab11 has been involved in the composition of the plasma membrane and the establishment of cell polarity, including ciliogenesis and cell migration.

Rab11 effectors are functionally diverse including molecular motors, guanine nucleotide exchange factors (GEFs) of Rabs, actin cytoskeleton regulators and the Rab11-family interacting proteins (Rab11-FIPs) and WDR44. Rab11-FIPs include five scaffold proteins (FIP1-FIP5) that have been highly characterized. In contrast, WDR44 has been poorly studied, even though it was the first Rab11 effector identified.

WDR44 binds to the GTP-bound Rab11 through its Rab-binding domain (RBD) and contains a FFAT-like domain, a proline rich domain and seven WD40 repeats. A truncated

version of WDR44 including the RBD inhibited the transferrin receptor recycling (TfR), thus involving Rab11 in the recycling pathway. However, the function of WDR44 in endocytic recycling remains unknown. WDR44 also interacts through its FFAT-like domain with the ER transmembrane proteins VAMP-Associated Protein A and B (VAPA and VAPB), recruiting WDR44 to the ER. VAPA/B are tether proteins that mediate the ER contacts with several organelles and have been involved in protein trafficking between the ER and the Golgi complex. Whether WDR44 is involved in protein transport at the ER-Golgi interface has not been explored.

We propose **the hypothesis** that "*WDR44 functions in endocytic recycling and protein trafficking between the endoplasmic reticulum and the Golgi complex".*

We characterized WDR44 tagged to EGFP interactome by GFP-trap and mass spectrometry analysis in comparison with the Rab11a-EGFP interactome. Our WDR44 interactome displays an enrichment of proteins involved in protein transport from early to late endosomes and from the ER-to-Golgi and Golgi-to-ER protein trafficking. Instead, Rab11a interactome is enriched in proteins of the endocytosis and exocytosis machinery. Potential interactors of WDR44 include subunits of the COPI coat complex, Rab1 and Rab6, involved in Golgi-to-ER transport, as well as Rab4 of the endocytic pathway. Our co-immunoprecipitation experiments validated the interactions with Rab1a, Rab1b, Rab6A, Rab4a and Rab4b. Immunofluorescence analysis revealed colocalizations of WDR44 with Rab11a, Rab4a and Rab4b in perinuclear recycling endosomes, partially in early endosomes and not in the Golgi complex. We did not find colocalization with Rab1a, Rab1b or Rab6. Consistently, GTPγS decreases the interaction of WDR44 with Rab1b, suggesting that WDR44 preferentially binds to the GDP-bound Rab1b in the cytoplasm.

To study the role of WDR44 we performed silencing experiments with shRNA and the effect of Rab11 silencing. We did not detect an effect of WDR44 nor Rab11 depletion in TfR

endocytic recycling. However, we observed a decreased recycling to the cell surface of the epidermal growth factor receptor (EGFR) previously accumulated at perinuclear recycling endosomes, where the GTP-bound Rab11 is associated. Therefore, WDR44 seems to be functional in endocytic recycling from the perinuclear recycling endosome and very likely does not affect the recycling of TfR from early sorting endosomes. WDR44 depleted cells also displayed decreased levels of migration and invasion, similar to Rab11 silenced cells, that might reflect a common regulated process.

We also observed that WDR44 silencing induces Golgi fragmentation, which is a phenotype associated to defects in ER-Golgi interface trafficking. WDR44 localizes to the ER and its depletion decreased the Golgi-to-ER retrograde transport of the KDEL receptor (KDELR). The KDELR cycles between the ER and the Golgi returning back to the ER the KDEL-containing chaperones. Consistently, WDR44 depleted cells missorted the KDEL-protein disulfide isomerase (PDI) to the plasma membrane, suggesting a saturation of the KDELR with KDEL-chaperones in the Golgi due to its deficient transport to the ER.

WDR44 depletion induced the unfolded protein response (UPR), increasing the levels of PERK and revealing a sustained ER stress condition. Although WDR44 depletion induces the mRNA expression of UPR associated genes, it decreased the protein levels of ER chaperones. Particularly intriguing is the remarkable decrease in the levels of the transmembrane and normally abundant ER chaperone calnexin, also observed in Rab1a/b silenced cells, suggesting a kind of impairment of the ER homeostasis previously undescribed.

During the course of this thesis, WDR44 was described to be involved in the vesicular transport towards the recycling endosome and in the regulation of ciliogenesis. Our findings add a role of WDR44 in the recycling from the endosomal perinuclear recycling compartment and the Golgi-to-ER transport.

1. INTRODUCTION

1.1. Problem Statement

The composition of the plasma membrane and organelles is mainly regulated by the vesicular protein transport that includes the exocytic and the endocytic routes. The exocytic, or biosynthetic, route transports neosynthesized proteins from the Endoplasmic Reticulum (ER) to the plasma membrane passing through the Golgi apparatus and the recycling endosomes, where they are sorted to specific cell surface domains (Mellman and Nelson 2008, Mani and Thattai 2016, Viotti 2016). The endocytic pathway internalizes plasma membrane and extracellular proteins into early endosomes, where they are delivered for degradation to lysosomes or sorted for recycling to the cell surface (Elkin, Lakoduk et al. 2016). Endocytic recycling involves a fast recycling route directly from the early endosomes and a slow recycling through perinuclear recycling endosomes, before arrival to the plasma membrane (Sheff, Pelletier et al. 2002). Thus, the perinuclear recycling endosome functions as a sorting regulation station where the secretory and the endocytic pathways converge. Additionally, organelles homeostasis require a retrograde pathway that retrieve escaped proteins to their original compartment, which includes the protein trafficking from the plasma membrane and endosomes to the TGN and from the Golgi to the ER (Johannes and Popoff 2008, Spang 2013).

Vesicular protein trafficking involves several steps including selection of the cargo, vesicle formation, transport, tethering and fusion with the target membrane. Each of these processes require a regulated and specific machinery with diverse molecular functions that ensures the proper protein delivery (Bonifacino and Glick 2004).

Protein transport is mainly regulated by Rab GTPases. Rabs cycle between a cytosolic inactive GDP-bound and a membrane-associated active GTP-bound state. GTP-bound Rabs interact with effector proteins with different molecular functions, allowing Rabs to regulate several steps of the transport process (Pfeffer 2017).

Rab11 is one of the main regulators of endocytic recycling and localizes to the *trans*-Golgi Network (TGN), Golgi-derived vesicles and perinuclear recycling endosomes (Urbe, Huber et al. 1993, Ullrich, Reinsch et al. 1996, Chen, Feng et al. 1998). Rab11 regulates the slow endocytic recycling from the perinuclear recycling endosomes towards to the plasma membrane of several cargoes including nutritional receptors, signaling receptors and adhesion proteins (Kelly, Horgan et al. 2012). Rab11 regulates several cellular processes that require cell surface polarization including ciliogenesis, cytokinesis, cell migration and invasion (Welz, Wellbourne-Wood et al. 2014) and it has been related to many diseases including ciliopathies, Alzheimer's disease, epithelial polarization disorders and cancer (Greenfield, Leung et al. 2002, Kampf, Schneider et al. 2019, Chen, Kelley et al. 2021, Ferro, Bosia et al. 2021).

The functions of Rab11 rely in the interaction with effector proteins. The first known Rab11 effector was WDR44, described in 1999, but its function has been poorly studied (Zeng, Ren et al. 1999). Other Rab11 effectors include several motor proteins; Sec15, an exocyst subunit; Rabin 8, the GEF of Rab8; and the Rab11 Family interacting proteins (Rab11-FIPs) that include five members (FIP1-FIP5), that work as scaffold proteins (Wallace, Lindsay et al. 2002, Knodler, Feng et al. 2010, Lindsay, Jollivet et al. 2013, Ji, Yao et al. 2019, Escrevente, Bento-Lopes et al. 2021). FIPs bind to other small GTPases like Rac1 and to motor proteins as MyoVb, kinesin II and dynein (Schonteich, Wilson et al. 2008, Horgan, Hanscom et al. 2010, Gidon, Bardin et al. 2012, Bouchet, Del Rio-Iniguez et al. 2016). Thus, Rab11 recruits effectors with several molecular functions regulating different steps in protein trafficking.

WDR44 localizes to recycling endosomes where it binds to GTP-bound Rab11 through a Rab11-binding domain (RBD) (Zeng, Ren et al. 1999). WDR44 has other protein-protein binding domains, including a FFAT-like domain, a proline rich domain (PRD) and seven WD40 repeats. The overexpression of WDR44 without the WD40 repeats, decreased the Transferrin receptor (TfR) recycling, revealing that it works as a dominant negative of Rab11 (Zeng, Ren et al. 1999). However, the particular role of WDR44 in endocytic recycling remains unknown. WDR44 also localizes to the ER (Lucken-Ardjomande Hasler, Vallis et al. 2020) where it binds to VAPA and VAPB through the FFAT-like domain (Baron, Pedrioli et al. 2014). VAPA/B are ER-associated tethering proteins that mediate ER membrane contacts with the plasma membrane and several organelles and they also regulate protein trafficking at the ER-Golgi interface (Soussan, Burakov et al. 1999, Rocha, Kuijl et al. 2009, Kuijpers, Yu et al. 2013, Baron, Pedrioli et al. 2014). Additionally, WDR44 interacts with the COPII complex subunit Sec13, that mediates the ER-to-Golgi protein transport (Mammoto, Sasaki et al. 2000). Whether WDR44 functions in protein transport between the ER and the Golgi complex has not been addressed.

In this thesis we looked for new WDR44 interacting proteins related with vesicular protein trafficking and we studied the role of WDR44 in endocytic recycling and protein transport at the ER-Golgi interface.

1.2. Literature review

1.2.1. Vesicular protein trafficking routes

The vesicular protein transport mediates protein sorting to the plasma membrane and organelles, regulating the interaction of the cell with the environment and the function of cellular compartments. The protein trafficking comprises the secretory and the endocytic pathways. The secretory route, also known as the biosynthetic route, begins in the ER, where newly synthesized proteins are glycosylated and properly folded (Barlowe and Miller 2013). Following the canonical secretory route, the proteins leave the ER and are transported to the ER-Golgi intermediate compartment (ERGIC) (Viotti 2016). From the ERGIC, proteins are delivered to the cis-Golgi where they continue their maturation process until they arrive to the trans-Golgi network (TGN) (Mironov, Beznoussenko et al. 2005, Mani and Thattai 2016, Zhang and Wang 2016). From the TGN, proteins are directly transported to the plasma membrane or they transit through the recycling endosome before they arrive to the cell surface, following a *trans*-endosomal route (Guo, Sirkis et al. 2014).

The endocytic pathway comprises the internalization of cell surface proteins and extracellular components. Internalized vesicles converge into highly dynamic tubulo-vesicular compartments, called early endosomes. The proteins destined for degradation are transported to late endosomes and subsequently to lysosomes (Elkin, Lakoduk et al. 2016). On the other hand, proteins that are destined to return to the cell surface might follow a fast recycling route directly from the early endosomes, or a slow recycling pathway through the perinuclear recycling endosome (Sheff, Pelletier et al. 2002).

The retrograde route returns proteins back to their original compartment. There are retrograde pathways towards the TGN from the early, recycling and late endosomes, and also there is a retrograde route from the Golgi/ERGIC to the ER (Pavelka, Neumuller et al. 2008, Klinger, Siupka et al. 2015, Ma and Burd 2020).

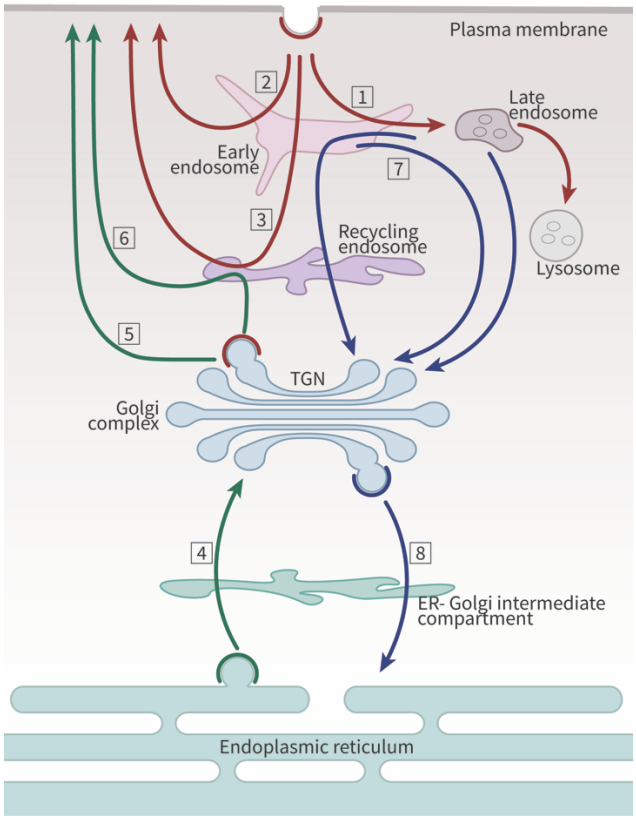

Figure 1. Graphical representation of vesicular protein trafficking routes. Endocytosis (red arrows) involves the internalization of proteins and lipids from the plasma membrane. Endocytosed proteins converge in early endosomes from where they might be destined for degradation in lysosomes (1) or recycle back to the plasma membrane. Endocytic recycling includes the fast recycling (2) and slow recycling (3) routes. Secretory route (green arrows) involves the transport of newly synthetized proteins from the endoplasmic reticulum (ER) to the Golgi complex passing through the ER-Golgi intermediate compartment (ERGIC) (4) until they arrive to the trans-Golgi network (TGN), from where they are directly sorted to the cell surface (5) or they transit through the recycling endosomes before to arrive to the plasma membrane (6). Organelle homeostasis requires the retrograde route which returns proteins back to their original compartment (blue arrows). Proteins are returned to the Golgi from different populations of endosomes (7) and from Golgi to the ER (8).

1.2.2. Steps of vesicular protein trafficking

The vesicle-mediated protein transport involves several sequential steps carried out by specific proteins. First, transmembrane cargo is selected by the recognition of a signal motif which usually consists in four to seven amino-acid residues or post-translational modifications in their cytosolic domains. Luminal proteins require recognition by a transmembrane receptor that mediates their selection at the cytoplasmic level through adaptors and coat-complex proteins. As an example of a transmembrane cargo, the transferrin receptor (TfR) possess a YXXΦ (where Y is a tyrosine residue, X is any amino acid residue and Φ is a bulky hydrophobic residue) motif that is recognized by the adaptor protein complex 2 (AP-2) at the plasma membrane mediating its endocytosis (Collawn, Stangel et al. 1990). In addition, the newly synthesized TfR is sorted by a GDNS motif from the recycling endosome to the basolateral plasma membrane domain in recently polarized epithelial cells in an AP1B-deppendent manner (Odorizzi and Trowbridge 1997, Gravotta, Deora et al. 2007). On the other hand, luminal ER chaperones possess a KDEL motif that is recognized by the transmembrane KDEL-receptor (KDELR) at the *cis*-Golgi (Semenza, Hardwick et al. 1990, Lewis and Pelham 1992). Protein kinase A (PKA) phosphorylates the cytosolic tail of the KDELR which is recognized by the COPI coat complex at the Golgi, and together with the KDEL-containing ER chaperones they are transported back to the ER (Cabrera, Muniz et al. 2003).

Coat protein complexes mediate the vesicle formation at the membrane of specific compartments with a particular lipid and protein composition. The AP-2 and the clathrin coat recognize cargoes at the plasma membrane mediating their endocytosis (Boucrot, Saffarian et al. 2010). COPII-coated vesicles transport cargoes from the ER to the ERGIC/cis-Golgi (Sato and Nakano 2007), while the retrograde Golgi-to-ER route is mediated by the COPI coat complex (Arakel and Schwappach 2018). From the *trans*-Golgi and recycling endosomes cargoes are selected by the adaptor protein complex 1 (AP-1) that recruits clathrin and sorts

proteins towards the plasma membrane (Faini, Beck et al. 2013). The retrograde transport from the endosomes to the *trans*-Golgi relies in the retromer complex that mediates cargo sorting and vesicle coating (Burd and Cullen 2014).

Although coat proteins induce membrane curvature, they are not enough to detach the vesicle from the donor compartment. The vesicle scission requires the incorporation of small head phospholipids as phosphatidic acid (PA) at the neck of the emerging vesicle which stimulate its negative curvature (Zhukovsky, Filograna et al. 2019). CtBP/BARS proteins (C-terminal-binding protein/brefeldin A ADP-ribosylated substrate) recruit phospholipase D and activate to lysophosphatidic acid acyltransferase types δ and γ, that in turn increases PA. In addition to lipids remodeling, mechanoenzymatic proteins as dynamin GTPase, constrict the neck of the vesicle, leading its release to the cytoplasm (Renard, Johannes et al. 2018).

Once the vesicle is released, the phosphatidylinositols are modified, which triggers partial vesicle uncoating allowing the association of molecular motors which are responsible for vesicle transport along the actin or microtubule cytoskeleton (Karcher, Deacon et al. 2002, Trahey and Hay 2010). When the vesicle reaches its destination, its docking is mediated by tethering factors (Yu and Hughson 2010). Finally, vesicular SNARE (Soluble NSF Attachment Protein Receptor, v-SNARE) proteins bind to the target SNARE (t-SNARE), that fuse the lipid bilayer of the vesicle with the membrane of the target compartment (Han, Pluhackova et al. 2017).

1.2.3. Rab GTPases as master regulators of vesicular trafficking

RabGTPases (Rabs) play a key role in the regulation of the molecular machinery involved in vesicular protein trafficking. Rabs are the largest family of small GTPases including more than 60 members in humans; they interact with effectors with highly diverse molecular functions, allowing to regulate the vesicular protein transport at several steps including vesicle formation, transport and fusion with target membrane (Zhen and Stenmark 2015).

Rabs switch between an active GTP-bound and an inactive GDP-bound state, that is regulated by two classes of proteins: the guanine nucleotide exchange factors (GEFs) and the GTPase activating proteins (GAPs). GEFs eject the GDP from the inactive GDP-bound Rab, which is easily replaced by a GTP from the cytoplasm. Once activated, the GTP-bound Rab is targeted to specific subcellular compartments by membrane-targeting sequences and lipid modification, where it interacts with effector proteins with several molecular functions. GAPs stimulate the intrinsic GTPase activity and let the Rab associated to GDP, that in turn releases the Rab from the membrane. At the cytoplasm, the GDP-bound Rab is recognized by a guanine nucleotide dissociation inhibitor (GDI) that sequesters the inactive Rab until they encounter a GEF (Pfeffer 2017, Song, Cong et al. 2019).

Rabs have been proposed as proteins that determine the membrane compartment identity that is a key element for proper protein destination within the cell (Pfeffer 2013). Particular Rabs decorate specific compartments in their cytosolic face (Chavrier, Parton et al. 1990). Each Rab recruit a specific set of effector proteins that regulates the constitution and movement of vesicles from their resident membrane, and also the targeting of incoming vesicles from another compartments.

At the endosomes, Rabs also provide a platform for the binding of divalent GEFs, that sequentially recruit different Rabs to the same compartment in segregated membrane domains, a process that is known as “Rab cascade” (Sonnichsen, De Renzis et al. 2000, Barbero, Bittova

et al. 2002, de Renzis, Sonnichsen et al. 2002). Since each Rab binds to specific effectors, different Rabs constitute functionally distinct membrane microdomains, allowing to endosomes work as sorting stations. Additionally, an ordered GAP recruitment during a Rab cascade lets to a sequential removal of previously bound Rabs, that enhances their segregation and finally it might result in a complete Rab conversion. Rabs replacement change the kind of carriers that are recruited, that in turn modify the luminal and membrane composition of the original endosome, constituting a compartment functionally different (Rink, Ghigo et al. 2005, Pfeffer 2013). The Rab conversion model was first coined from live-cell imaging studies that revealed that Rab5 is replaced by Rab7 during early to late endosome progression (Rink, Ghigo et al. 2005). More recently, this process has also been observed in the Rab11 to Rab8 conversion of the large ciliary vesicle at the early stages of ciliogenesis (Westlake, Baye et al. 2011, Walia, Cuenca et al. 2019).

Additional studies also revealed new insights about the conversion model. It seems that the complete replacement of a particular Rab for another, requires an additional step in which some Rabs membrane domains, and their cargo associated proteins, are first removed by tubule fission, previous to the transition to another kind of endosome. Thus, Rabs segregation by tubule scission, might efficiently decreases the diversity of Rabs at the endosome, facilitating the Rab conversion in a following step (Mesaki, Tanabe et al. 2011).

The function of Rabs in vesicular protein transport relies in their interaction with effector proteins. A GTP-bond Rab interacts with several effectors with distinct molecular functions, including adaptor proteins, coat complexes, molecular motors, tethering factors and SNAREs. The effectors are not exclusive for a particular Rab; in fact, they might be shared between related Rabs that commonly display partial colocalization, contributing to the sequentially of transport events.

Although the high homology and similar structure of Rabs, the binding of GTP and the membrane interaction induce conformational changes that increase the variability in conserved regions, conferring specificity for the effector binding (Merithew, Hatherly et al. 2001). As we mentioned, effectors are structurally and functionally diverse and most of them seem do not have common Rab-binding domains (RBD), however some effectors compete for the binding to the same Rab which also contributes to the Rab conversion process (Meyers and Prekeris 2002).

1.2.4. Rabs in the secretory and the endocytic recycling

Several Rabs participate along the biosynthetic and the endocytic routes, including Rab1, Rab6, Rab4 and Rab11.

Rab1. Rab1 functions at early secretory pathway regulating protein transport between the ER and the Golgi. Rab1 family comprises two isoforms, Rab1a and Rab1b, which predominantly localize to ERGIC and cis-Golgi (Marie, Dale et al. 2009). During the ER-to-Golgi anterograde transport, Rab1 is recruited to COPII vesicles, where it interacts with the COPII components Sec23, Sec24 and Sec31 and it promotes the binding of the tethering factor p115 (Allan, Moyer et al. 2000, Slavin, Garcia et al. 2011). Additionally, Rab1 binds and regulates the assembly of the tethering complex GM130-GRASP65 at the ERGIC and cis-Golgi membranes, which together with the vesicle associated-p115, allow the docking of COPII-coated vesicles (Moyer, Allan et al. 2001). Moreover, Rab1 depletion decreases the size of COPII structures and causes a delay in cargo sorting at the ER (Slavin, Garcia et al. 2011). Rab1 has also been related to the Golgi-to-ER retrograde transport. Rab1 interacts with GBF1, which is the GEF of the Arf1GTPase (Arf1) that mediates the recruitment of COPI complex (Monetta, Slavin et al. 2007). Consistently, the loss of function of Rab1 induces the release of COPI in the cytosol and the overexpression of constitutively active Rab1 increases GTP-bound

Arf1 and COPI in Golgi membranes (Alvarez, Garcia-Mata et al. 2003). Rab1 depletion induces strong Golgi fragmentation which might relies in its key role in bi-directional transport between the ER and Golgi and on its interaction with the p115-GM130-GRASP65 complex, which in addition to work in vesicle tethering, it mediates the interaction between cis-Golgi cisterna (Weide, Bayer et al. 2001, Marra, Salvatore et al. 2007, Slavin, Garcia et al. 2011, Jarvela and Linstedt 2012, Galea and Simpson 2015).

Rab6. Rab6 is the most abundant Rab-GTPase at the Golgi, mainly distributed in the medial/trans cisterna. There are three Rab6 in humans: Rab6A, Rab6A' and Rab6B. Rab6A regulates the Golgi-to-ER protein transport and is involved in Golgi structure maintenance through interactions with golgin proteins (Heffernan and Simpson 2014). Rab6A' also regulates the Golgi-to-ER protein trafficking and it works in the endosome to TGN transport (Mallard, Tang et al. 2002). Additionally, Rab6A and Rab6A' function in intra-Golgi trafficking (Dickson, Liu et al. 2020). Rab6B is as a neuron-specific Rab and it regulates the retrograde traffic from Golgi to the ER in neurons (Opdam, Echard et al. 2000). Rab6 regulates the Golgi-to-ER transport in a COPI independent manner, participating at the budding, elongation and fission of transport carriers, through its interaction with microtubule and actin molecular motors (White, Johannes et al. 1999, Matanis, Akhmanova et al. 2002, Miserey-Lenkei, Bousquet et al. 2017). Rab6 depletion increases the Golgi cisternal continuity and its overexpression redistributes Golgi resident proteins into the ER (Martinez, Antony et al. 1997, Galea and Simpson 2015).

Rab4. Rab4 family includes Rab4a and Rab4b and localize to early sorting endosomes where it colocalizes with transferrin (Tf) and partially with EEA1(Van Der Sluijs, Hull et al. 1991, Sonnichsen, De Renzis et al. 2000). Rab4 regulates the rapid endocytic recycling from the early sorting endosomes towards the cell surface, while Rab11 regulates the slow recycling route from the perinuclear recycling compartment (Van Der Sluijs, Hull et al. 1991, de Renzis, Sonnichsen et al. 2002). Rab4 regulates the endocytic recycling of several receptors and

adhesion proteins including the TfR (Yamamoto, Koga et al. 2010), α5β3 integrin (Roberts, Barry et al. 2001), glucose transporter type 4 (GLUT4) (Imamura, Huang et al. 2003), beta-2 adrenergic receptor (B2AR) (Yudowski, Puthenveedu et al. 2009) and the oxytocin receptor (Conti, Sertic et al. 2009). Rab4 regulates the fission of early endosomes and the formation of recycling vesicles from this compartment (Chavrier, van der Sluijs et al. 1997, de Wit, Lichtenstein et al. 2001), in a process that involves the adaptor complexes AP-1, AP-3 and GGA-3 (D'Souza, Semus et al. 2014). Additionally, Rab4 function in the fusion of recycling vesicles with the plasma membrane through its interaction with t-SNARE protein syntaxin 4 (Li, Omata et al. 2001) and it also regulates the cargo sorting from early endosomes to perinuclear recycling compartments (Eggers, Schafer et al. 2009).

1.2.5 Rab11 and its effectors

Rab11 family involves three members: Rab11a, Rab11b and Rab11c (Rab25). They regulate the “slow” endocytic recycling route and localize to perinuclear recycling endosomes, TGN and Golgi-derived vesicles (Urbe, Huber et al. 1993, Ullrich, Reinsch et al. 1996, Chen, Feng et al. 1998). The Rab11-perinuclear recycling endosome is a dynamic compartment where converge newly synthesized and endocytosed proteins. From here, proteins are sorted to specific plasma membrane domains affecting directly the cell surface composition and polarization. In fact, Rab11 regulates cellular processes as cytokinesis, ciliogenesis and cell migration and invasion, all of them highly dependent on cell surface polarization (Welz, Wellbourne-Wood et al. 2014). Consistently, Rab11 has been related to many diseases as ciliopathies, epithelial polarization disorders and cancer (Kampf, Schneider et al. 2019, Chen, Kelley et al. 2021, Ferro, Bosia et al. 2021)

In addition to the endocytic recycling, Rab11 regulates the sorting of newly synthesized proteins following a *trans*-endosomal route in polarized cells (Lock and Stow 2005). Rab11-

positive compartments also function as a primary platform for autophagosome assembly, by its interaction with WIPI2 (WD repeat domain phosphoinositide-interacting protein 2), which recruits autophagy machinery (Puri, Vicinanza et al. 2018). Additionally, Rab11 regulates the homeostasis of endosomal-lysosomal biogenesis through the regulation of cation-independent mannose 6-phosphate receptor (CI-M6PR) recycling between the late endosomes and the TGN (Zulkefli, Houghton et al. 2019). Rab11 also is involved in late stages of Ca^{2+}-induced lysosome exocytosis (Escrevente, Bento-Lopes et al. 2021). In addition, Rab11 was detected in BFA-induced Golgi-derived carriers and it depletion inhibits Golgi-to-ER retrograde transport, but in a lesser extent than Rab1a or Rab1b silencing (Galea and Simpson 2015).

Rab11 interacts with several effectors with different molecular functions. The first discovered Rab11 effector was WDR44, that structurally seems to be a scaffold protein, but its function has been poorly studied (Zeng, Ren et al. 1999). Rab11 binds to molecular motors including, MyoVa and MyoVb (Lindsay, Jollivet et al. 2013, Ji, Yao et al. 2019). Rab11 also interacts with the exocyst subunit Sec15 (Escrevente, Bento-Lopes et al. 2021) and with Rabin8, the GEF of Rab8 (Knodler, Feng et al. 2010). In addition, there is a family of Rab11-interacting proteins (Rab11-FIPs) which involve five members: FIP1/RCP, FIP2, FIP3, FIP4 and FIP5/Rip11, that function in the trafficking of specific cargoes including TfR, α5β1 integrin, EGFR, α-amino-3-hydroxy5-methylisoxazole-4-propionic acid (AMPA) and GLUT4 (Peden, Schonteich et al. 2004, Caswell, Chan et al. 2008, Schonteich, Wilson et al. 2008, Wang, Edwards et al. 2008).

FIPs are scaffold proteins for Rab11. FIP2 binds to MyoVb and together with Rab11, work in the formation of vesicles from the pericentriolar recycling endosome and also in their targeting to the plasma membrane (Gidon, Bardin et al. 2012). Rip11 interacts with kinesin II, regulating the anterograde transport of Rab11-positive vesicles (Schonteich, Wilson et al. 2008), while FIP3 binds to dynein light intermediate chain 2 subunit (DLIC-2) and regulates the

movement of peripheral endosomes toward the centrosome and the perinuclear recycling compartment (Horgan, Hanscom et al. 2010). FIP3 also interacts with Rac1, a small GTPase protein from Rho family, that regulates the formation of branched actin networks (Bouchet, Del Rio-Iniguez et al. 2016).

1.2.6. WDR44

WDR44 is a protein of 913 residues with several protein-protein binding domains, including a FFAT-like domain, a proline rich domain (PRD), the Rab11 binding domain (RBD) and seven WD40 repeats. The RBD is located between the residues 334-504 and mediates the interaction with the GTP-bound and membrane-associated Rab11 (Zeng, Ren et al. 1999). WDR44 cofractionates with Rab11 and they colocalize in perinuclear endosomes in CHO cells (Zeng, Ren et al. 1999). The overexpression of the residues 1-504 of WDR44, which lacks the WD40 repeats, but not the complete WDR44, decreases the TfR recycling, revealing that it works as a dominant negative of Rab11 and that the WD40 domain is required to the Rab11-related functions (Zeng, Ren et al. 1999).

Recent studies have revealed new insights about the WDR44 function. WDR44 binds to Rab11 at the base of the primary cilia, which blocks the recruitment of FIP3 and Rabin8 and in turn decreases ciliogenesis (Walia, Cuenca et al. 2019). The interaction of WDR44 and Rab11 is enhanced by the Akt-mediated phosphorylation at Ser342/344 of WDR44, and consistently, the phosphomimetic mutation inhibits ciliation (Walia, Cuenca et al. 2019). Moreover, WDR44 and FIP3 compete for Rab11 interaction, suggesting a common binding site and a sequential coupling to Rab11 function (Walia, Cuenca et al. 2019). Additionally, it has been suggested that WDR44 is involved in the transport of the endocytosed ß1-adrenergic receptor (ß1-AR)-containing vesicles toward to the perinuclear recycling endosome (Gardner, Hajjhussein et al. 2011).

WDR44 also interacts with the ER integral membrane proteins VAMP-Associated Protein A and B (VAPA and VAPB) through its FFAT-like domain (Baron, Pedrioli et al. 2014) and all together colocalize in the ER (Lucken-Ardjomande Hasler, Vallis et al. 2020). VAPA/B are tether proteins that mediate ER contacts with lysosomes, mitochondrion, Golgi, endosomes and autophagosomes (Rocha, Kuijl et al. 2009, De Vos, Morotz et al. 2012, Dong, Saheki et al. 2016, Zhao, Liu et al. 2018). Additionally overexpression of VAPA, inhibits the ER-to-Golgi transport of VSGV, decreasing the VSGV incorporation into budding ER vesicles due to a reduced lateral mobility in the ER (Prosser, Tran et al. 2008). VAPB depletion reduces the delivery of membrane from soma to dendrites, affecting their morphology (Kuijpers, Yu et al. 2013). Using in vitro assays it was described that blockade of VAPB decreases the fusion of COPI-coated vesicles (Soussan, Burakov et al. 1999). Moreover VAPA binds to Bet1 and Sec22 which are SNARE proteins associated to the Golgi and ER, respectively (Hay, Hirling et al. 1996, Weir, Xie et al. 2001). WDR44 also interacts with Sec13, a COPII subunit, that mediates the ER-to-Golgi protein transport (Mammoto, Sasaki et al. 2000).

In summary, WDR44 is a Rab11 effector that binds to the ER tethering proteins VAPA and VAPB, and might be functionally involved in endocytic recycling and protein trafficking between the ER and the Golgi complex.

1.3. Hypothesis and objectives

1.3.1. Hypothesis:

"WDR44 functions in endocytic recycling and protein trafficking between the Endoplasmic Reticulum and the Golgi complex".

1.3.2. Objectives:

1. To Identify proteins that interact with WDR44.

    1.2 To characterize the WDR44 interactome and their cellular functions.

    1.3 To validate WDR44 interactions with protein transport-related proteins.

2. To characterize the subcellular localization of WDR44.

    2.1 To analyze the distribution of WDR44 relative to its protein interactors.

    2.2 To analyze the WDR44 localization relative to subcellular protein markers.

3. To evaluate the function of WDR44 in endocytic recycling.

    3.1 To evaluate the effect of WDR44 silencing on early and recycling endosomes distribution.

    3.2 To assess the effect of WDR44 depletion in the endocytic recycling.

    3.3 To evaluate the effect of WDR44 silencing in cell migration and invasion.

4. To evaluate the function of WDR44 in protein transport at the ER-Golgi interface.

    4.1 To assess the effect of WDR44 silencing in the anterograde and retrograde transport between the ER and the Golgi complex.

    4.2 To assess functional consequences of WDR44 depletion, related to protein transport at the ER-Golgi interface (ER stress/Unfolded Protein Response).

2. MATERIALS AND METHODS

2.1. Materials.

2.1.1. Cell lines

HeLa and Hek293T human cell lines were maintained in Dulbecco's Modified Eagle's Medium (DMEM 4.5 g/l glucose) supplemented with 10% fetal bovine serum (FBS), 100 Units/ml penicillin and 0.1 mg/ml streptomycin (SigmaAldrich, ST Louis, MO).

2.1.2. Antibodies

The following antibodies were used: Rabbit anti-WDR44 (Novus Biological), rabbit anti-Rab11a (Invitrogen), rabbit anti-Rab1a, rabbit anti-PDI, rabbit anti-Calnexin, rabbit anti-BiP, rabbit anti-ERO1, rabbit anti-PERK, rabbit anti-Ire1α (Cell signaling), rabbit anti-Rab1b (Santa cruz), rat anti-GFP (Chromotek), sheep anti-TGN46 (Serotec, Oxford, UK), mouse anti-GM130, mouse anti-EEA1 (Transduction Laboratories, Lexington, KY), mouse anti-γ-Adaptin (Sigma), mouse anti-Transferrin receptor (Invitrogen), rabbit anti-Epidermal growth factor receptor (EGFR984) produced in our laboratory as described (Salazar and Gonzalez 2002). Primary antibodies were recognized with horseradish peroxidase (HRP) conjugated antibodies (Rockland) for western blots (1:5000 dilution) or with Alexa conjugated antibodies (Molecular Probes) for immunofluorescence (1:1000 dilution).

2.1.3. Reagents

Lipofectamine 2000, Opti-MEM medium, penicillin/streptomycin (P/S), Dulbecco's Modified Eagle Medium (DMEM), nitrocellulose membrane (88018), fetal bovine serum (FBS), Fluoromont G, Trizol reagent, from Invitrogen. Bradford reagent from Bio-Rad. D-Propranolol (P0689), Tunicamycin, Ampicillin, MESNA (M1511), Iodoacetamide and AP solution in tablets from Sigma. EZ-Link sulfo NHS-Biotin (21217), EZ-Link Sulfo-NHS-SS-Biotin (cleavable biotin) (21331), Neutravidin-agarose (29201) and BCA assay from Thermo. Immobilon Forte Western

HRP substrate (WBLUF0500) from Millipore. GoTaq Flexi and M-MLV Reverse Transcriptase from Promega. GFP-trap agarose beads (Chromotek). SYBR Green Super mix (Biorad).

2.1.4. Plasmids

Human WDR44 cloned in pEGFP-N1(WDR44-EGFP) and bovine WDR44 cloned in pCDNA3.1-HA (Bt-HA-WDR44) were donated by Dr. David Sabatini (NYU). Bovine WDR44 was cloned during this thesis in pmCherry-N1 (Bt-WDR44-mCherry). shRNA lentiviral vectors for WDR44 (RHS3979-201780280, 201780281, 201780282, 201780283, 201780284) and Rab11a (cat. No. RHS3979-201786829, 201788691,201791571, 201793166, 201795938) shRNAs were purchased from Dharmacon. pLKO.1 empty vector was donated by Dr. María Paz Marzolo (PUC). pVSVG and pΔR were used as viral delivery system.

2.2. Methods.

2.2.1. Indirect immunofluorescence and imaging. Cells grown on coverslips were washed three times with PBS Ca-Mg. Cells were fixed with 4% PFA in PBS Ca-Mg during 20min at room temperature (RT) and then they were washed three times with PBS 0.1 mM $CaCl_2$ and 1 mM $MgCl_2$ (PBS Ca-Mg). Fixed cells were permeabilized with PBS 0.05% saponin during 15min at RT. Coverslips were incubated with primary antibodies diluted in PBS 0.05% saponin during 30min at 37ºC. Then, coverslips were washed with PBS and incubated with secondary antibody as the primary. Coverslips were mounted on slide with Fluoromount-G (Invitrogen) and incubated at 60ºC during 15min. IFIs were imaged with a Leica TCS SP8 spectral confocal microscopy (63X oil immersion objective), processed with ImageJ software (NIH) and colocalizing analysis were performed using JaCoP plugin.

2.2.2. Semiquantitative RT-PCR. RNA was obtained from HeLa cells using the Trizol (Invitrogen) isolation reagent following the manufacturer's instructions. Complementary DNA (cDNA) was made using the M-MLV Reverse Transcriptase kit (Promega). PCR was performed using GoTaq Flexi kit (Promega) at 50ºC annealing temperature and using the following

primers: ACTB forward (5′-TGACCCAGATCATGTTTGGAG-3′); ACTB reverse (5′-TTCTCCTTAATGTCACGCAC-3′); WDR44 forward (5´-GGTATTAAAGCCCACAATGCAG-3′); WDR44 reverse (5′- AATGCTCCAGTGAAGTCAGC-3′).

2.2.3. Quantitative RT-PCR (qRT-PCR). RNA and cDNA was obtained as in section 2.2.2. qPCR was performed using SYBR Green Super mix (Biorad) and the Rotor-Gene Q (QIAGEN). Primers used in this study were from (van Galen, Kreso et al. 2014): ACTB forward (5'-CCTGTACGCCAACACAGTGC-3'); ACTB reverse (5'-ATACTCCTGCTTGCTGATCC-3'); CHOP forward (5'-GGAGCATCAGTCCCCCACTT-3'); CHOP reverse (5'-TGTGGGATTGAGGGTCACATC-3'); ERDJ4 forward (5'-TCGGCATCAGAGCGCCAAATCA-3'); ERDJ4 reverse (5'-ACCACTAGTAAAAGCACTGTGTCCAAG-3'); GADD34 forward (5'-CCCAGAAACCCCTACTCATGATC-3'); GADD34 reverse (5'-GCCCAGACAGCCAGGAAAT-3'); BiP forward (5'-TGACATTGAAGACTTCAAAGCT-3'); BiP reverse (5'-CTGCTGTATCCTCTTCACCAGT-3'); XBP1s forward (5'-CGCTTGGGGATGGATGCCCTG-3´); XBP1s reverse (5'-CCTGCACCTGCTGCGGACT-3').

2.2.4. Gel electrophoresis and western blot. Protein samples were resolved in sodium dodecyl sulfate polyacrylamide gel electrophoresis (SDS-PAGE) at different percentages depending on the protein of interest. Loading buffer contained 100 mM DTT as a reducing agent. After electrophoresis, samples were transferred into a PVDF (Thermo) membrane in 25 mM Tris-HCl, Glycine 192 mM and 20% methanol at 450 mA for 1.5 h. After transferring, membranes were blocked with PBS-5% skim milk for 1h at RT. Primary antibodies were incubated ON at 4ºC in blocking buffer and then washed three times for 10 min with PBS 0.5% Tween 20. Secondary antibodies conjugated with horseradish peroxidase (HRP) were incubated 1h in blocking buffer then washed. HRP conjugated antibodies were developed with chemiluminescent HRP substrate following manufacturer's instructions. Chemiluminescent

images were acquired in G:Box gene tools detection system (Syngene) with the corresponding filter. Densitometric band analysis was performed with FIJI software.

2.2.5. GFP-Trap precipitation and mass spectrometry analysis. HeLa cells ($5x10^6$ cell/100mm dish) were transfected with Lipofectamine 2000 (Invitrogen) according to the protocol of manufacture. 24 hours after transfection, cells were harvest in PBS 0.05% trypsin and lysed in 500µL GFP-trap lysis buffer (25mM Tris pH 7.5, 50 mM NaCl, 0.1%NP40) during 30min at 4ºC. Cell lysate were passed three times through 29-gauge needle and centrifugated at 14.000 rpm during 10 min. Supernatant was collected and incubated with 25uL GFP-trap agarose beads (Chromotek) during 1h at 4ºC with constant rotation. Beads were washed three times with GFP-trap lysis buffer and resuspended in SDS sample buffer for subsequent immunoblotting or mass spectrometry. Co-precipitated proteins were sequenced by mass spectrometry according to (Telot, Rousseau et al. 2018) at the Université Paris Diderot, Sorbonne Paris Cité, Proteomics/Mass spectrometry core facility, Institut Jacques Monod, Paris, French (in collaboration with Dr. Stephanie Miserey-Lenkei from Institut Curie, Paris, French).

2.2.6. Recombinant lentiviral production and transduction. HEK293T (2.5x105 cell/well in 6-well plates) were cotransfected with pVSVG (50ng), pΔR(500ng), and pLKO.1 (500ng) vectors containing WDR44 or Rab11a specific short hairpin RNA or empty pLKO.1 as control. Plasmid were diluted in Optimem (50µL) supplemented with 6% FUGENE and added to culture media (DMEM 10% FBS). 24 and 48 h post transfection the virus-containing media was centrifugated at 320g during 5 min, aliquoted and frozen at -80ºC.

For cells transduction, HeLa cells were incubated with 25% virus-containing media diluted in DMEM 10% FBS without antibiotics. After 24h post-transduction, culture media was replace by DMEM 10% FBS supplemented with 2µg/ml puromycin during 48h. Cells were used for different assays after 48h of puromycin selection.

2.2.7. Transferrin endocytosis and recycling assay. HeLa cells ($2x10^5$ cell/well in 6-well plates) were transduced and puromycin selected for 48h. Then, cells were incubated in serum-free DMEM during 1h at 37ºC. For endocytosis assay in continuing exposure to transferrin, cells were incubated with 25µg/mL Transferrin Alexa-488 (Tf-488) in DMEM 1%BSA for different times at 37ºC. For pre-loaded transferrin endocytosis assay, cells were washed three times with cold PBS at 4ºC and they were incubated with 25ug/mL Transferrin Alexa-488 (Tf-488) in PBS during 30min at 4ºC in darkness. To remove the unbound Tf-488, cells were washed three times with cold PBS Ca-Mg at 4ºC and then, they were incubated with previously warmed DMEM at 37ºC for different times, to allow Tf-488 internalization. In both, pre-loaded and continuing exposure to Tf-488 assays, cells were washed on ice with cold PBS Ca-Mg for Tf-488 uptake stopping. Remaining cell surface Tf-488 was removed by three washes with acid PBS Ca-Mg pH 5.0 followed by three washed with PBS Ca-Mg at 4ºC before cells fixing.

For Tf-488 recycling assay, cells were under 30min of pre-loaded transferrin endocytosis with a subsequent acid wash to remove the remaining cell surface Tf-488. Then, cells were incubated in previously warmed DMEM 1% BSA supplemented with 250µg/mL unlabeled transferrin (Biotin-Tf, Invitrogen) for different times at 37ºC to allow transferrin receptors recycle back to the plasma membrane. Then, cells were washed three times with acid PBS Ca-Mg pH 5.0 followed by three washed with PBS Ca-Mg at 4ºC before cells fixing.

In all conditions, cells were incubated with PBS 5mM EDTA, 0.05% trypsin during 15min at 4ºC, transferred to a 1.6mL tube and centrifugated at 1100g for 3min at 4ºC. Cells were washed three times with FACS Buffer (PBS 2%BFS) and they were fixed by incubation in PFA 2% in PBS 1%BFS during 16h at 4ºC in darkness. Finally, cells were washed three times and resuspended in FACS buffer before their cytometry analysis.

2.2.8. EGFR biotinylation recycling assay. HeLa cells ($2x10^5$ cell/well in 6-well plates) were seeded, transduced and puromycin selected as previously described. After puromycin treatment, cells were incubated in serum-free DMEM during 4h at 37ºC. Then, the cells were washed twice with cold PBS Ca-Mg during 5min at 4ºC each time. Cell surface proteins were biotinylated by adding 0.2mg/mL EZ-Link Sulfo-NHS-SS-biotin (#21331; Thermo Scientific, Waltham, MA, USA) in PBS Ca-Mg for 30min at 4ºC. Then, cells were washed twice as described before and incubated with 100µM propranolol in previously warmed DMEM for 30min at 37ºC to allow the internalization of biotinylated plasma membrane proteins. Cells were washed twice with cold PBS Ca-Mg for uptake stopping. Remaining cell surface biotin was removed by incubation with fresh reduction solution (20mM MESNA, 50mMTris, 100mM NaCl, pH 8.6) for 45min at 4ºC. After Biotin reduction, cells were washed twice as previously described and remaining reducing agent was quenched by incubation with fresh diluted 20mM Iodoacetamide in PBS Ca-Mg at 4ºC for 10min. Then, cells were washed twice with cold PBS Ca-Mg and incubated a second time with previously warmed DMEM for 30min at 37ºC to allow protein recycling back to the plasma membrane. Then, cells were washed twice with cold PBS Ca-Mg and biotin re-exposed at the cell surface was removed by a second MESNA solution treatment. Cells were washed and remaining MESNA was quenched with Iodoacetamide as previously described.

Cell proteins were extracted with lysis buffer and biotinylated proteins were pulled down with Neutravidin-agarose beads (Thermo Scientific) for 1h at 4ºC. Beads were washed three times with lysis buffer at 4ºC for 5min each time. Finally, beads were resuspended with loading buffer and incubated at 90ºC for 10min before western blotting.

2.2.9.Transwell migration and invasion assay. For invasion assay, 100µL of Matrigel matrix (200µg/mL in serum-free DMEM) was added to each Transwell insert (8 µm PET membrane, Corning, #3464) and incubated during 2 hour at 37ºC for Matrigel gelling. $5x10^4$ transduced and puromycin selected HeLa cells were diluted in serum-free DMEM and seeded over Matrigel or uncoated filters for invasion and migration assay respectively. The lower chambers were supplemented with serum in all conditions. Cells were incubated for 16h at 37ºC before staining with 0.2 % crystal violet/50 % ethanol for 10 min. Cells at the top side of the upper chamber were removed using moistened cotton swabs and the Transwell inserts were washed twice with PBS to remove unbound crystal violet and then air-dried. Cells that migrated to the bottom side of the membrane were photographed and counted.

2.2.10. Inverted Invasion Assay. Matrigel (Corning, #35423) 5 mg/mL, mixed with fibronectin (25µg/mL), was polymerized in 24-well Transwell polycarbonate filters 8-µm pore size inserts (Corning, #3422) for 1 h at 37 °C. Inserts were inverted, and $5x10^4$ cells were seeded to the bottom of the filter and allowed to adhere for 4–5 h at 37 °C in 5% CO2 before returning to the right side up. Serum free media was added to the wells of the transwell plate and media with FBS 10% was added in the upside of the chamber on top of the Matrigel plug and cells were maintained during 5 days at 37ºC in 5% CO2. Matrigel plugs were fixed with 4% PFA, treated with 0.2% Triton X-100 and stained with Hoechst. Cells at the bottom of the filter that failed to migrate through the filter were removed using tissue. Images at 10µm intervals were taken with a spectral confocal microscope (SP8, Leica) using the 10X objective. ImageJ software (NIH) was used to determine the integrated density of each image section to calculate the invasion index = (∑ integrated density of first 30 µM)/(∑ integrated density of invasion) expressed as a fold change (Barra, Cerda-Infante et al. 2021).

2.2.11. Fluorescence loss in photobleaching (FLIP). FLIP experiments were performed by first defining the regions of interest (ROI) that considered the whole cell body avoiding the perinuclear region with Golgi morphology. ROIs were repeatedly bleached, while an image was acquired with reduced laser power (0.5% output) at the start of the experiment and after 100 bleaching events. Remaining fluorescence at each ROI was manually quantified and corrected with a non-photobleached area from a different cell in the same image. Data was normalized to the mean of 10 frames before the photobleaching using ImageJ software.

2.2.12. Bioinformatic analysis.

2.2.12.1 Multiple protein sequence alignment. Amino acid sequences were aligned using the program Clustal Omega supported by the European Bioinformatics Institute (EBI) (Sievers and Higgins 2018).

2.2.12.2 Gene Ontology (GO) enrichment analysis. The Biological Process (BP), Cellular Component (CC) and Molecular Function (MF) GO enrichment analysis were made using the DAVID database and considering the complete human genome as background. Data visualization was made using the python library plotnine (based on ggplot2) and considering fold-enrichment, enrichment significance (p-value) and number of proteins related to each GO term.

2.2.12.3 Protein-protein interacting (PPI) network. Physical PPI analysis was made using STRING database, considering high-throughput lab experiments, textmining and previous knowledge in curated databases. PPI network results were plotted using the Cytoscape program and the interaction scores were manually added.

2.2.13. Statistical analysis. Student's t test was used for two-group comparison, and one- or two-way analysis of variance (ANOVA) was used for comparisons of more than two groups with Bonferroni's post-hoc test, $p<0.05$ was considered statistically significant higher p values were considered non-significant (ns). All analysis was performed using the GraphPad PRISM software. Data points and error bars in the figures represent mean and standard error of the mean (SEM).

3. RESULTS

To address the role of WDR44 we first analyzed its structural characteristics and performed an interactome analysis, to then use this information to design dedicated experiments testing its potential function.

3.1 WDR44 structure and bioinformatic analysis.

Human WDR44 is a protein of 913 residues of a theoretical molecular weight of 101KDa, that possesses a FFAT-like domain, a proline rich domain (PRD), a Rab11 binding domain (RBD) and seven WD40 repeats (Figure 2A). The FFAT-like domain is located within the residues 9-15 and has been described to interact with the ER membrane proteins VAPA and VAPB, which recruit WDR44 to the ER (Baron, Pedrioli et al. 2014, Lucken-Ardjomande Hasler, Vallis et al. 2020). The PRD encompasses the residues 210-256 and mediates the interaction of WDR44 with the tubulating protein GRAF2 through its SH3 domain in tubular endosomes closely associated to the ER (Lucken-Ardjomande Hasler, Vallis et al. 2020). The Rab11 binding domain (RBD) is located between the residues 334-504 and mediates the interaction with Rab11 in a GTP- and membrane-associated manner (Zeng, Ren et al. 1999). A recent study described that Akt phosphorylates WDR44 at Ser342/344 (Figure 2A) enhancing its binding to Rab11-GTP (Walia, Cuenca et al. 2019).

The RBD of WDR44 has not been analyzed in detail. Therefore, we compared its sequence with the RBD of the Rab11 family-interacting-proteins (FIPs), which includes five members (Figure 2A) (Hales, Griner et al. 2001, Wallace, Lindsay et al. 2002). FIPs have a RBD of 62 residues that forms a coiled-coil involved in Rab11a-GTP binding and FIPs homodimerization, thus conforming a heterotetrameric complex [Rab11-$(FIP)_2$-Rab11] (Wallace, Lindsay et al. 2002, Jagoe, Lindsay et al. 2006, Shiba, Koga et al. 2006). The 62

residues of RBD of FIPs align within the residues 334-399 in RBD of WDR44 (Figure 2B). However, the identity of sequences within that region is lower for WDR44 (12.5-21.05%) compared with the identity found among the FIPs (21.43-62.9%) (Figure 2C and 2D). Some residues are highly conserved in all these proteins and are likely involved in the binding of Rab11 (Figure 2B).

Figure 2. Comparison between the Rab11 binding domain (RBD) of WDR44 and the RBD of Rab11 Family Interacting proteins (FIPs). A. Schematic structure representation of WDR44 and human Rab11 family interacting proteins (FIP); FIP-1, FIP-2, FIP-3, FIP-4 and FIP-5. **B.** Amino acid sequence alignment of RBD from WDR44 and FIPs. Code color is according to Clustal Omega multiple sequence alignment program and is detailed in the legend. (*) indicates perfect alignment, (:)represents a site belonging to group exhibit strong similarity and (.) weak similarity. Black boxes regions outline the RBD from crystal structures of FIP-2 and FIP-3 (Jagoe, Lindsay et al. 2006, Shiba, Koga et al. 2006). Red asterisk above the sequences indicate Akt-mediated phosphorylation sites in WDR44 (Walia, Cuenca et al. 2019). **C.** Sequence identity heatmap showing the pairwise percentage identity between all RBD sequences calculated by Clustal Omega alignment. The X and Y axes indicate the protein names. Identity scores are shown as a color-coded matrix, calculated by comparing every sequence to each other. Sequence identity increases from yellow to blue. **D.** Guide tree produced by Clustal Omega considering the sequence identity shown in C.

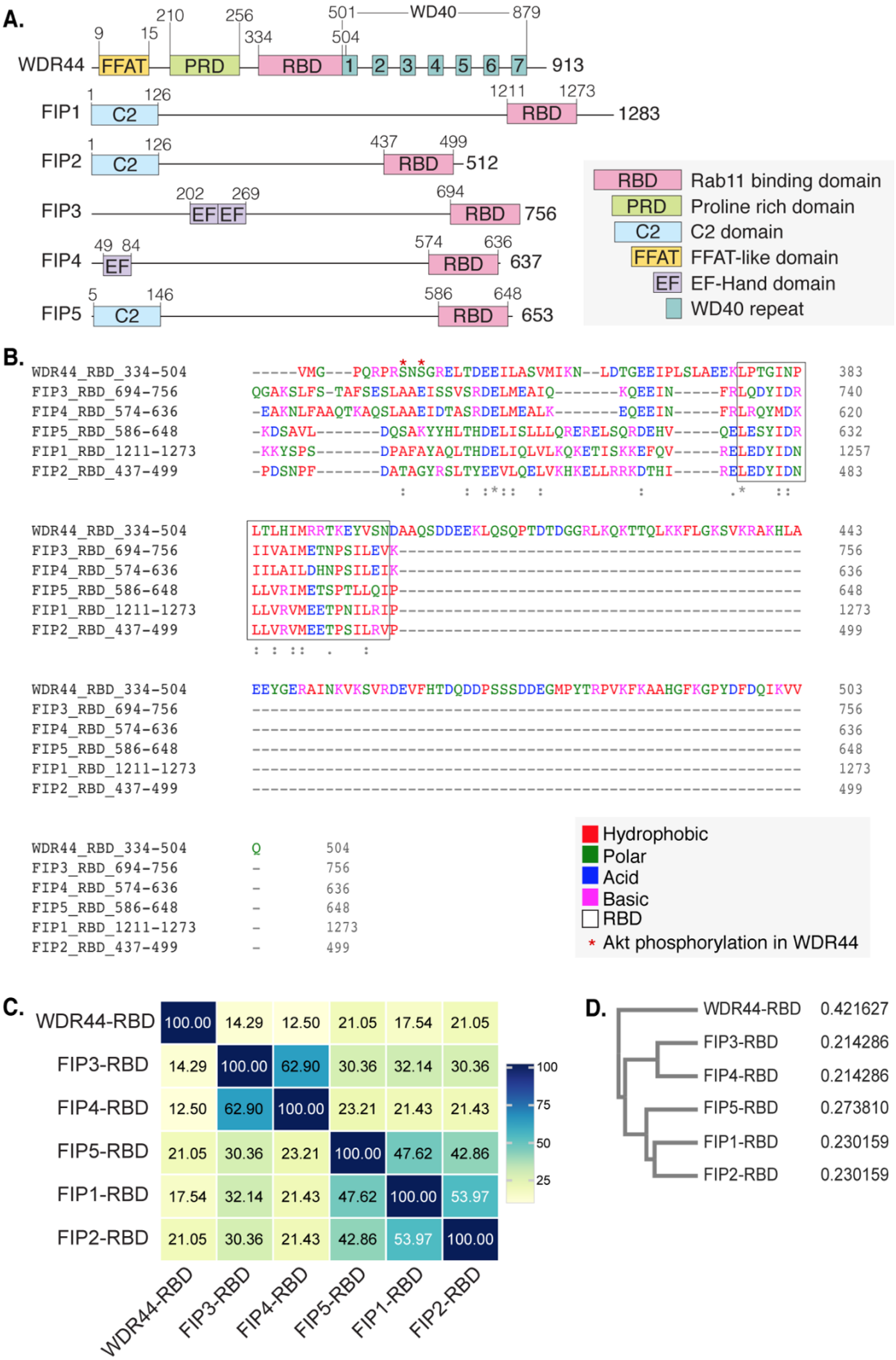
A.
WDR44
FFAT
PRD
RBD
WD40
913
FIP1
C2
1283
FIP2
512
FIP3
EF
756
FIP4
637
FIP5
653
RBD Rab11 binding domain
PRD Proline rich domain
C2 C2 domain
FFAT FFAT-like domain
EF EF-Hand domain
WD40 repeat
B.
WDR44_RBD_334-504
FIP3_RBD_694-756
FIP4_RBD_574-636
FIP5_RBD_586-648
FIP1_RBD_1211-1273
FIP2_RBD_437-499
Hydrophobic
Polar
Acid
Basic
RBD
* Akt phosphorylation in WDR44
C.
WDR44-RBD 100.00 14.29 12.50 21.05 17.54 21.05
FIP3-RBD 14.29 100.00 62.90 30.36 32.14 30.36
FIP4-RBD 12.50 62.90 100.00 23.21 21.43 21.43
FIP5-RBD 21.05 30.36 23.21 100.00 47.62 42.86
FIP1-RBD 17.54 32.14 21.43 47.62 100.00 53.97
FIP2-RBD 21.05 30.36 21.43 42.86 53.97 100.00
100
75
50
25
D.
WDR44-RBD 0.421627
FIP3-RBD 0.214286
FIP4-RBD 0.214286
FIP5-RBD 0.273810
FIP1-RBD 0.230159
FIP2-RBD 0.230159

3.2 WDR44 interactome suggests interactions with a variety of proteins including other Rabs beyond Rab11.

3.2.1 Interactome data analysis.

To identify new proteins that interact with WDR44 we performed a proteomics study by transiently expressing WDR44-EGFP in HeLa cells followed by GFP-trap-agarose precipitation. We used empty GFP plasmid and GFP pull-down as negative controls. Given that Rab11 is the first known WDR44 interactor (Zeng, Ren et al. 1999), we also included an analysis with Rab11a-EGFP for comparison. Co-precipitated proteins were sequenced by mass spectrometry at the Université Paris Diderot, Sorbonne Paris Cité, Proteomics/Mass spectrometry core facility, Institut Jacques Monod, Paris, French (in collaboration with Dr. Stephanie Miserey-Lenkei from Institut Curie, Paris, Francia).

We analyzed the data and filtered the results according to the scores obtaining a dataset of 132 proteins within the WDR44-EGFP precipitates (Table I). The interactome suggests that WDR44 interacts with other Rabs in addition to Rab11, including Rab4a, Rab4b, Rab1b, Rab6A and Rab10. The interactome also corroborates previously described WDR44 interactions, such as those with VAPA and VAPB, two ER membrane proteins involved in ER interactions with several other organelles (Wu, Carvalho et al. 2018, Neefjes and Cabukusta 2021).

Rab11a-EGFP data set included 272 interacting proteins (Table II), among which only 54 proteins share an interaction with WDR44. We analyzed the function and location associated to each protein of WDR44 and Rab11a interactomes by a Gene Ontology (GO) enrichment analysis, using the complete human genome as background in DAVID database. We found common biological processes GO terms as cell-cell adhesion, actin filament bundle assembly, regulation of organelle assembly and translational initiation. Among exclusive processes enriched in WDR44 interactome, we found regulation of early endosome to late endosome

transport, Golgi-to-ER and ER-to-Golgi vesicle-mediated transport; while Rab11a interactome was enriched in regulation of endo and exocytosis (Figure 3).

Among cellular component GOs, WDR44 and Rab11a interacting proteins were associated to perinuclear region, cell-cell adherent junction, focal adhesion and mitochondria. Particularly, WDR44 interactome was enriched in proteins of COPI coat complex, while Rab11a interactome was enriched in exocyst and clathrin-coated vesicles (Figure 4).

Both interactomes were also enriched in molecular functions related with GTP, GTPase and cadherin binding. WDR44 interactome was also enriched in FFAT motif binding and actin and myosin V binding. Rab11 interactors shown molecular functions related with clathrin adaptor activity and Ral GTPase and Ran GTPase binding (Figure 5). Thus, even though WDR44 interactor proteins are involved in common processes with Rab11a interactome, they are also related with specific cellular functions that include vesicular protein transport at the ER and Golgi level.

In order to analyze how the 132 proteins in WDR44 interactome are physically related, we constructed a protein-protein interacting (PPI) network using the STRING database. We considered high-throughput lab experiments, textmining and previous knowledge in curated databases (Figure 6). The analysis revealed 179 interactions between these 132 proteins with an average node degree of 2.71 interactions associated to each protein. Proteins found in this WDR44 interactome have more interactions among themselves than would be expected for a random set of proteins of similar size, drawn from the genome. This is indicated by the PPI enrichment p-value <1,0E-16, suggesting that WDR44 interacting proteins are biologically connected as a group.

Our PPI network analysis showed that Rab4a is the main co-precipitated protein according to its interaction score (Figure 6). Additionally, the PPI network let us to visualize clusters of proteins associated with common GO biological processes. WDR44 appeared as the hub of the cluster associated to cell-cell adhesion and ER organization. We also identified that Rab1b works as the hub of the cluster related with vesicular protein transport between the ER and the Golgi. Ezrin, an actin filament binding protein, is the hub of the cluster related with the regulation of organelle and actin filament bundle assembly (Figure 6).

Table 1: WDR44 interactome dataset. WDR44-EGFP interacting proteins identified by a GFP-trap assay followed by Mass Spectrometry analysis. Score value indicates level of interaction with WDR44.

Protein	Score	Protein	Score	Protein	Score	Protein	Score
WDR44	1719	RPL24	124	COPB1	81	NARF	62
RAB4A	742	YWHAB	120	GCN1	79	PDE12	62
IQGAP1	379	DNAJC10	118	PRDX5	79	COX17	61
VAPA	302	CYFIP1	117	RPL15	79	ISOC2	60
RAB11A	293	COPA	116	CENPM	78	GPX1	59
VAPB	282	IDH3B	114	SESTD1	78	TUBAL3	59
GDI2	250	SHC1	113	RPL12	77	SLC1A5	58
MSN	235	NARS	111	NAP1L1	76	LIN7C	57
HARS	233	QARS	110	CYFIP2	75	RDX	57
CAST	232	ITPK1	107	ASNS	74	RPL18	57
YARS	211	HSDL2	104	GDA	74	ADO	56
RAB4B	209	ACTN4	103	RAB10	74	ANP32E	56
HSP90B1	207	APEH	103	RAB1B	74	DDX6	56
TARS	203	EZR	101	RAB6A	74	NSUN2	56
MAGED2	184	SRP14	101	FSTL4	73	RUVBL2	56
PGLS	171	FSCN1	100	RPL14	73	SPRYD4	55
PPP2R1A	170	PSME1	99	BUB1B	72	RPL26	54
EPRS	165	SH3GL2	99	COASY	71	RPL35	54
CNN2	160	SH3KBP1	99	LARS	71	TRAF5	54
RPS21	160	CNN3	98	SPAG7	71	ACOT9	53
ACYP2	156	PSME2	97	IBA57	70	EIF4E	53
VCP	156	NT5DC2	96	TMEM109	70	PBK	53
ANP32B	155	RPL22	96	S100A6	69	PSMC3	53
KRT80	145	EXOSC9	95	PPA2	68	TIPRL	52
PCBP2	145	OGFR	95	MLKL	67	C2orf69	51
PTPN11	136	PCYT1A	94	TNPO1	67	NEK9	51
PRDX6	135	RPL38	94	RPL31	66	SRR	51
NUBP2	133	ACTN1	93	ARCN1	65	UNC45A	51
SKP1	133	PFKP	93	KPNA3	65	ANKRD54	50
SET	129	YWHAG	93	EIF2S1	64	DCTPP1	50
HDGF	126	ARL1	86	AAMP	63	GLUL	50
IARS	125	GSPT1	84	LGALS1	62	GOLGA4	50
ANP32A	124	KCTD6	82	MACROD1	62	RPS19	50

Table 2: Rab11a interactome dataset. Rab11a-EGFP binding proteins identified by a GFP-trap assay followed by a Mass Spectrometry analysis. Score values represent the level of interaction with Rab11a.

Protein	Score	Protein	Score	Protein	Score	Protein	Score	Protein	Score
RAB11A	9003	GEMIN4	147	EXOC1	100	MAGED2	73	EIF3D	58
GCN1	3204	DNAAF5	145	RPL14	97	PRPF19	73	PPP1R12A	58
MTOR	1913	IPO4	145	PCYT1A	97	GSPT1	73	LIMS1	58
GDI2	1156	XRCC5	143	TTI1	97	CTNND1	72	KIF2A	58
IQGAP1	778	PPP2R2A	142	AP2S1	97	LPL	72	COPA	58
RAB4A	486	SURF4	138	GAPDH	96	LPCAT2	71	EDF1	57
RAB11FIP1	460	TNPO3	138	PACSIN2	96	SPTLC1	71	SH3BP4	57
GDI1	431	VPS13C	136	EXOSC9	95	LDHB	71	MOCS2	57
TNPO1	389	XPO7	134	ARL6IP5	95	PDCD6	71	TNPO2	57
ECM29	368	XPO4	133	EXOC3	95	TCOF1	71	CSNK1E	57
PHB2	359	ABCF1	131	RAB5C	93	BRAT1	71	NCAPD2	56
BZW2	358	ATP6V1A	127	PPA1	92	EHD2	71	TRABD	56
KPNB1	346	IDH3B	126	CPT1A	92	ATP5O	70	PRPF8	56
IPO9	331	CYFIP1	125	ATP2A2	91	EXOSC2	69	SLC7A5	56
FANCI	325	STOML2	125	TCEA1	91	HSPA4	69	CPPED1	56
RICTOR	319	CANX	124	TECR	91	KDELR1	69	ITPK1	55
EVI5	291	ARFGEF1	123	EHD4	91	PRKAR1A	68	ASNS	55
RAB11FIP5	285	RAB11FIP2	123	ARL1	89	RPL17	68	SPDL1	55
MSN	285	RPL22	122	S100A16	89	RDX	67	H2AFZ	55
ARFGEF2	275	VPS28	122	AP2M1	89	RPL9	67	SERPINB8	54
PPP2R1A	255	AP2A1	121	BOP1	89	PARVA	66	L2HGDH	54
MON2	246	VDAC1	119	ACSL3	88	LPCAT1	66	DHCR24	54
CNN2	235	MYO1E	119	CDC42	88	GCAT	66	FIBP	54
EIF5B	235	MAP2K3	118	GTF2I	87	ACSL4	66	GPAT4	54
PPIB	234	RTFDC1	117	PSMG1	87	PRPF31	65	ARHGAP17	54
WDR44	225	AP1B1	117	LRRC59	86	PRAF2	64	BCAP31	54
PRKDC	218	RAB34	117	ALDH3A2	85	ALDOA	64	CBX1	54
GBF1	217	EXOC2	116	ERLIN1	85	MTHFD2	64	SET	54
ACTN4	215	TRIO	115	EXOC7	84	HSD17B12	64	PSMC3	53
EZR	212	ERLIN2	113	LGALS1	84	AP2A2	64	TMX1	53
NPM1	209	EXOC4	113	TELO2	83	PAWR	64	ESYT2	53
KRT80	198	RPL7A	112	POLD1	82	EVI5L	63	SEC23IP	53
EIF2S1	196	RAB4B	112	ATR	82	FUS	63	FARSA	53
AP2B1	195	CYFIP2	111	RPL12	82	PCID2	63	TBRG4	52
XPO5	194	EFTUD2	111	TARBP1	81	CHM	62	TUBAL3	52
PCBP2	184	MLKL	110	IPO13	81	RPN2	62	SEPT7	51
PSME1	176	SSR4	110	AAAS	80	U2AF1	62	SUGT1	51
CCT2	175	PRDX6	109	ERC1	80	APOB	62	AP3D1	51
SNRNP200	173	STOM	109	UNC13D	80	BAX	62	NELFB	51
IPO8	172	S100A13	108	LDHA	80	EIF3I	61	CCDC47	51
SRP14	170	EIF5A	107	RFC2	79	SNX9	61	PES1	51
GSTP1	164	DHX16	107	SLC2A1	79	KIF5B	61	PARP1	51
UNC45A	161	HEATR1	107	RPL18	79	NCDN	61	TNFAIP2	51
PFKP	157	MTCH2	105	EPRS	78	XRCC6	60	GPX1	51
XPO6	157	MMS19	105	RPS27	78	CDKN2A	60	ADO	51
MLST8	156	TTK	103	HADHB	78	BSCL2	60	SDHA	50
IARS	156	EXOC5	103	C8orf82	77	VDAC2	60	NELFA	50
MYOF	155	NSUN2	102	RAB7A	77	DTD1	60	SCCPDH	50
SEC61A1	155	EIF3F	102	CEP170	77	EIF3E	60	THOC3	50
NAP1L1	154	DDX46	102	COG5	77	COMMD9	60	AGPAT2	50
PTRF	154	GALNT2	102	U2AF2	77	PPP2R2D	60	SESTD1	50
RPS6	154	COASY	101	FEN1	76	AGPS	59	EFHD2	50
HADHA	153	PLAA	101	UCKL1	75	SLC7A11	59		
ACTN1	152	CSNK2A1	101	TBC1D15	74	CC2D1A	59		
ACYP2	147	CCT6A	100	RPL31	74	RUVBL2	59		

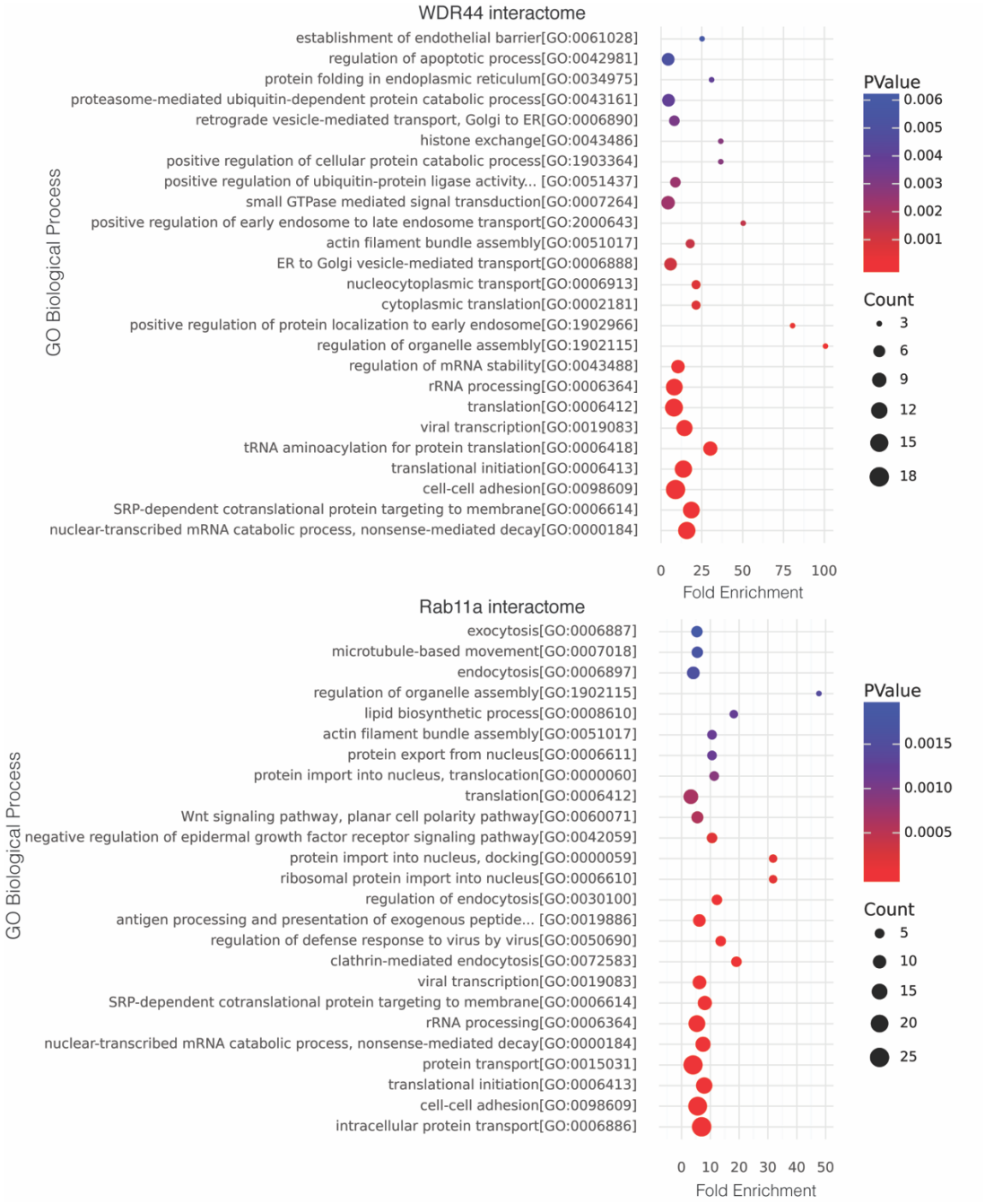

Figure 3. Biological process Gene Ontology (GO) enrichment analysis of WDR44 and Rab11a interactome. Analysis of Biological processes GO terms enriched in WDR44 and Rab11a interactomes. The complete human genome was used as background in DAVID database. The bubble charts show the 25 more significant GO terms with lower p-values. X-axis indicates fold enrichment among the complete genome. Color bubble represent p-value associated to each GO term. Bubble size indicates the number of proteins related to each biological process. The bubble charts were made using the python library plotnine (based on ggplot2).

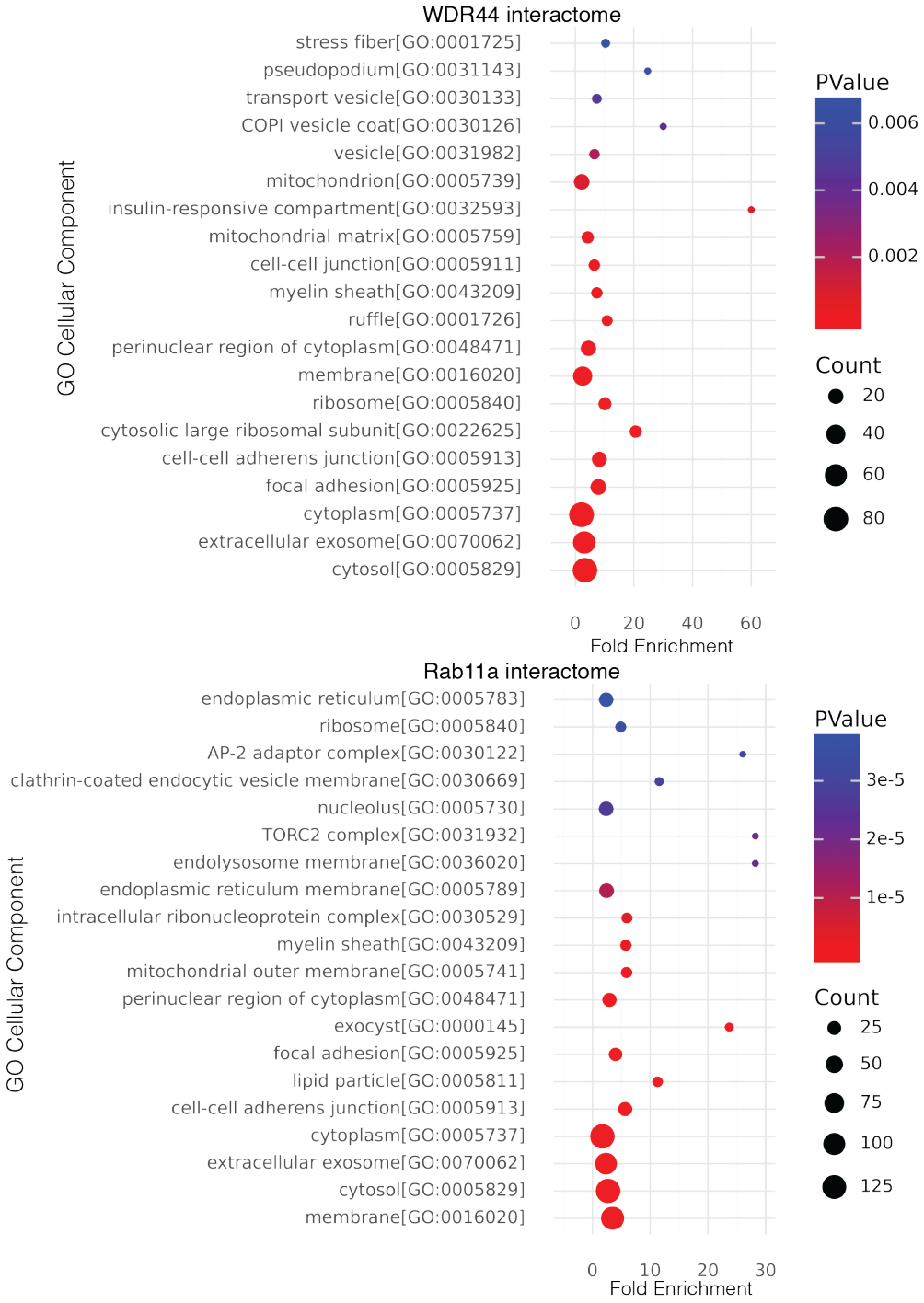

Figure 4. Cellular component GO enrichment analysis of WDR44 and Rab11a interactome. Analysis of Cellular Component GO terms enriched in WDR44 and Rab11a interactomes. The complete human genome was used as background in DAVID database. The bubble charts show the 20 more significant GO terms with lower p-values. X-axis indicates fold enrichment among the complete genome. Color bubble represent p-value associated to each GO term. Bubble size indicates the number of proteins related to each cellular component. The bubble charts were generated as in Figure 2.

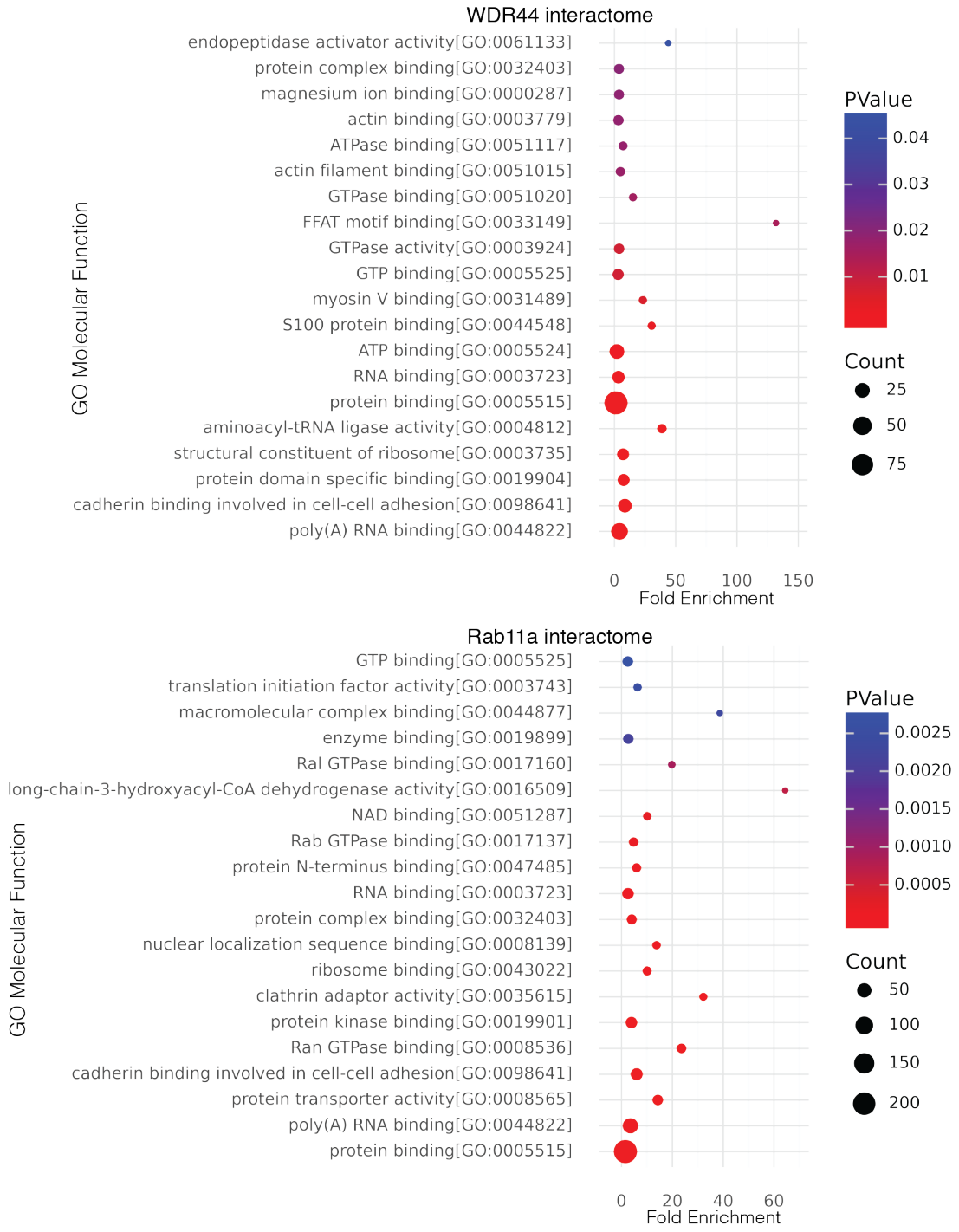

Figure 5. Molecular Function GO enrichment analysis of WDR44 and Rab11a interactome. Analysis of Molecular Function GO terms enriched in WDR44 and Rab11a interactomes. The complete human genome was used as background in DAVID database. The bubble charts show the 20 more significant GO terms with lower p-values. X-axis indicates fold enrichment among the complete genome. Color bubble represent p-value associated to each GO term. Bubble size indicates the number of proteins related to each cellular component. The bubble charts were generated as in Figure 2.

Figure 6. Analysis of physical interactions between the proteins of WDR44 interactome dataset. Protein-protein interacting (PPI) network among the WDR44 interactome dataset, generated by Cytoscape using PPI analysis of STRING database. The PPI network considers high-throughput lab experiments, textmining and previous knowledge in curated databases. Nodes represent each protein of WDR44 interactome. Color node indicates the interaction score with WDR44, according to the interactome Mass Spec information (Table 1). The edges represent physical interaction between the proteins and the thickness indicates the edge confidence according to the legend. Note that the figure includes isolated nodes without described physical interaction with any other protein of WDR44 interactome. Grey boxes enclose cluster of proteins functionally related. The biological processes GO terms associated to each cluster is indicated within the grey box and p-value of enrichment analysis is included in brackets. Stars indicate proteins that also were found in Rab11a interactome dataset (Table 2).

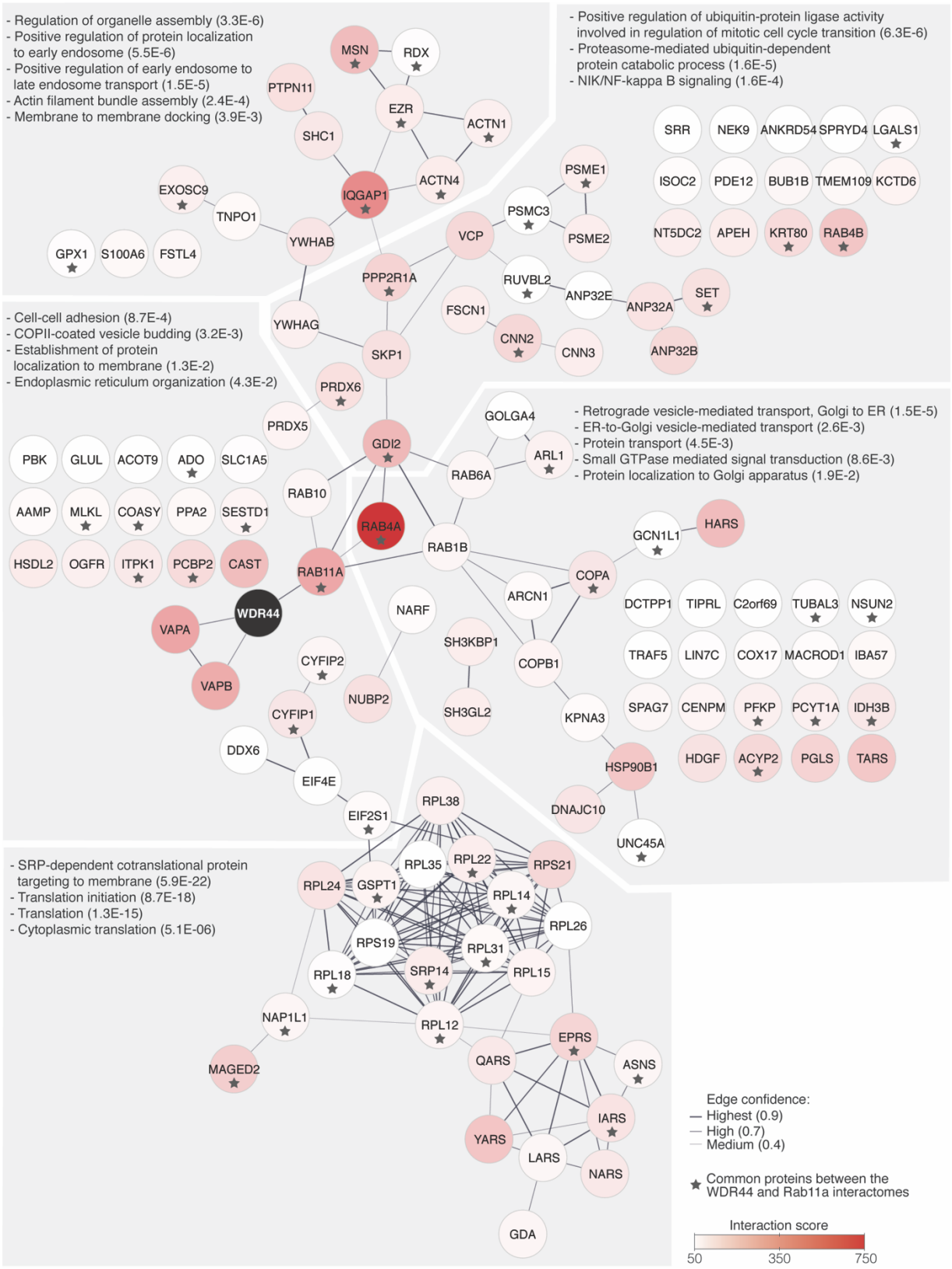
- Regulation of organelle assembly (3.3E-6)
- Positive regulation of protein localization to early endosome (5.5E-6)
- Positive regulation of early endosome to late endosome transport (1.5E-5)
- Actin filament bundle assembly (2.4E-4)
- Membrane to membrane docking (3.9E-3)
- Positive regulation of ubiquitin-protein ligase activity involved in regulation of mitotic cell cycle transition (6.3E-6)
- Proteasome-mediated ubiquitin-dependent protein catabolic process (1.6E-5)
- NIK/NF-kappa B signaling (1.6E-4)
- Cell-cell adhesion (8.7E-4)
- COPII-coated vesicle budding (3.2E-3)
- Establishment of protein localization to membrane (1.3E-2)
- Endoplasmic reticulum organization (4.3E-2)
- Retrograde vesicle-mediated transport, Golgi to ER (1.5E-5)
- ER-to-Golgi vesicle-mediated transport (2.6E-3)
- Protein transport (4.5E-3)
- Small GTPase mediated signal transduction (8.6E-3)
- Protein localization to Golgi apparatus (1.9E-2)
- SRP-dependent cotranslational protein targeting to membrane (5.9E-22)
- Translation initiation (8.7E-18)
- Translation (1.3E-15)
- Cytoplasmic translation (5.1E-06)
MSN
RDX
PTPN11
EZR
ACTN1
SHC1
ACTN4
IQGAP1
EXOSC9
TNPO1
YWHAB
GPX1
S100A6
FSTL4
PSME1
PSMC3
PSME2
VCP
SRR
NEK9
ANKRD54
SPRYD4
LGALS1
ISOC2
PDE12
BUB1B
TMEM109
KCTD6
NT5DC2
APEH
KRT80
RAB4B
PPP2R1A
RUVBL2
ANP32E
ANP32A
SET
FSCN1
CNN2
CNN3
ANP32B
YWHAG
SKP1
PRDX6
PRDX5
GDI2
GOLGA4
ARL1
RAB6A
PBK
GLUL
ACOT9
ADO
SLC1A5
AAMP
MLKL
COASY
PPA2
SESTD1
HSDL2
OGFR
ITPK1
PCBP2
CAST
RAB10
RAB4A
RAB1B
RAB11A
GCN1L1
HARS
COPA
ARCN1
DCTPP1
TIPRL
C2orf69
TUBAL3
NSUN2
TRAF5
LIN7C
COX17
MACROD1
IBA57
SPAG7
CENPM
PFKP
PCYT1A
IDH3B
HDGF
ACYP2
PGLS
TARS
WDR44
VAPA
VAPB
NARF
SH3KBP1
SH3GL2
COPB1
CYFIP2
CYFIP1
NUBP2
KPNA3
DDX6
EIF4E
HSP90B1
DNAJC10
UNC45A
EIF2S1
RPL38
RPL35
RPL22
RPS21
RPL24
GSPT1
RPL14
RPL26
RPS19
RPL31
RPL18
SRP14
RPL15
NAP1L1
RPL12
EPRS
QARS
ASNS
MAGED2
IARS
YARS
LARS
NARS
GDA
Edge confidence:
Highest (0.9)
High (0.7)
Medium (0.4)
Common proteins between the WDR44 and Rab11a interactomes
Interaction score
50
350
750

3.2.2 Validation of WDR44 interactions with Rabs including Rab11.

In order to validate WDR44 and RabGTPases interactions we transfected HeLa cells with the relevant GFP-tagged Rabs and evaluated the presence of WDR44 in GFP-trap precipitation of each Rab. Immunoblot detection of WDR44 required previous characterization of WDR44 antibody as described below.

3.2.2.1 WDR44 protein forms detected by immunoblot suggest protein cleavage at the amino terminus.

Previous to validate the interactome we characterized the WDR44 antibody. We analyzed the endogenous WDR44 in HeLa cell lysates by immunoblot using a polyclonal antibody that recognizes a region between residues 175-225 of human WDR44 (Figure 7A). As previously described (Baron, Pedrioli et al. 2014), we detected three bands at 143KDa, 124KDa and 108KDa (Figure 7B, non-transfected lane). The lower migration in SDS page of WDR44 compared to the theoretical (101KDa) is a common characteristic of proteins that contains proline rich domains, probably related with a lower incorporation of SDS (Ziemer, Mason et al. 1982, Castle, Stahl et al. 1992).

Immunoblot analysis of exogenously expressed human WDR44 tagged with EGFP at the carboxyl terminus (HsWDR44-EGFP), revealed seven bands recognized by anti-EGFP antibody (Figure 7D; lane HsWDR44-EGFP). Among them, bands 172 KDa, 158 KDa and 140 KDa corresponded to endogenous WDR44 (143KDa, 124KDa and 108KDa) plus EGFP. Considering that HsWDR44-EGFP cDNA lacks splicing sites, our results suggest that WDR44 can be proteolytically cleaved before residues 175-225.

Using an anti-EGFP we also detected a band of 101 KDa in HsWDR44-EGFP, which does not correlate with the mass weight of any band of endogenous WDR44 plus EGFP (Figure

7D). This suggests that WDR44 may be proteolyzed within or downstream the residues 175-225 giving a product that is not detected by the anti-WDR44 antibody.

We obtained similar results when expressing bovine WDR44 tagged to mCherry at the carboxyl terminus (BtWDR44-mCherry), which shares a 93.8% identity and 96.2% similarity with human WDR44 (Figure 7 B and C).

Finally, we expressed the bovine WDR44 tagged with HA within the residues 10-24. Immunoblot analysis using anti-HA antibody revealed only one band of 150 KDa, suggesting that a proportion of Bt-HA-WDR44 loss HA tag, leading undetectable smaller forms of BtWDR44. Thus, these results reinforce the idea of proteolytic cleavage of WDR44 within the amino terminus region.

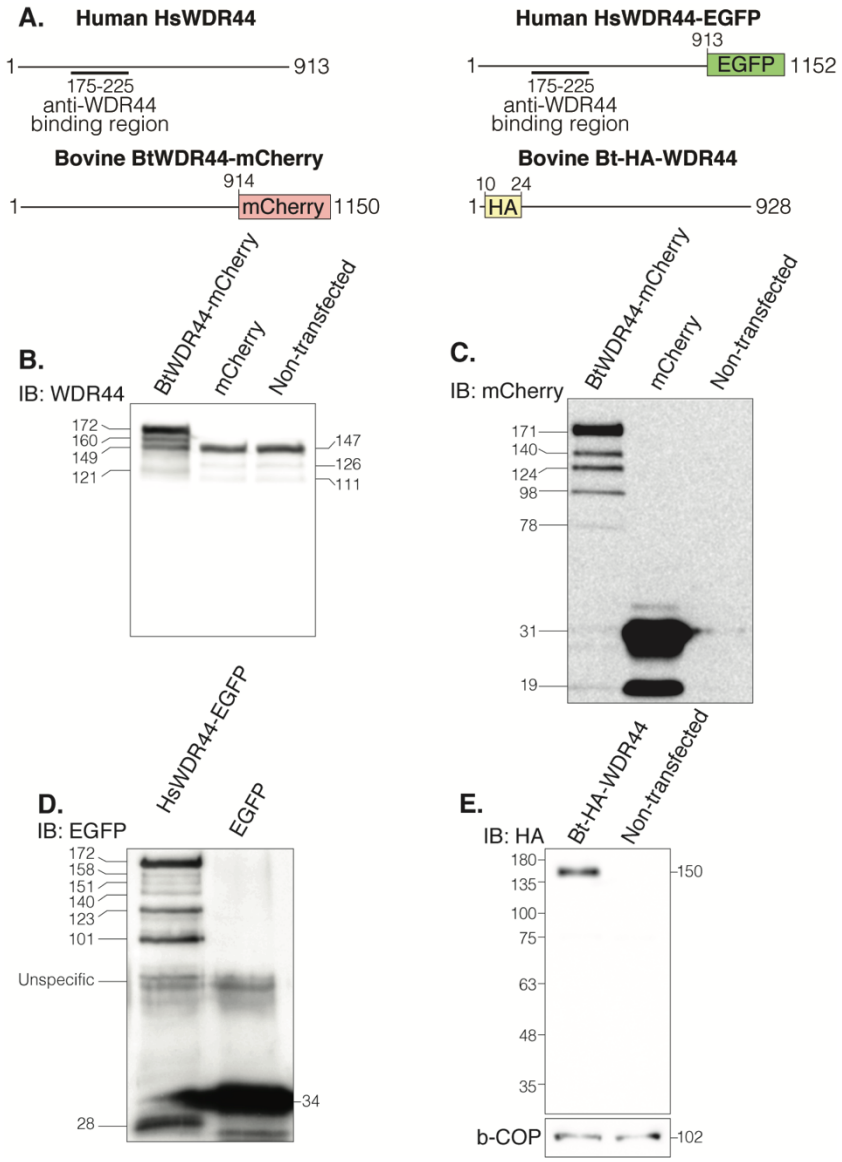

Figure 7. Characterization of WDR44 antibody reveals several WDR44 isoforms and suggests protein cleavage at the amino terminus. A. Schematic representation of different variation of WDR44 analyzed by immunoblot (IB). The scheme shows the anti-WDR44 binding region in endogenous human WDR44 (HsWDR44) and HsWDR44 tagged to EGFP (HsWDR44-EGFP). Bovine WDR44 (BtWDR44) tagged with m-Cherry or HA are also included. Numbers represent amino acid positions within each protein sequence. **B, C.** IB analysis of endogenous HsWDR44 and transfected BtWDR44-mCherry or empty mCherry plasmid in HeLa cells, using WDR44 antibody (B) or anti-mCherry (C). **D.** IB analysis of transfected HsWDR44-EGFP or empty EGFP vector using anti-EGFP antibody. **E.** IB detection of Bt-HA-WDR44 transfection using anti-HA antibody. For the immunoblots, the molecular size of each band was estimated by a relative motility standard curve (n=1).

3.2.2.2 Rab1a/b, Rab4a/b and Rab6A precipitate different WDR44 isoforms.

As expected, Rab11a-EGFP precipitated the three forms of WDR44. Rab11a also immunoprecipitated Rab coupling protein (RCP), which is a well-known Rab11a effector (Jin and Goldenring 2006) and therefore served as internal positive control (Figure 8A). Important to note, the amount of the WDR44 isoforms coprecipitated with Rab11a was proportional to their amount in the lysate, suggesting a similar interaction of Rab11 with each isoform. This contrasted with the interaction of Rab4a and Rab4b with WDR44. Rab4a-GFP and Rab4b-GFP also co-immunoprecipitated WDR44 but preferentially its smaller isoform (Figure 8A). The functionally diverse interactome of WDR44 and its different isoforms highly suggest potential unexplored functions of WDR44.

Considering the importance of Rab1a, Rab1b and Rab6A in protein trafficking, we also proceeded to evaluate their interaction with WDR44. All three Rab GTPases coprecipitated the full-length WDR44 isoform, but in a lesser extent than Rab11a-GFP (Figure 8B). These results are congruent with the score of interactions shown in the interactome for each of these Rabs. Rab11a showed an score of 293 while Rab1a, Rab1b and Rab6A have an score of 74 (Figure 6 and Table I). Altogether these results suggest that Rab1a/b, Rab4a/b and Rab6A are new interactors of WDR44, with variations depending on the WDR44 isoform.

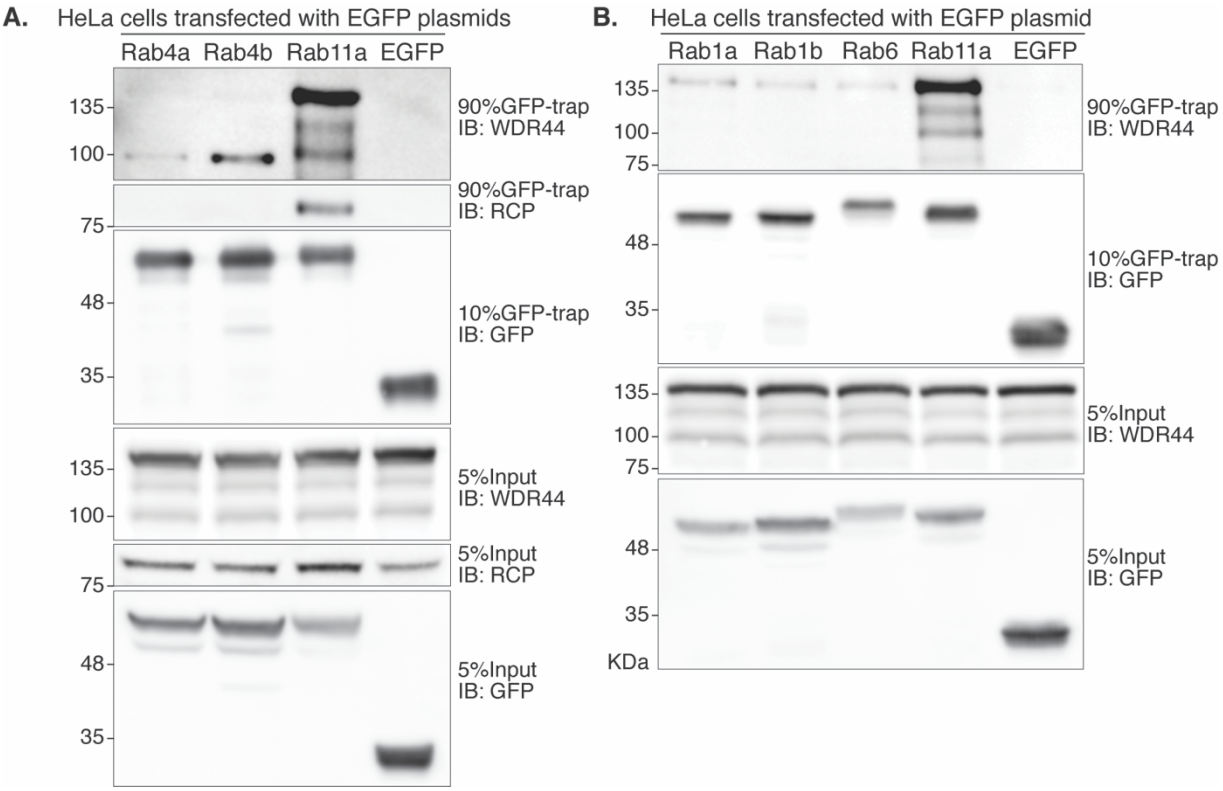

Figure 8. Validation of the interaction of WDR44 with Rab proteins suggested by the WDR44 interactome. HeLa cells were transfected with Rab4a-EGFP, Rab4b-EGFP (**A**) and Rab1a-EGFP, Rab1b-EGFP and Rab6a-EGFP (**B**). Rab11a-EGFP was used as positive control of WDR44 interacting protein and EGFP empty vector was used as negative control. After 16h of expression, EGFP-tagged Rab proteins were precipitated with GFP-trap agarose beads and WDR44 was analyzed by immunoblot (n=2).

Rab GTPases interact with their effectors mainly in a GTP-dependent manner. Therefore, to test whether the coprecipitations of WDR44 with Rabs reflect a functional interaction we performed the GFP-trap assay in presence of GTPγS, a non-hydrolysable analog of GTP. We observed that GTPγS increases Rab11a-GFP and WDR44 co-immunoprecipitation (Figure 9A), as previously described for the interaction between WDR44 and rab11a (Zeng, Ren et al. 1999). In contrast, GTPγS decreased Rab1b-GFP and WDR44 interaction, suggesting that it takes place with the GDP-bound form of Rab1b.

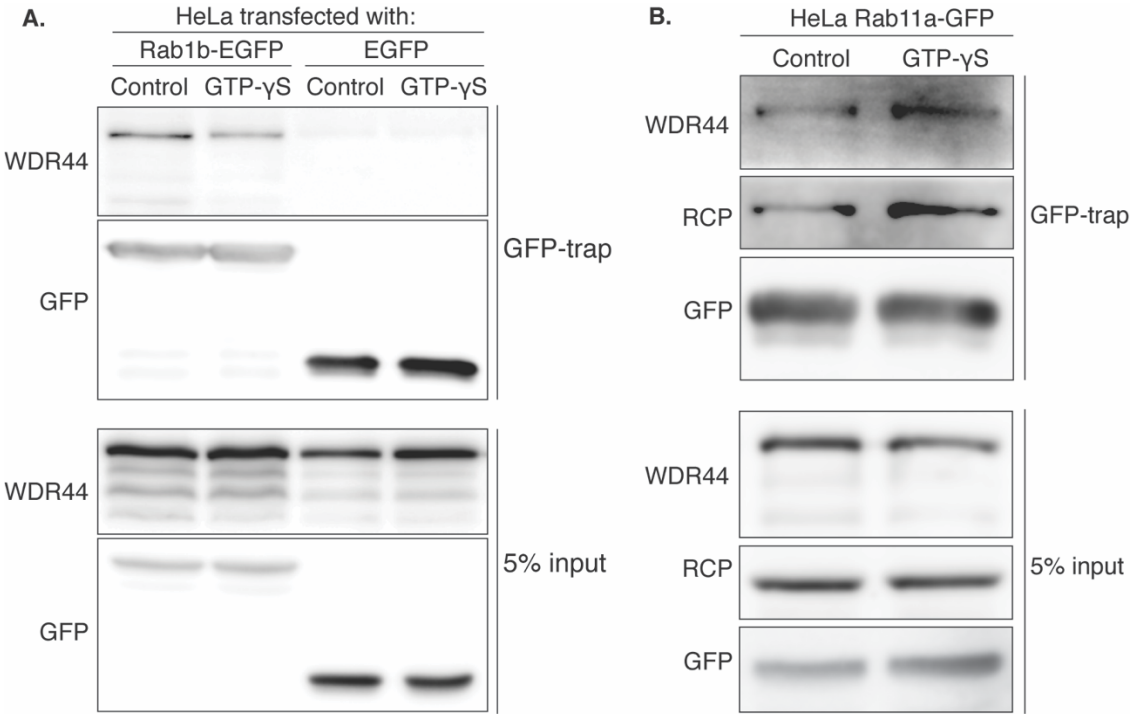

Figure 9. GTPγS reduces the interaction of WDR44 and Rab1b-EGFP interaction. Hela cells were transfected with Rab1b-EGFP or EGFP empty vector (**A**) and Rab11a-EGFP (**B**). After 16h expression, fresh cell lysates were incubated with or without GTPγS during 15min at room temperature. Then, EGFP-tagged proteins were precipitated with GFP-trap and the presence of WDR44 was analyzed by immunoblot. A, n=2; B, n=1.

3.2.3 WDR44 subcellular distribution and colocalization with Rabs.

Additionally, we evaluated the distribution of endogenous WDR44 relative to the RabGTPases. Considering that specific mouse anti-RabGTPases antibodies are scarce, we decided to exogenously express the RabGTPases fused to EGFP. HeLa cells were transfected with different Rab-GFP plasmids and we waited for protein expression, then IFI was carried out and cells with lower expression of Rabs were imaged. As we expected, endogenous WDR44 colocalized with Rab11a-GFP in peripheral endosome structures and also in the perinuclear region (Figure 10, Table 3). In addition, Rab4a-EGFP and Rab4b-EGFP also showed some partial colocalization with WDR44 (Figure 11, Table 3). However, we did not see colocalization between WDR44 and Rab1a-EGFP, Rab1b-EGFP or Rab6A-EGFP (Figure 12 and 13, Table 3). Rab overexpression seems do not affect the WDR44 distribution (Figure 14)

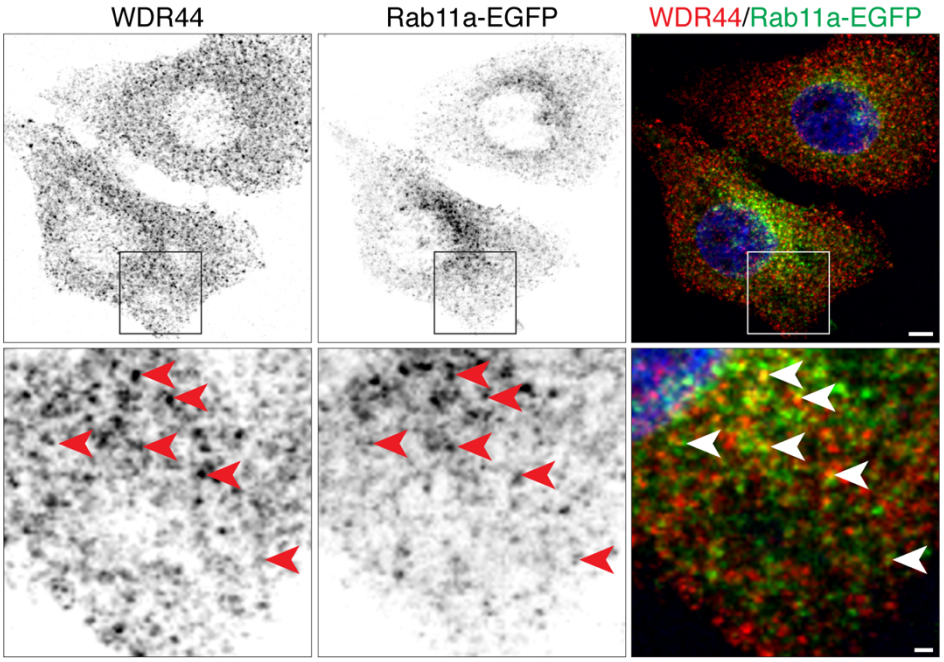

Figure 10. Analysis of distribution of endogenous WDR44 relative to Rab11a-EGFP. HeLa cells were transfected with Rab11a-EGFP plasmid and after 16h of expression the IFI with anti-WDR44(red) and Hoechst stain (blue) was carried out. Cells were imaged by confocal microscopy; the figure shows a single plane from a z-stack. Lower panels show magnification of the boxed areas in upper panels. Arrowheads indicate WDR44 and Rab11a-EGFP colocalization. Scale bars: upper panel, 5 μm; magnification, 1μm.

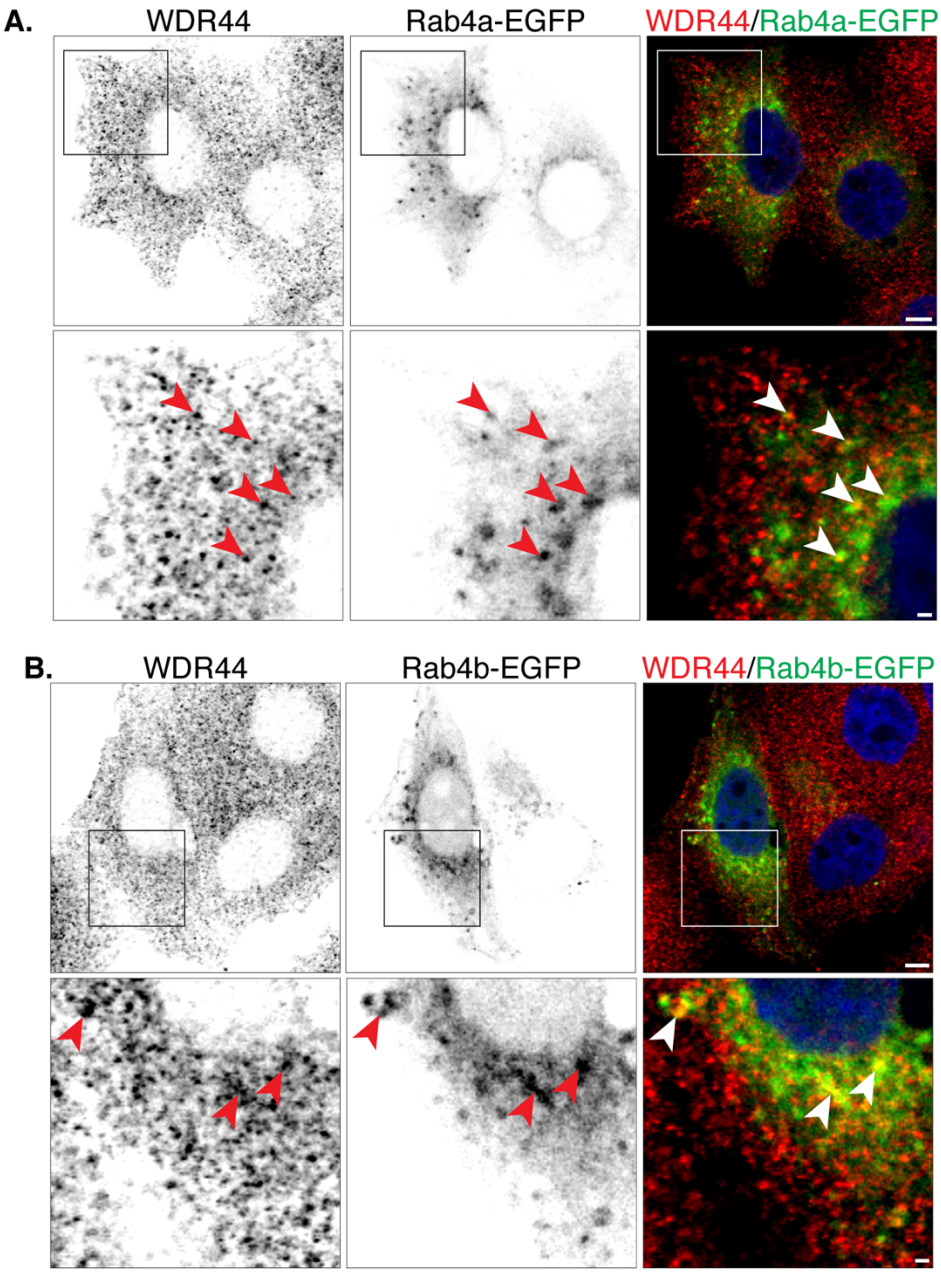

Figure 11. Distribution of endogenous WDR44 relative to Rab4a-EGFP and Rab4b-EGFP. HeLa cells were transfected with Rab4a-EGFP or Rab4b-EGFP plasmids and after 16h of cDNA expression, the protein distribution was evaluated by IFI with anti-WDR44(red) and Hoechst stain (blue). Cells were imaged by confocal microscopy; the figure shows a single plane from a z-stack. Lower panels show magnification of the boxed areas in upper panels. Arrowheads indicate WDR44 and Rab4a/b-EGFP colocalization. Scale bars: upper panel, 5 μm; magnification, 1μm.

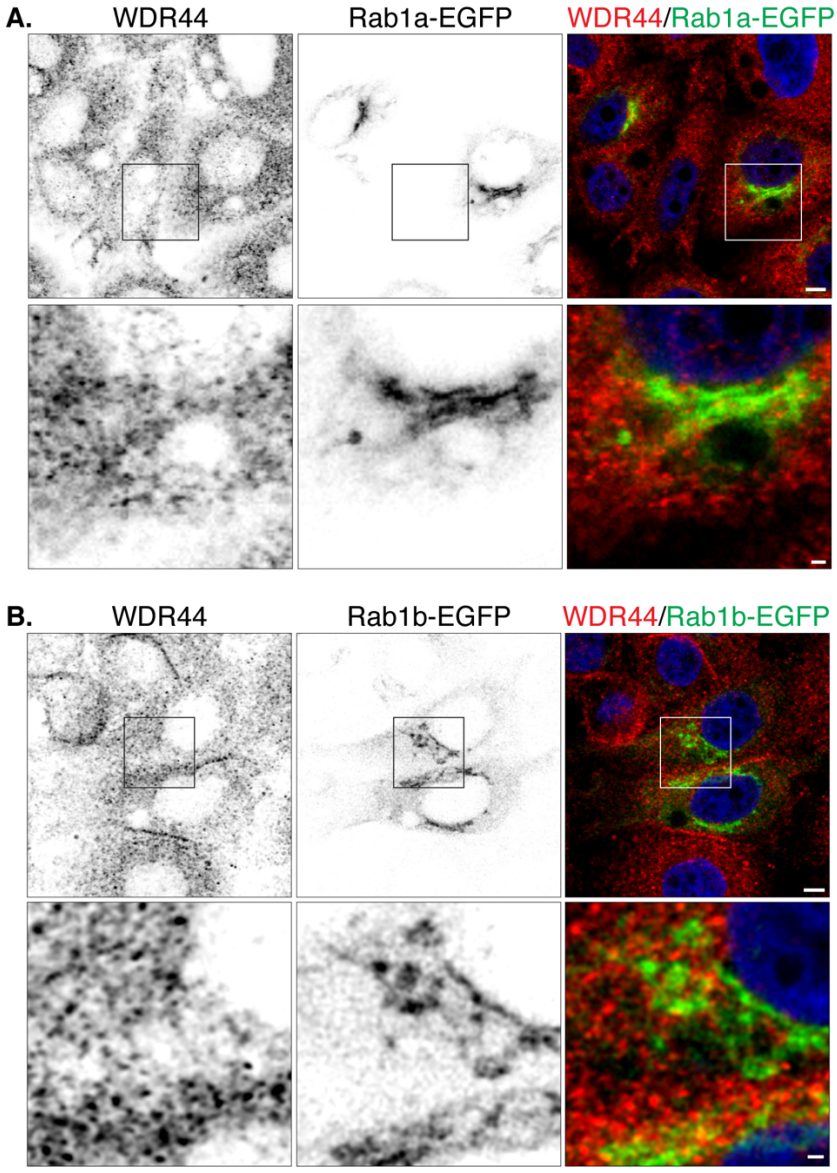

Figure 12. Localization of endogenous WDR44 relative to Rab1a-EGFP and Rab1b-EGFP. HeLa cells were transfected with Rab1a-EGFP or Rab1b-EGFP plasmids and after 16h of cDNA expression, the protein distribution was evaluated by IFI with anti-WDR44(red) and Hoechst stain(blue). Cells were imaged by confocal microscopy; the figure shows a single plane from a z-stack. Lower panels show magnification of the boxed areas in upper panels. Scale bars: upper panel, 5 μm; magnification, 1μm.

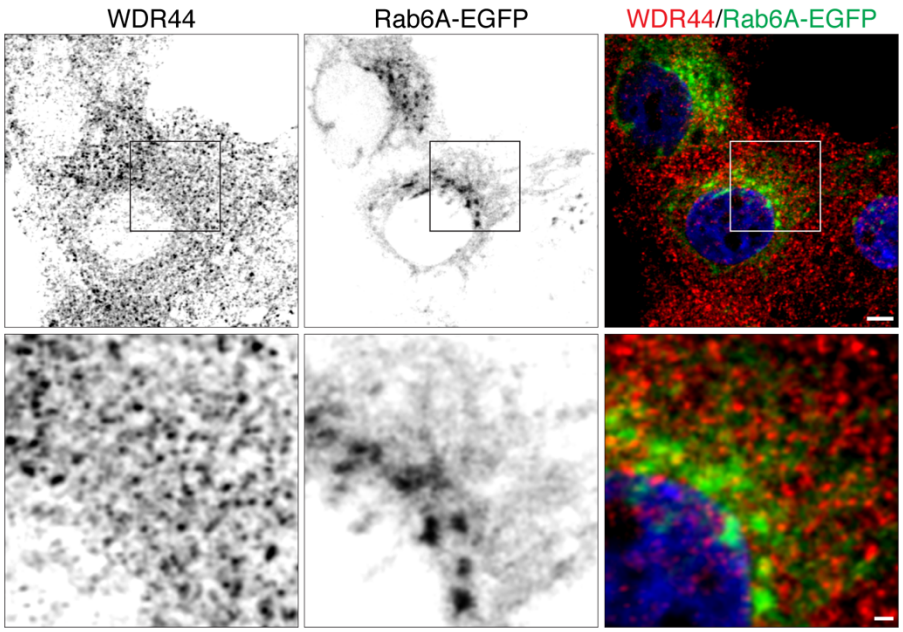

Figure 13. Localization of endogenous WDR44 relative to Rab6A-EGFP. HeLa cells were transfected with Rab6A-EGFP plasmid and after 16h of expression the IFI with anti-WDR44 (red) and Hoechst stain (blue) was carried out. Cells were imaged by confocal microscopy; the figure shows a single plane from a z-stack. Lower panels show magnification of the boxed areas in upper panels. Scale bars: upper panel, 5 μm; magnification, 1μm.

Table 3. Colocalization of endogenous WDR44 with transfected Rabs. Endogenous WDR44 was colocalized with transfected Rabs tagged to EGFP (Rab-EGFP, figures 10-13). Table shows Mander's and Pearson's coefficients (mean ± SE, n = 20-30 cells).

Rab-EGFP	Mander's coefficient (% ± SE)		Pearson's coefficient ± SE
	WDR44 / Rab	Rab / WDR44	
Rab11a	15.06 ± 0.92	15.50 ± 0.74	0.67 ± 0.01
Rab4a	13.75 ± 1.28	17.24 ± 1.37	0.72 ± 0.01
Rab4b	13.30 ± 1.36	16.25 ± 1.56	0.68 ± 0.02
Rab1a	3.51 ± 0.36	12.17 ± 1.23	0.61 ± 0.01
Rab1b	4.52 ± 0.65	17.08 ± 1.92	0.61 ± 0.03
Rab6A	4.57 ± 0.67	9.7 ± 1.09	0.57 ± 0.01

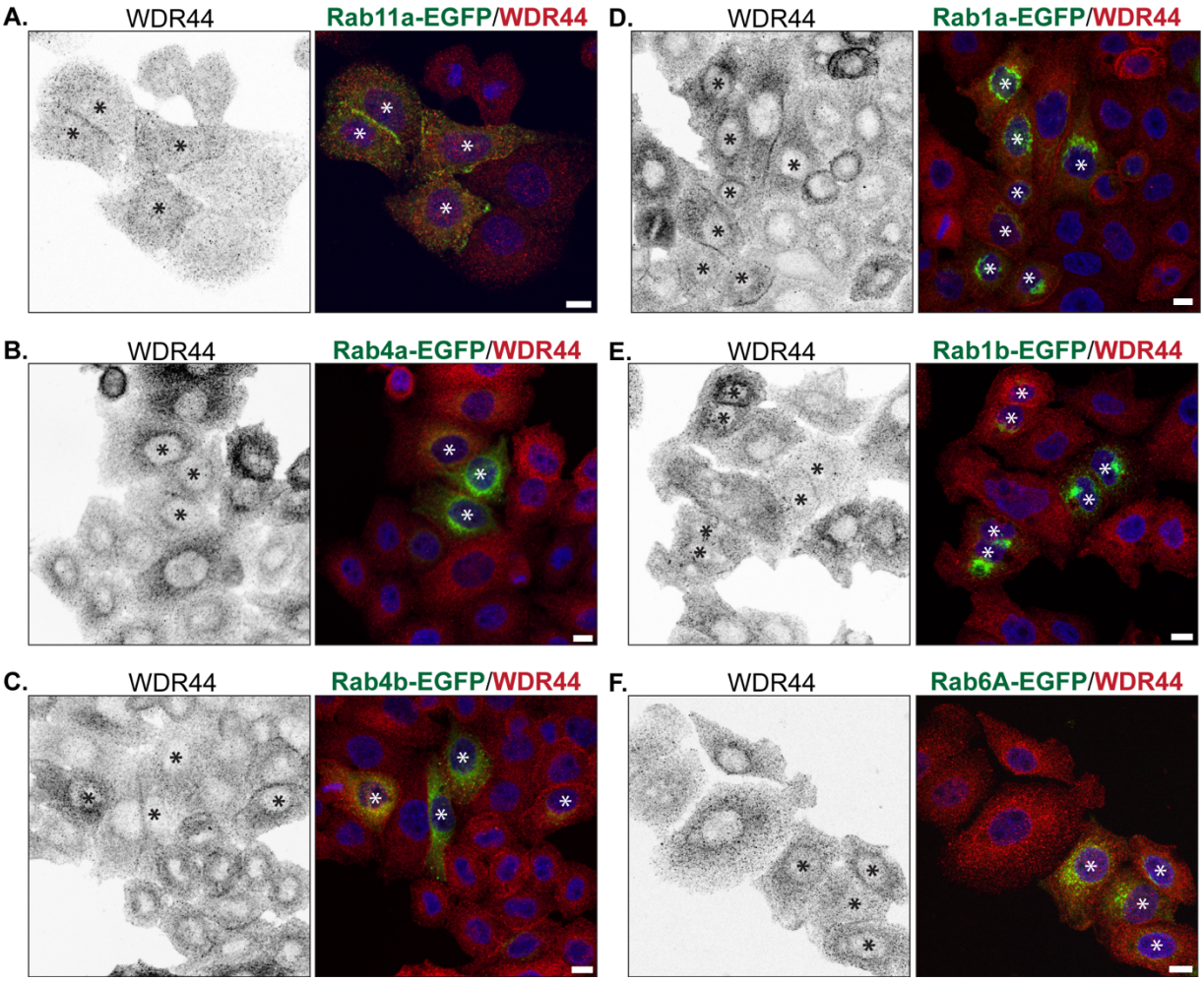

Figure 14. Effect of Rab overexpression on WDR44 distribution. Representative images of HeLa cells transfected with Rabs tagged to EGFP and WDR44 distribution was evaluated by IFI. Asterisks indicate transfected cells. Scale bars represent 10 μm.

To get further information on WDR44 and its possible function we proceeded to analyze its distribution respect with cellular compartments of the vesicular trafficking pathway. First, we evaluated the distribution of WDR44 with Rab11-related compartments by immunofluorescence. Rab11 has been related with recycling endosomes, which contain the constitutively recycling Transferrin Receptor (TfR) (Ullrich, Reinsch et al. 1996). AP1 clathrin adaptor can be used to label the TGN, although it has been also found in recycling endosomes (Pagano, Crottet et al. 2004). In addition, Rab11 has been involved in the trafficking step between EEA1 positive early endosomes and perinuclear recycling endosomes (Mu, Callaghan et al. 1995, Schafer, McRae et al. 2016). We observed that endogenous WDR44 partially co-localized with punctate intracellular structures labeled with TfR and γ-Adaptin (Figure 15, Table 4). Additionally, WDR44 seems to surround EEA1 positive endosomal structures (Figure 16).

The WDR44 interactome suggested that WDR44 interacts with proteins related with protein trafficking between the ER and the Golgi. Thus, we also evaluated the WDR44 localization respect to Golgi and ER. GM130 is a cytoplasmic protein that preferentially binds to cis-Golgi membranes (Nakamura, Rabouille et al. 1995), while the cytosolic protein p230 associates with the trans-Golgi region and post-Golgi vesicles (Gleeson, Anderson et al. 1996). Endogenous WDR44 did not co-localized with GM130 or p230 suggesting that it is not associated with Golgi membranes (Figure 17, Table 4). BiP is an abundant HSP70 molecular chaperone localized within the lumen of the ER (Gething 1999). The distribution of endogenous WDR44 was similar to the localization pattern of BiP and both proteins show co-localization in perinuclear and peripheral regions (Figure 18, Table 4). This suggests that WDR44 associates to ER membranes which has been previously described by the WDR44 and Calnexin colocalization (Lucken-Ardjomande Hasler, Vallis et al. 2020).

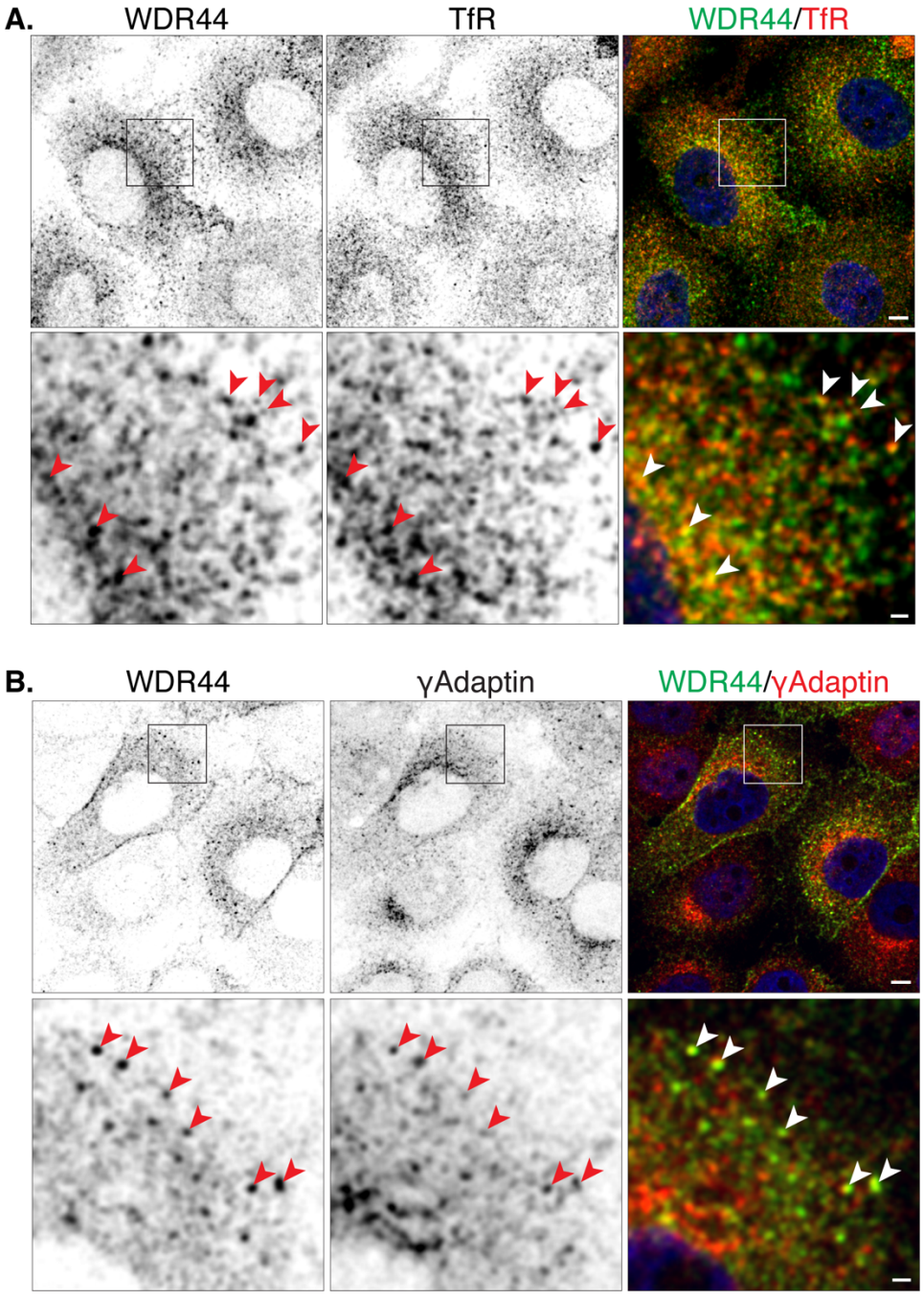

Figure 15. Subcellular distribution of endogenous WDR44 relative to recycling endosomes labeled with Transferrin receptor (TfR) or γ-Addaptin. WDR44 distribution was analyzed by IFI using TfR **(A)** or γ-Addaptin **(B)** as recycling endosomes markers. Cells were imaged by confocal microscopy; the figure shows a single plane from a z-stack. Arrowheads indicate colocalization with WDR44 in endosomal structures. Blue represent Hoechst stain. Lower panels show magnification of the boxed areas in upper panels. Scale bars: upper panel, 5 μm; magnification, 1μm.

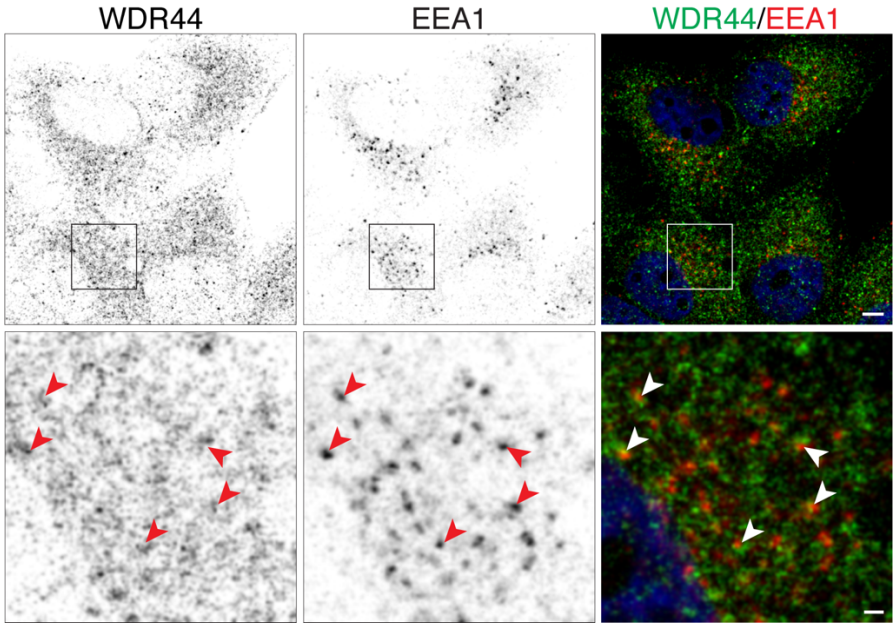

Figure 16. Subcellular distribution of endogenous WDR44 relative to early endosomes labeled with EEA1. WDR44 distribution was analyzed by IFI using EEA1 as early endosomes markers. Cells were imaged by confocal microscopy; the figure shows a single plane from a z-stack. Arrowheads indicate WDR44 surrounding EEA1 positive endosome structures. Blue represent Hoechst stain. Lower panels show magnification of the boxed areas in upper panels. Scale bars: upper panel, 5 μm; magnification, 1μm.

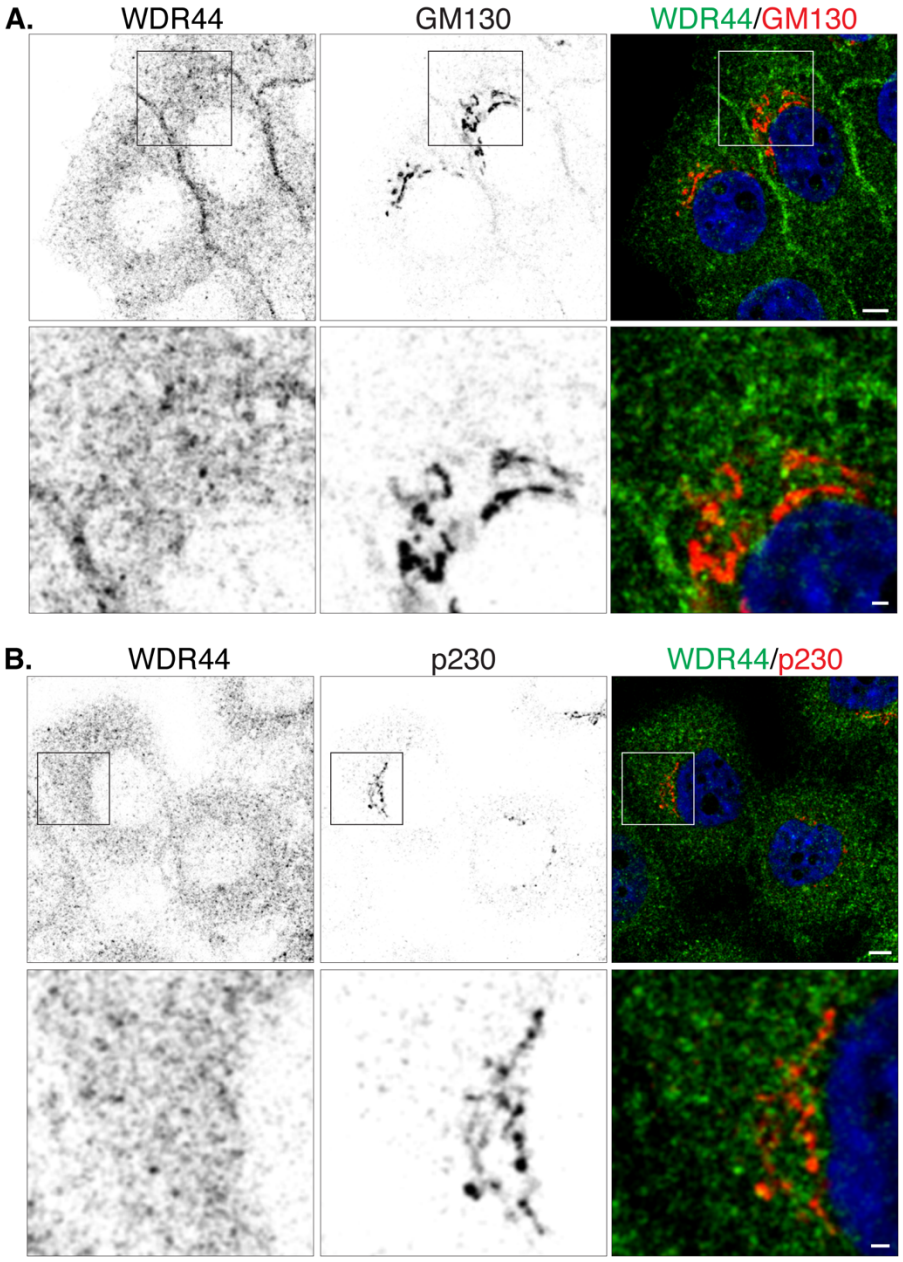

Figure 17. Subcellular distribution of endogenous WDR44 relative to Golgi apparatus. WDR44 distribution was analyzed by IFI using GM130 **(A)** and p230 **(B)** as Golgi markers. Cells were imaged by confocal microscopy; the figure shows a single plane from a z-stack. Blue represent Hoechst stain. Lower panels show magnification of the boxed areas in upper panels. Scale bars: upper panel, 5 μm; magnification, 1μm.

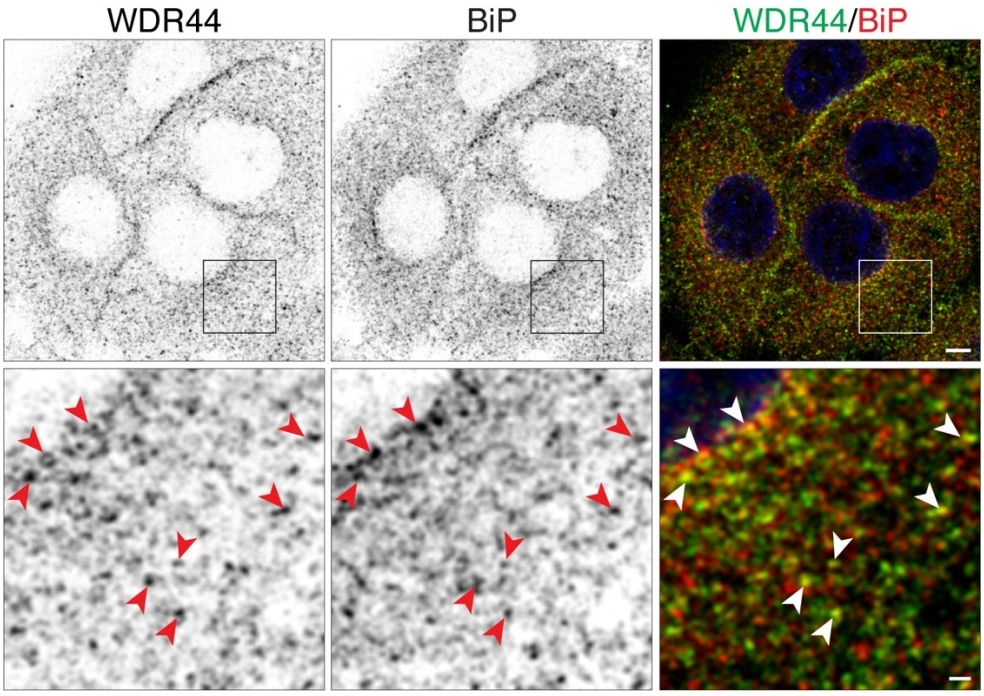

Figure 18. Subcellular distribution of endogenous WDR44 relative to the Endoplasmic Reticulum. WDR44 distribution was analyzed by IFI using BiP as an ER marker. Cells were imaged by confocal microscopy; the figure shows a single plane from a z-stack. Arrowheads indicate WDR44 and BiP colocalization. Blue represent Hoechst stain. Lower panels show magnification of the boxed areas in upper panels. Scale bars: upper panel, 5 μm; magnification, 1μm.

Table 4. Colocalization of endogenous WDR44 with endogenous protein markers. Endogenous WDR44 was colocalized with several protein markers (Figures 14-17). Table shows Mander's and Pearson's coefficients (mean ± SE, n = 20-30 cells).

Marker (A)	Mander's coefficient (% ± SE)		Pearson's coefficient ± SE
	WDR44 / A	A / WDR44	
TfR	18.05 ± 1.18	14.63 ± 0.95	0.65 ± 0.02
γ-adaptin	13.79 ± 0.96	15.99 ± 0.79	0.65 ± 0.01
BiP	18.54 ± 1.02	14.10 ± 0.84	0.65 ± 0.01
GM130	2.66 ± 0.21	14.13 ± 0.87	0.44 ± 0.02

Finally, we also analyzed the distribution of WDR44 respect to actin and microtubule cytoskeleton. Phalloidin is a toxin that binds specifically to F-actin and when is labeled to fluorescent dye is a useful tool for studies of actin cytoskeleton distribution (Wieland 1976). WDR44 endosomal structures seem to decorate Phalloidin-Alexa555 filamentous close to the cell cortex (Figure 19A). Consistently, Jaime Venegas, a PhD student from our laboratory, observed colocalization between WDR44 endosomes and Actinin-4 (data not shown), an F-actin cross-linking protein that also was strongly suggested as a WDR44 and Rab11a interactor in the interactome analysis (Table 1 and Table 2). Additionally, WDR44 endosomes also colocalized with tubulin filaments, both at perinuclear and peripheral regions (Figure 19B).

Altogether these results show that WDR44 is associated to recycling endosomes and it co-precipitates and colocalizes with Rab11a, Rab4a and Rab4b. Additionally, our results support that WDR44 is also associated to ER membranes and reveals close localization to actin and microtubule cytoskeleton.

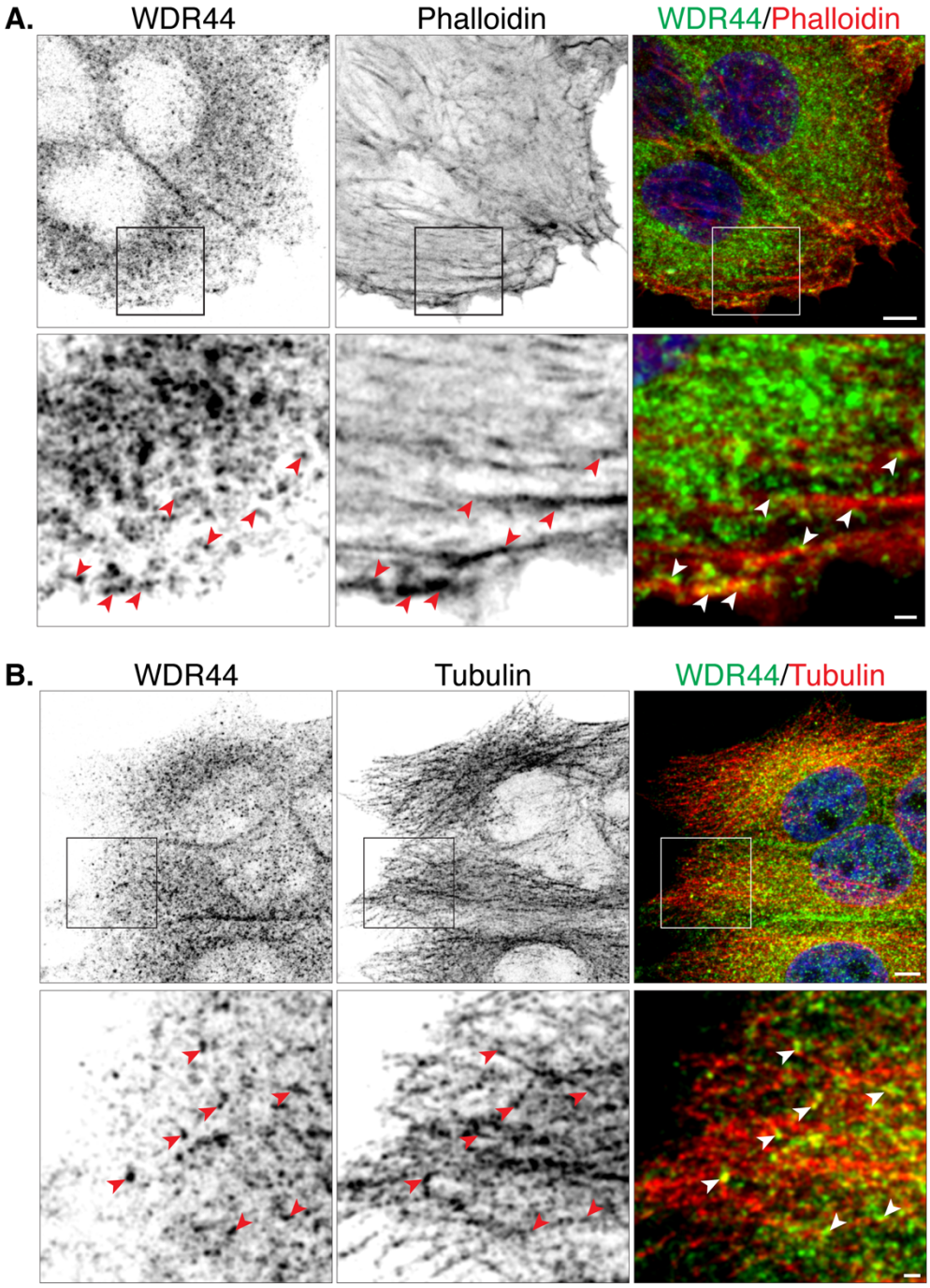

Figure 19. Subcellular distribution of endogenous WDR44 relative to actin and microtube cytoskeleton. WDR44 distribution was analyzed by IFI using Phalloidin-Alexa555 as F-actin stain **(A)** and tubulin as microtubule protein marker **(B)**. Cells were imaged by confocal microscopy; the figure shows a maximum intensity Z-projection in order to visualize filamentous structures. Arrowheads indicate colocalization with WDR44. Blue represent Hoechst stain. Lower panels show magnification of the boxed areas in upper panels. Scale bars: upper panel, 5 μm; magnification, 1μm.

3.3 Functional studies of WDR44 related to recycling endosome system.

3.3.1 WDR44 and Rab11a knock-down system.

To study the function of WDR44 in protein trafficking we generated a model of loss of function in HeLa cells transduced with shRNA against WDR44. Since Rab11a is the main interactor of WDR44, we also generated a similar model of Rab11a depletion. Both models allowed to us to compare the effects of WDR44 and Rab11a silencing in protein transport processes, using as control HeLa cells transduced with the empty pLKO vector.

Five different shRNAs were initially tested against WDR44 by immunoblot (IB) 72h post infection. Cells transduced with shWDR44 #3 and #5 showed a consistent decrease of WDR44 (Figure 20A). Transduction with shWDR44#3 decreased the levels of the three forms of WDR44 (Figure 20D). Semiquantitative RT-PCR corroborated a decrease of WDR44 mRNA levels (Figure 20B). For Rab11a silencing we also tested three different shRNA (#3, #4, #5), and found all of them effective in lowering the Rab11 levels (Figure 19C). We chose shRab11a #4 (Figure 20E) for the next experiments.

Interestingly, Rab11a silencing slightly increased the WDR44 levels (Figure 20D), whereas WDR44 silencing had no effect on Rab11a protein levels (Figure 20E). This suggests that WDR44 might be negatively regulated by Rab11a expression, which can be found elevated in cancer cells (Ferro, Bosia et al. 2021).

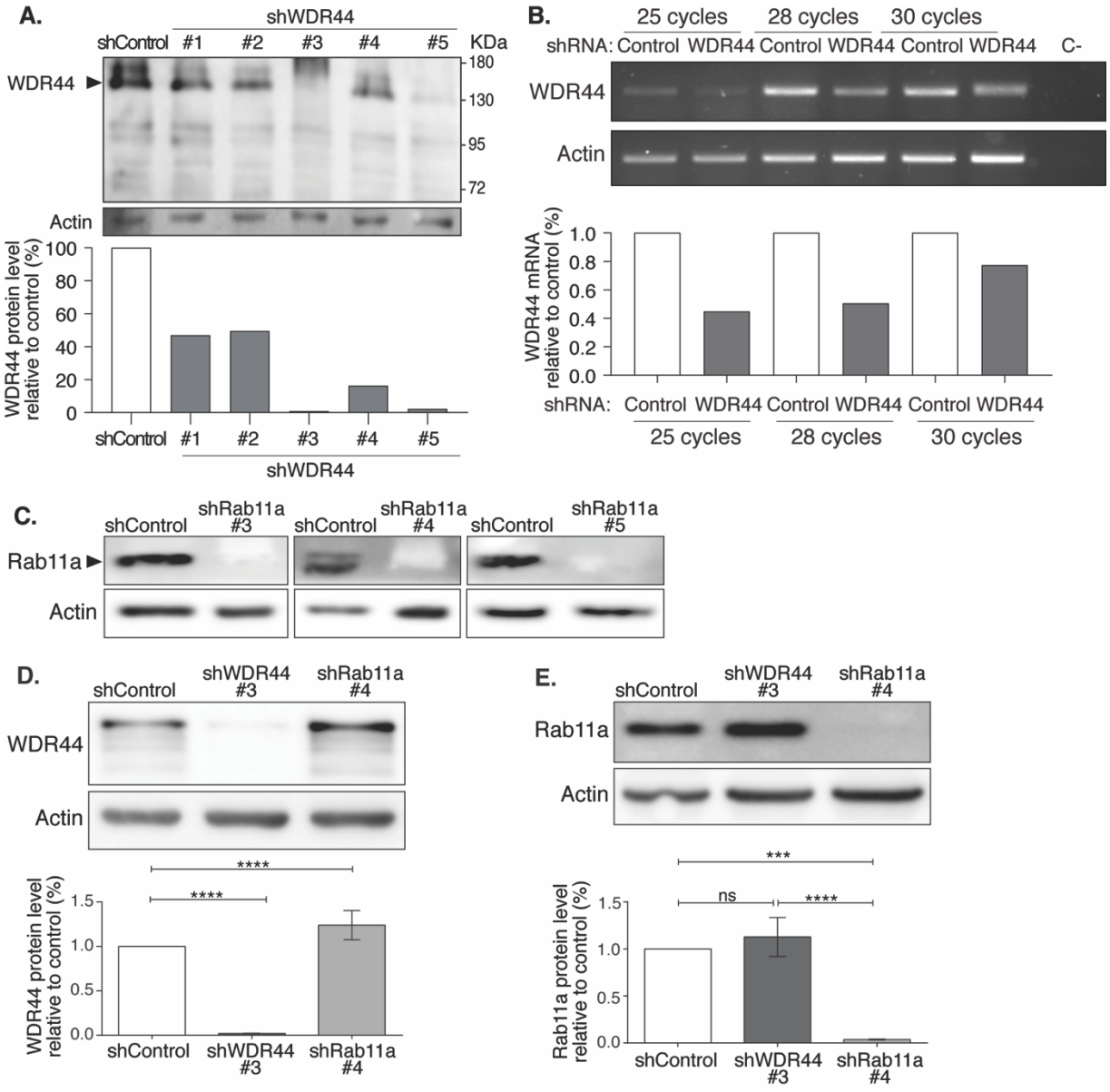

Figure 20. WDR44 and Rab11a silencing in HeLa cells. HeLa cells were transduced with different shRNA against to WDR44 **(A and B)** and Rab11a **(C)**, treated with puromycin during 48h and cell lysates were analyzed by immunoblot (N=1). **(B)** WDR44 mRNA levels were analyzed by semi-quantitative RT-PCR from HeLa cells transduced with shWDR44 #3 (N=1). WDR44 **(D)** and Rab11a **(E)** protein levels were analyzed by immunoblot from HeLa cells transduced with shWDR44#3 and shRab11a#4. All data represent the mean of five independent experiments ± SEM. Asterisks denote significant differences in one-way ANOVA * $p<0.05$, ** $p<0.01$, ***$p<0.001$, ****$p<0.0001$.

3.3.2 Analysis of WDR44 silencing in Rab11a and Rab4a subcellular localization.

Because WDR44 co-immunoprecipitated with Rab11a and Rab4a, we analyzed the effect of WDR44 silencing on the distribution of these Rab-GTPases. HeLa cells transduced to silence WDR44 or Rab11a for 72 h were subsequently transfected with different Rab-GTPases tagged with GFP and analyzed for their subcellular distribution after 16h using immunofluorescent organelle markers. Rab11a-GFP showed a perinuclear and peripheral distribution in shControl cells, which changed to a more peripheral endosomal distribution, losing the perinuclear location, in WDR44 silenced cells (Figure 21A). Neither WDR44 nor Rab11a silencing affected the typical Rab4a-GFP localization in perinuclear endosomes (Figure 21B).

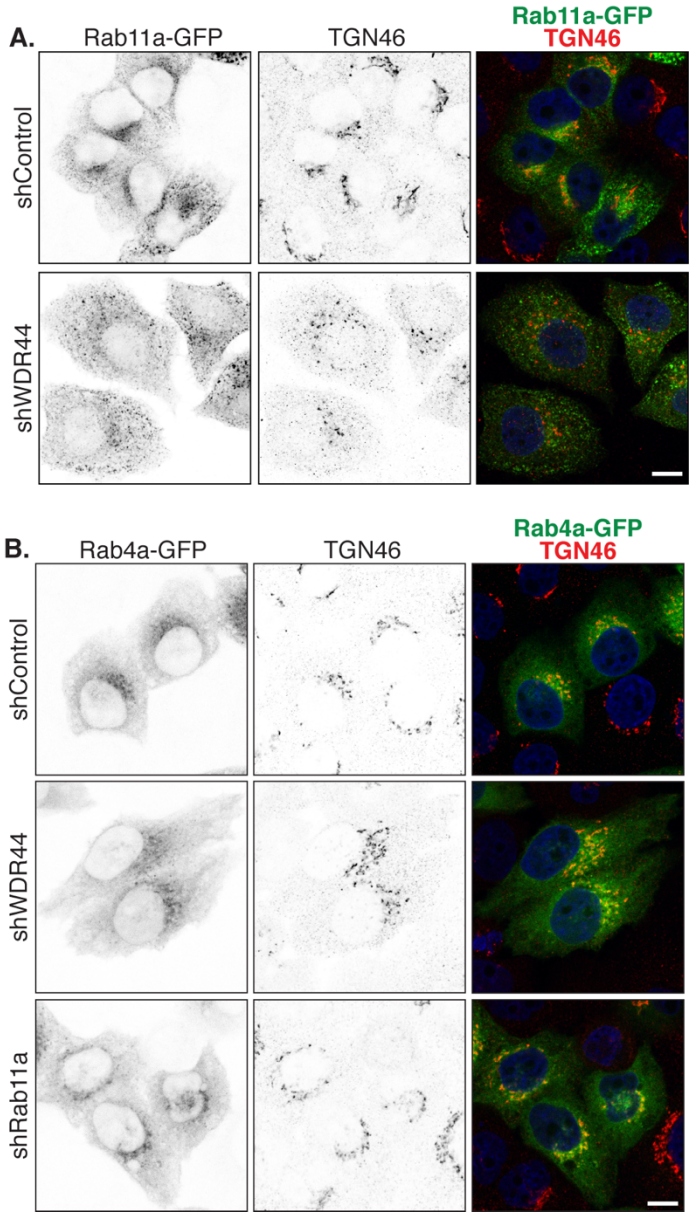

Figure 21. Effects of WDR44 KD in Rab11a and Rab4a subcellular distribution. HeLa cells silenced against WDR44 or Rab11a were transfected with Rab11a **(A)** or Rab4a **(B)** tagged to GFP. After over-night expression, cells were analyzed by IFI with anti-TGN46 antibody as a TGN marker. Cells were imaged by confocal microscopy and the figure shows a single plane from a z-stack. Scale bar represents 10μm.

3.3.4 Endocytosis and recycling.

The role of WDR44 in endocytic recycling has not been studied despite its original identification as a protein that interacts with Rab11a, which is involved in endocytic recycling. The transferrin receptor (TfR) is a well-known protein that traffics through Rab11a recycling endosomes during its endocytic pathway. Therefore, we analyzed whether WDR44 have any effect on TfR recycling. WDR44 silenced HeLa cells incubated with Transferrin alexa-488 (Tf-488) for different times at 37ºC showed no difference in the levels of internalized ligand, as quantified by FACS (Figure 22A). We also did not detect differences when the cells were previously incubated with this ligand on ice (Figure 22B). These results suggest that WDR44 does not participate in the endocytosis of TfR.

To evaluate endocytic recycling of the TfR the cells were first allowed to internalize Tf-488 at 37ºC for 30 min and the remaining Tf-488 at the cell surface was removed by acid wash. To allow the return of internalized Tf-488 we incubated the cells at 37ºC for different times and assessed the Tf-488 that remaining inside of the cells after washing out the cell surface at each time point. The results showed no differences in TfR recycling rates between shControl, shWDR44 cells (Figure 23).

These results suggest that WDR44 does not participate in TfR recycling, even though both proteins colocalize in endosome-like structures (see Figure 15A). However, our assay neither detected an alteration of TfR recycling in cells silenced for Rab11a (Figure 23). It might be that our assay is only detecting recycling from early endosomes and not from the perinuclear recycling endosomes where Rab11a participates (Campa, Margaria et al. 2018).

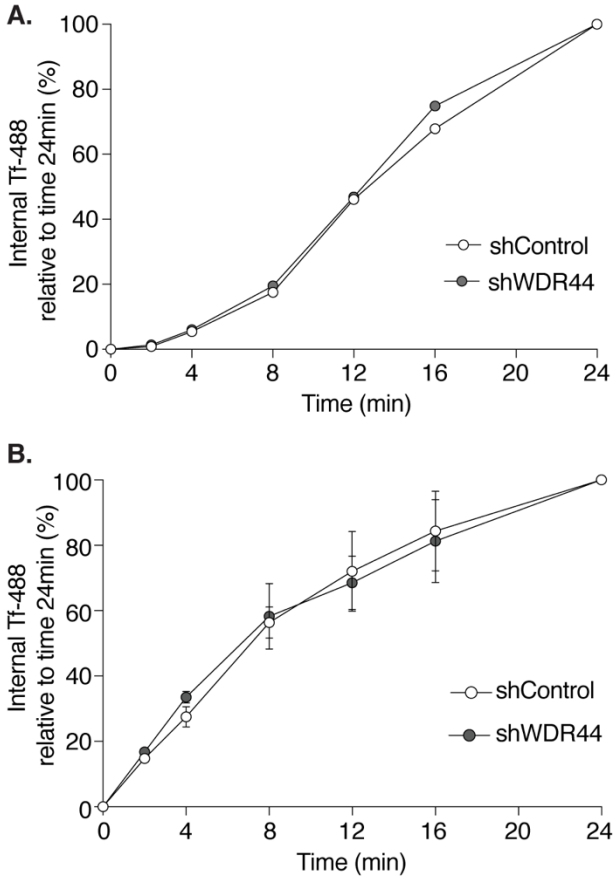

Figure 22. Effect of WDR44 silencing in TfR endocytosis. A. WDR44 KD HeLa cells were constantly incubated with fluorescent transferrin conjugates (Tf-488) during different times at 37ºC. Cell surface remaining Tf-488 was removed with an acid wash at 4ºC. Internal Tf-488 per cell was quantified by FACS. All data are the mean ± SEM of 10.000 cells from three different experiments. **B.** WDR44 KD HeLa cells were incubated with Tf-488 during 30min on ice. Then, cells were washed and incubated at 37ºC during different times to allow Tf-488 endocytosis. Remaining Tf-488 at the cell surface was removed with an acid wash on ice. Internal Tf-488 per cell was quantified by FACS. All data are the mean ± SEM of 10.000 cells from four different experiments.

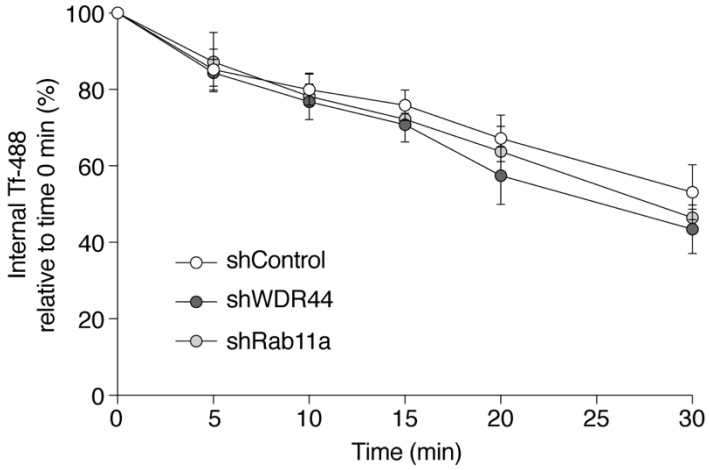

Figure 23. Effect of WDR44 and Rab11a silencing in TfR recycling. WDR44 and Rab11a KD HeLa cells were incubated with Tf-488 during 30min on ice. Then, cells were washed and incubated at 37ºC during 30min to allow Tf-488 endocytosis. Remaining Tf-488 at the cell surface was removed with an acid wash on ice. Then, cells were incubated during different times at 37ºC to allow transferrin receptors recycle back to the plasma membrane. Cell surface Tf-488 was removed with an acid wash on ice. Internal Tf-488 per cell was quantified by FACS. All data are the mean ± SEM of 10.000 cells from two different experiments.

To assess the recycling from the perinuclear recycling endosomes we used an assay based on previous data our laboratory, in which the epidermal growth factor receptor (EGFR) is induced to reversible accumulate at these endosomes by treating with propranolol. Our laboratory showed that inhibition of phosphatidic acid hydrolysis by propranolol induces EGFR ligand-independent endocytosis and its accumulation in juxtanuclear recycling endosomes (Norambuena, Metz et al. 2010). These endosomes are a site of function of Rab11 (Campa, Margaria et al. 2018) and accumulates EGFR under propranolol treatment. Furthermore, EGFR can then return to the plasma membrane upon propranolol removal (Norambuena, Metz et al. 2010), thus providing a model system to assess recycling from the perinuclear recycling endosomes. Therefore, we analyzed the effect of WDR44 silencing upon EGFR recycling after propranolol removal.

Cell surface proteins were biotinylated with EZ-Link Sulfo-NHS-SS-biotin and then were incubated with propranolol to induce EGFR endocytosis. The remaining biotin at the cell surface biotin was removed by incubating the cells with the reducing agent MESNA. The internal biotinylated EGFR then was allowed to return to the plasma membrane after washing out propranolol. A second round of cell surface biotin reduction leaved the intracellular biotinylated EGFR detectable by streptavidin precipitation followed by immunoblot. Our results show that propranolol removal decreases internal EGFR in shControl cells but not in WDR44 silenced cells (Figure 24B), suggesting that WDR44 plays a role in the trafficking from the perinuclear recycling endosomes. Interestingly, WDR44 KD cells show lower EGFR total protein (Figure 24A), but we do not study the mechanism of this effect. A possibility to study in future experiments is whether the silencing of WDR44 lead to alterations of the EGFR trafficking promoting its degradation in lysosomes.

Then in collaboration with Jaime Venegas we analyzed WDR44 distribution respect to EGFR. As is reported, serum starvation induced cell surface EGFR localization but did not change WDR44 distribution (Figure 25). Propranolol treatment induced EGFR endocytosis and its perinuclear accumulation, as we previously reported (Norambuena, Metz et al. 2010, Shaughnessy, Retamal et al. 2014, Barra, Cerda-Infante et al. 2021), without changing the distribution of WDR44 distribution. However, propranolol treatment induced EGFR and WDR44 colocalization in perinuclear endosomes (Figure 25).

Taken together, these results suggest that WDR44 is involved in the trafficking through the perinuclear recycling endosomes.

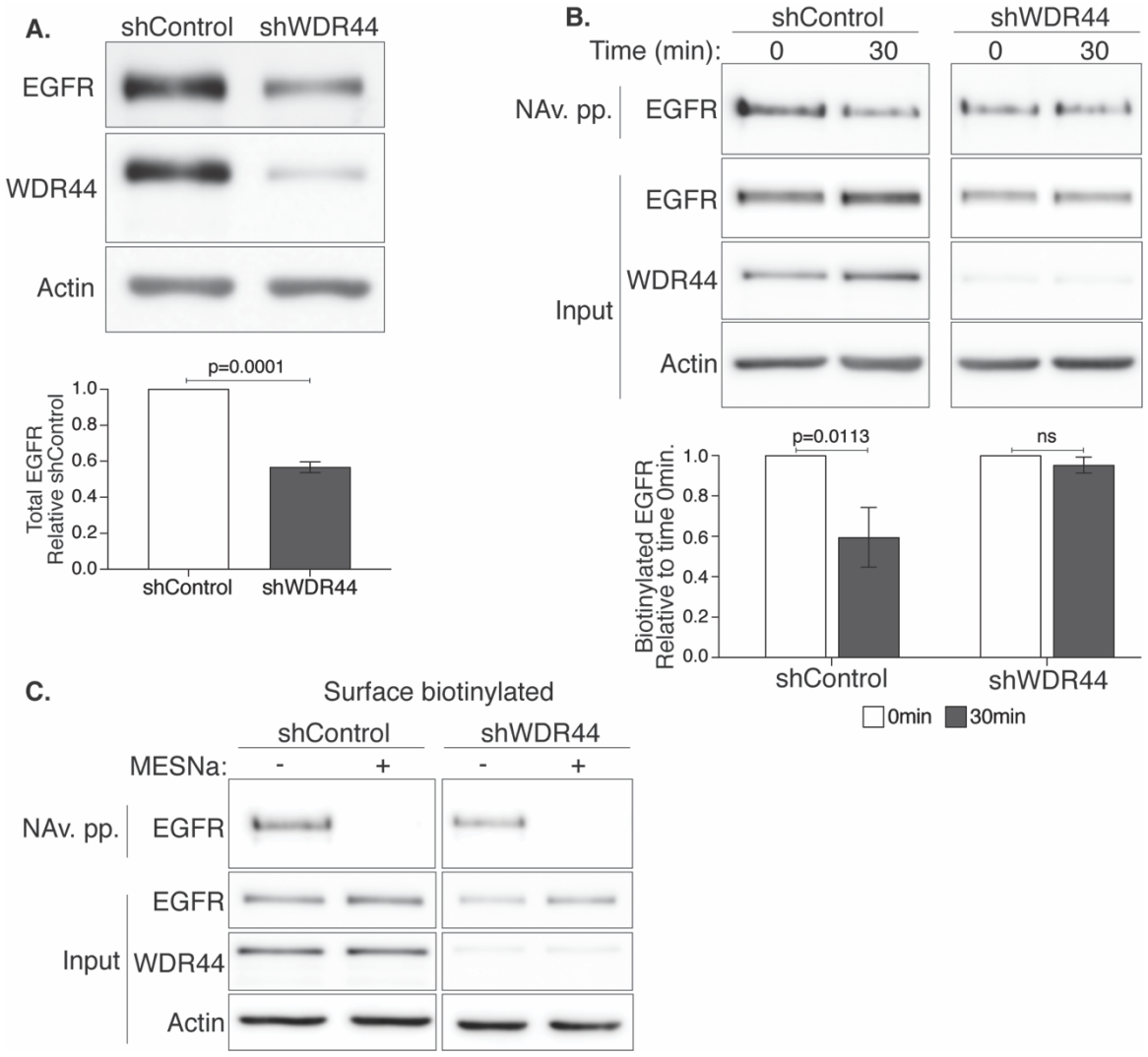

Figure 24. Effect of WDR44 KD in EGFR recycling from perinuclear endosomes. **A.** WDR44 KD HeLa cells were analyzed by immunoblot against to EGFR (n=3). **B.** EGFR recycling assay. Cell surface proteins were biotinylated with EZ-Link Sulfo-NHS-SS-biotin during 30min on ice and then were incubated with 100uM propranolol for 30min at 37ºC to allow the internalization of biotinylated plasma membrane proteins. Remaining cell surface biotin was removed by MESNa reduction solution. After Biotin reduction, cells were incubated a second time at 37ºC during 30min to allow protein recycling back to the plasma membrane. Biotin re-exposed at the cell surface was removed by a second MESNa solution treatment. Internal biotinylated proteins were precipitated with neutravidin and analyzed by immunoblot. All data are the mean ± SEM of three independent experiments. **C.** Control assay of MESNa reduction protocol in B.

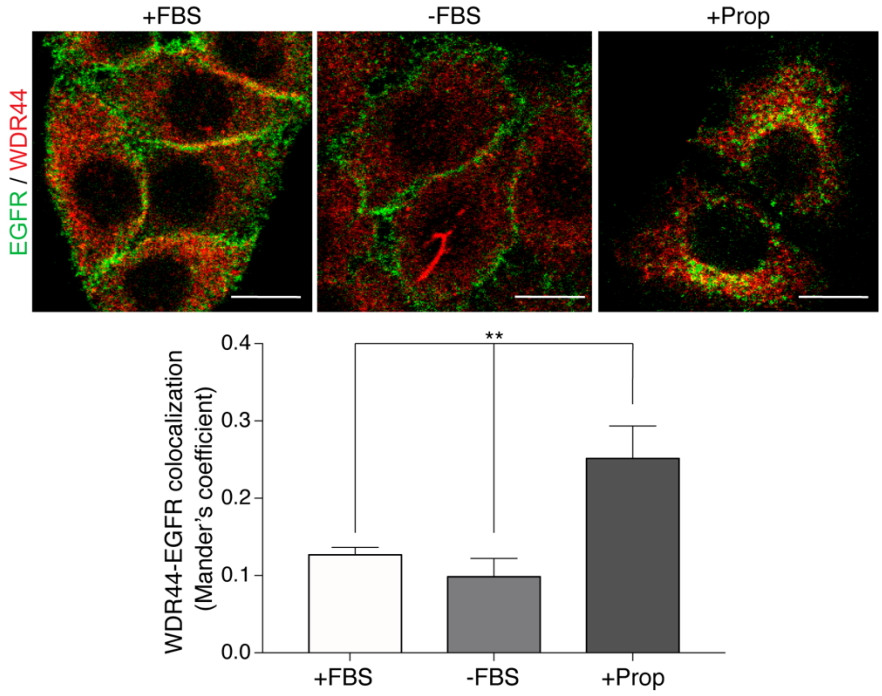

Figure 25. Analysis of WDR44 and EGFR distribution under propranolol treatment. WDR44 and EGFR distribution was analyzed by IFI in HeLa cells previously maintained with fetal bovine serum (FBS) supplemented media, FBS-depleted media or propranolol treatment (150μM) . Cells were imaged by confocal microscopy and WDR44 and EGFR colocalization was quantified in each condition. All data are the mean ± SEM of 10 cells from two independent experiments. Asterisks denote significant differences in one-way ANOVA **p<0.05. *The experiment and the figure were made by Jaime Venegas, a PhD. student from our laboratory.*

3.3.5 Cell migration and invasion.

Considering the interaction of WDR44 and Rab11a, we decided to study other cellular process, such as cell migration and invasion, in which the function of Rab11 has been involved. Rab11 participates in cell migration acting upon endocytic recycling, particularly of β1 integrins (Caswell and Norman 2006) and extracellular matrix remodeling, which in turn depends on secretion of metalloproteinases (Yu, Yehia et al. 2014).

First we evaluated cell migration by wound closure assay. WDR44 silenced cells showed a significant decrease in wound closure compared to control cells in serum-free conditions, but not in serum supplemented media where cell proliferation occurs shielding this effect (Figure 26).

We also analyzed cell migration by the classic trans-well assay. Again, shWDR44 cells showed lower trans-well migration than control cells using serum as a chemoattractant (Figure 27A). In addition, we studied cell invasion in matrigel matrix pretreated trans-wells. WDR44 silenced cells showed a significant decrease in cell invasion compared to control cells (Figure 27B). In collaboration with Jaime Venegas, we also analyzed cell invasion in matrigel assay visualized by confocal microscopy in WDR44 and Rab11a silenced cells. Both WDR44 and Rab11a silencing decreased cell invasion relative to shControl cells (Figure 28).

Altogether these results strongly suggest that WDR44 participates in cell migration and invasion processes very likely due to its role as Rab11a effector.

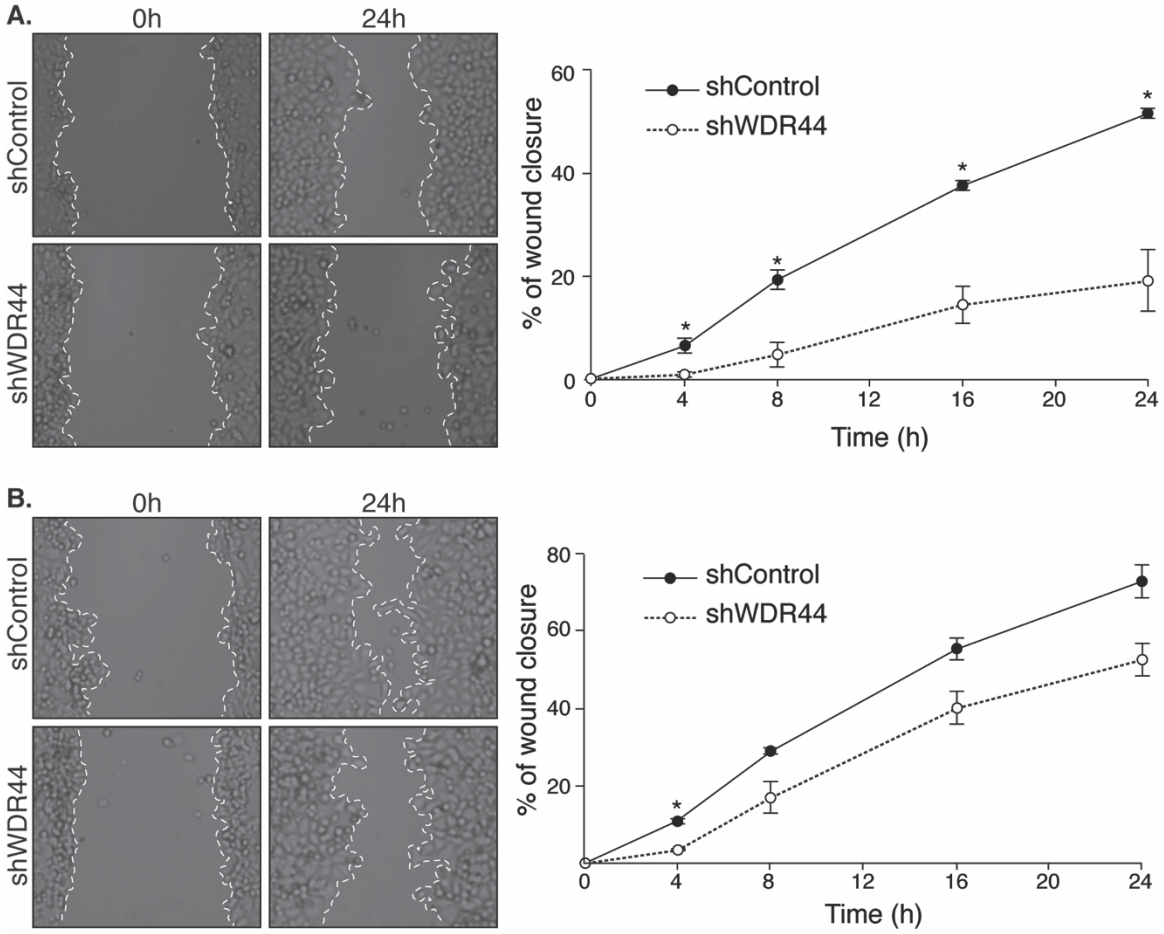

Figure 26. Analysis of cell migration by wound closure assay in shWDR44 cells. HeLa cells were seeded, transduced with shRNA and puromycin selected in a p24 wells plate. The wounds were made with a SPLScar scratcher and cells were imaged at different times without FBS **(A)** or 10% FBS supplementation **(B)**. The percentage of cell-covered area at each time point was calculated compared to the 0h time. All data are the mean from three independent experiments ± SEM. t-test was made for each time point, *p<0.05.

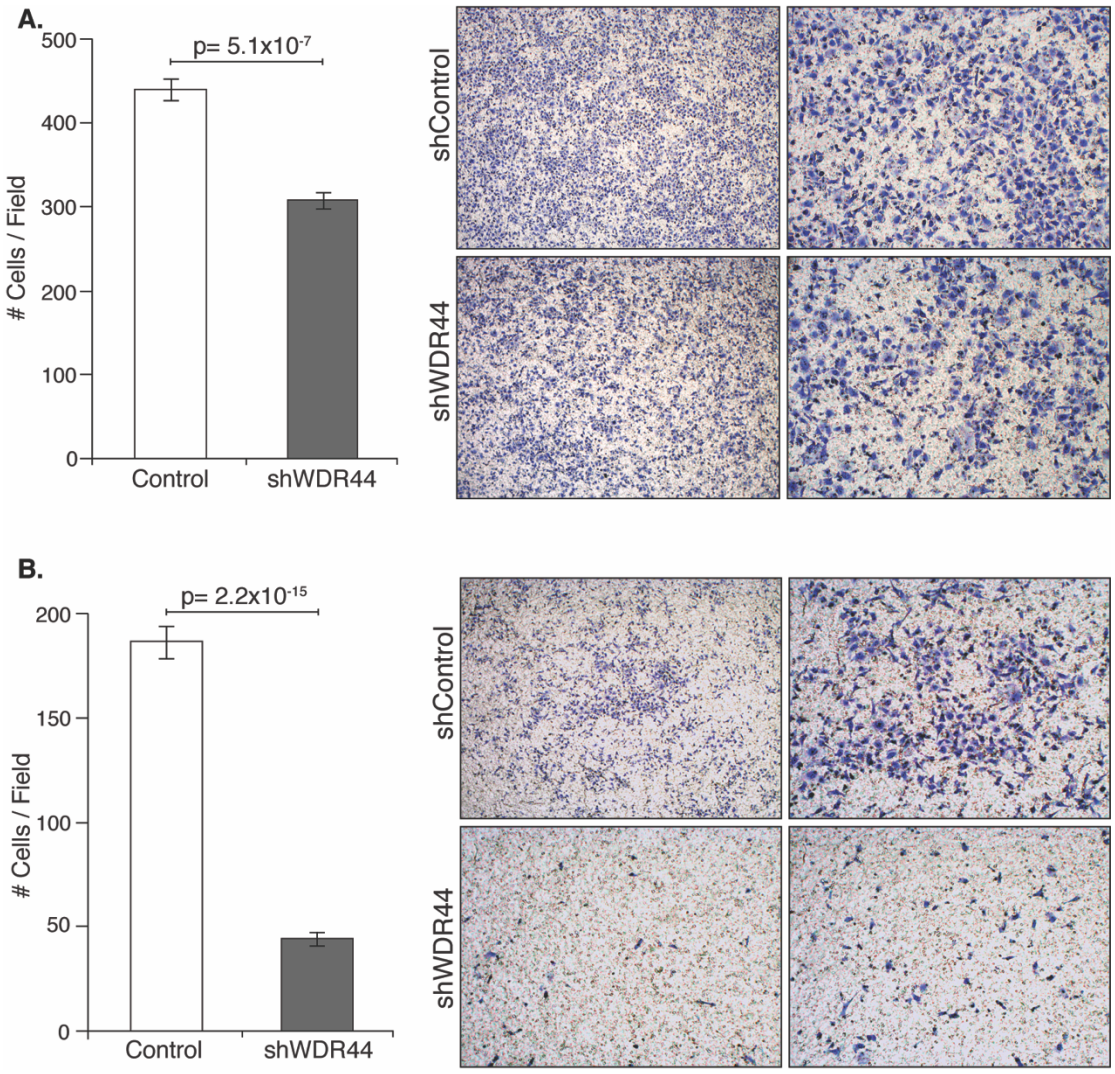

Figure 27. Effect of WDR44 silencing in cell migration and invasion. HeLa cells silenced against to WDR44 were seeded directly on transwell insert **(A)** or matrigel pretreated transwell **(B)** for migration and invasion assay, respectively. After 16h, cells were staining with 0.2 % crystal violet, imaged and counted. All data are the means from 15 images from three experiments ± SEM. The figure indicates p-value of t-test.

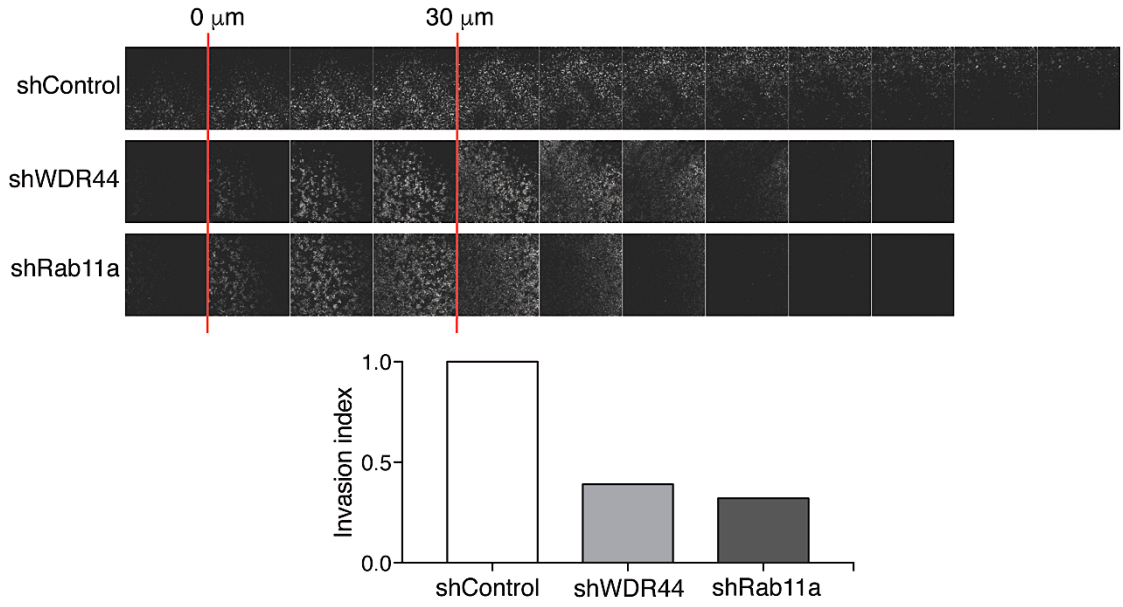

Figure 28. Effect of WDR44 and Rab11a depletion in cell invasion. HeLa cells depleted for WDR44 and Rab11a were seeded on matrigel pretreated transwell and maintained during 5 days. Matrigel was imaged at 10μm intervals by confocal microscope using the 10X objective. ImageJ software was used to determine the integrated density of each image section to calculate the invasion index = (∑ integrated density of first 30 μM)/(∑ integrated density of invasion) expressed as a fold change. Data represent the invasion index of one experiment. *The experiment and the figure were made by Jaime Venegas, a PhD. student from our laboratory.*

3.4 Protein trafficking between the ER and the Golgi complex

3.4.1 Depletion of WDR44 induces Golgi fragmentation

Considering that Golgi structure is crucial for a variety of cellular processes and their alterations have been described is several diseases (Li, Ahat et al. 2019), we further analyzed the effect of WDR44 silencing on Golgi markers. We used GM130 and TGN46 as cis and trans Golgi markers. WDR44 silencing showed disaggregation of both GM130 and TGN46 suggesting a Golgi fragmentation (Figure 29). Despite their disaggregated distribution, GM130 and TGN46 remained in close proximity indicating that some Golgi structure is still preserved. This Golgi fragmentation did not occur under Rab11a silencing conditions (Figure 29), as previously described (Galea, Bexiga et al. 2015). Therefore, WDR44 seems to play a role in Golgi structure independent of Rab11.

We also noted that visualization of TGN46 immunofluorescence in WDR44 KD cells required higher laser intensity scanning by confocal microscopy than control cells (data not shown). We evaluated by immunoblot the levels of several Golgi proteins and found decreased the levels of TGN46 and Furin, two TGN proteins, while Giantin, a TM *cis*-Golgi protein, did not change in WDR44 KD cells (Figure 30).

Altogether, these results reveal that WDR44 is involved in regulation of Golgi structure and homeostasis.

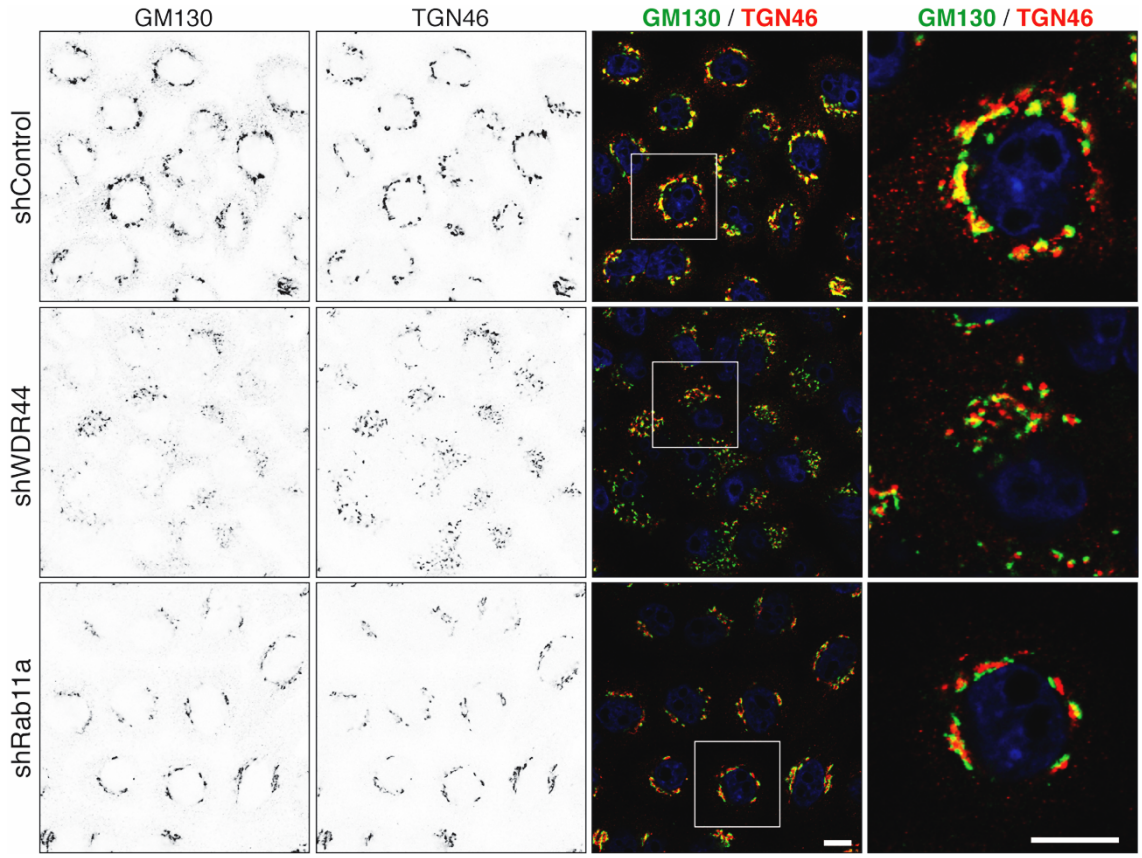

Figure 29. Analysis of Golgi morphology in WDR44 and Rab11a silenced cells. HeLa cells silenced against WDR44 and Rab11a were analyzed by IFI with anti-GM130 and anti-TGN46 antibodies as a cis-Golgi and TGN markers, respectively. Cells were imaged by confocal microscopy. Scale bars represent 10μm.

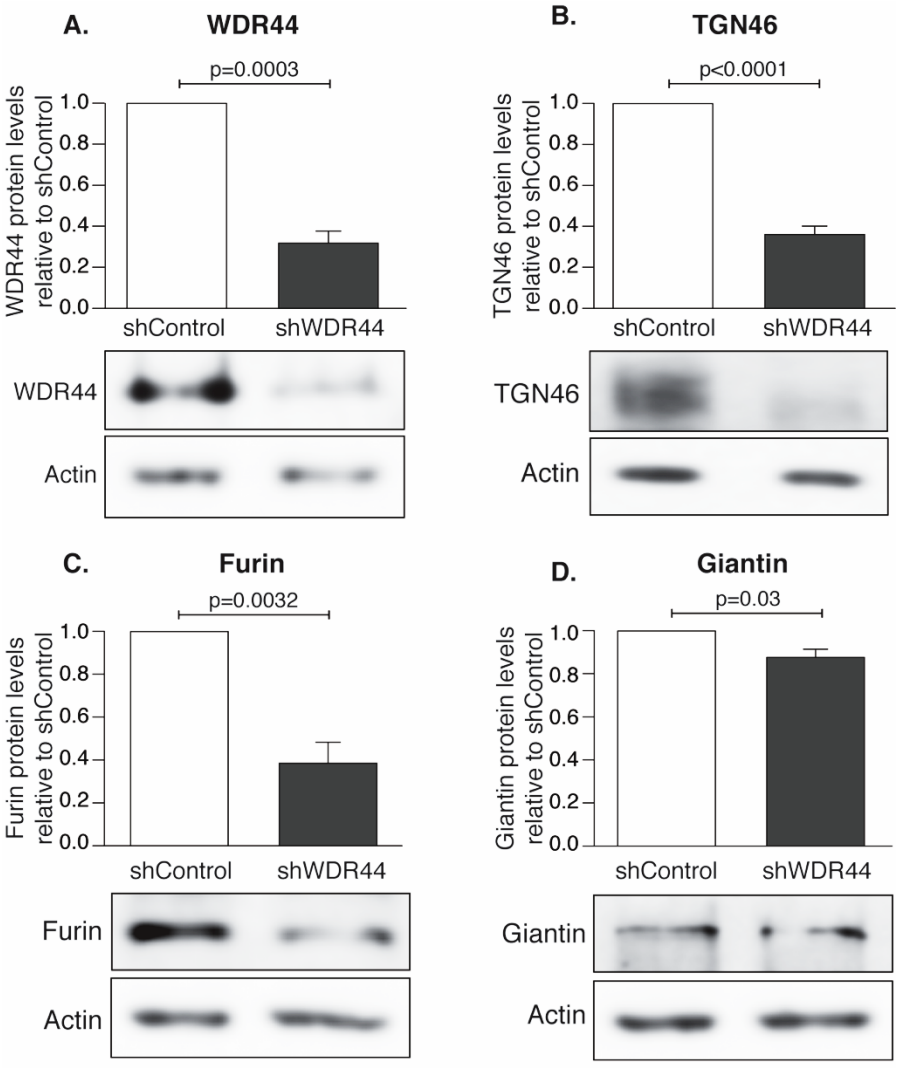

Figure 30. Analysis of Golgi resident proteins in WDR44 KD cells. HeLa cells were silenced against to WDR44 (shWDR44) or control (shControl). **A.** WDR44 silencing was confirm by immunoblot. Protein levels of TGN46 **(B),** Furin **(C)** and Giantin **(D)** were analyzed by immunoblot and quantified. All data represent the mean of three independent experiments ± SEM. The figure indicates t-test p-values.

3.4.2 Effects of WDR44 silencing in Rab1 and Rab6 localization

Rab1b-GFP and Rab6A-GFP, which are Golgi-associated Rab-GTPases, showed a perinuclear and compact distribution, colocalizing with the TGN46 Golgi marker in control cells (Figure 31). Silencing of Rab11a did not change their TGN location. In contrast, both Rab1b-GFP and Rab6A-GFP displayed a more disaggregated distribution together with TGN46 in WDR44 silenced cells (Figure 31). These results suggest that WDR44 silencing leads to the Golgi fragmentation and loss of its ribbon-like structure of the Golgi complex (Wei and Seemann 2010).

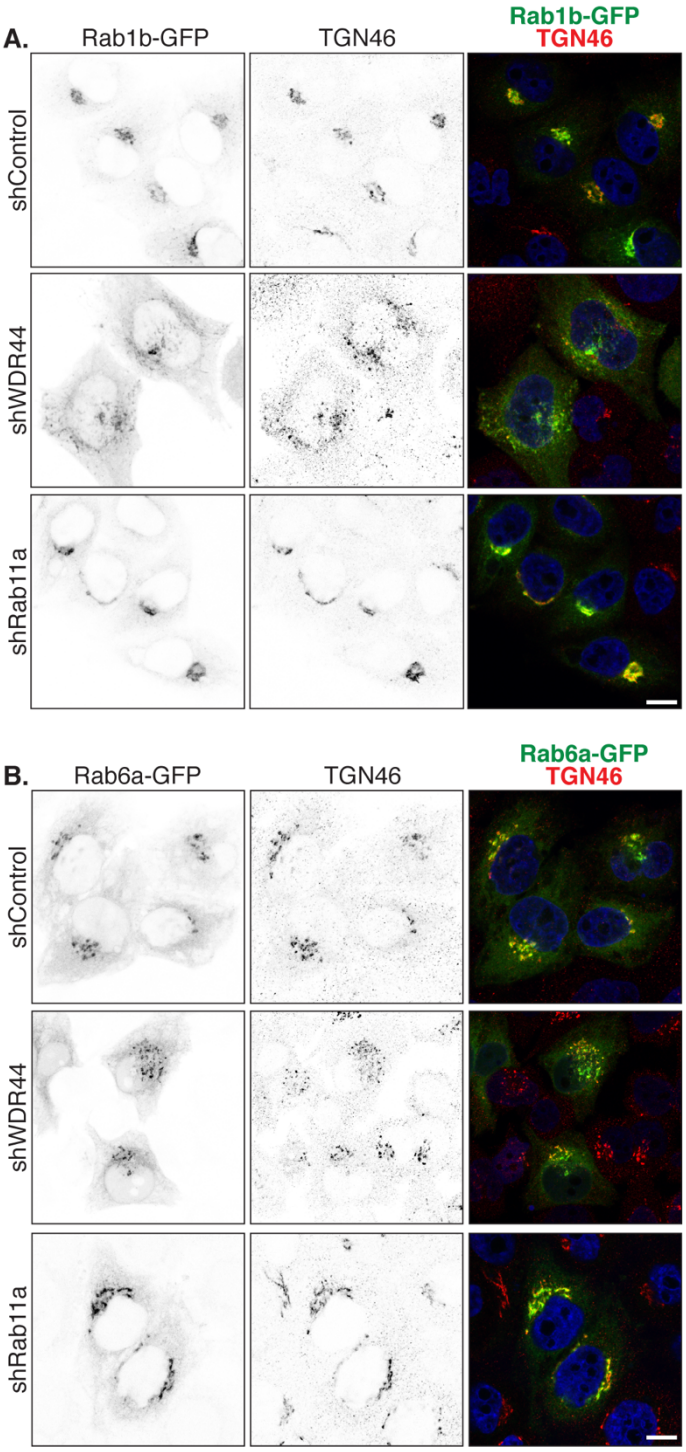

Figure 31. Effects of WDR44 and Rab11a KD in Rab1b and Rab6a subcellular distribution. HeLa cells silenced against WDR44 or Rab11a were transfected with Rab1b **(A)** or Rab6a **(B)** tagged to GFP. After over-night expression, cells were analyzed by IFI with anti-TGN46 antibody as a TGN marker. Cells were imaged by confocal microscopy and the figure shows a single plane from a z-stack. Scale bar represents 10μm.

3.4.3 Functional analysis of WDR44 in ER-Golgi interface transport

Golgi structure maintenance is highly dependent on protein trafficking routes in the ER-Golgi interface. For instance, (Galea, Bexiga et al. 2015) showed that Rab1a/b KD cells had fragmented Golgi phenotype and decreased Golgi-to-ER retrograde trafficking, Rab6A silencing induced a compacted Golgi structure. Considering our results suggesting that WDR44 interacts with Rab1a/b and Rab6 we studied the effects of WDR44 silencing on protein trafficking at the ER-Golgi interface using the KDEL receptor (KDELR) as model system.

KDELR mediates the retrieval of ER chaperones such as BiP and PDI from the Golgi apparatus by recognizing the KDEL motif present in their carboxyterminal region (Semenza, Hardwick et al. 1990, Vaux, Tooze et al. 1990). Once KDELR binds to the ligand at the cis-Golgi it is transported to the ER by COPI-coated vesicles (Majoul, Straub et al. 2001). The KDEL-ligand is released at the ER and the KDELR is transported back to the cis-Golgi through COPII-coated vesicles emerging from the ER (Majoul, Sohn et al. 1998). The KDELR is therefore normally found distributed in the cytoplasmic network typical of the ER and the perinuclear structure characteristic of the Golgi complex (Figure 32, Control cells)

3.4.3.1 Silencing of WDR44 decreases Golgi-to-ER retrograde transport of KDELR leading to its accumulation in cis-Golgi

To evaluate whether WDR44 is involved in Golgi-to-ER retrograde transport we first assessed the KDELR distribution in cells silenced for WDR44. We used a HeLa cell line that stably expresses KDELR tagged to GFP (KDELR-GFP). In control cells, KDELR-GFP showed a reticular distribution and colocalized with the *cis*-Golgi marker Giantin. Interestingly, shWDR44 cells showed higher KDELR-GFP colocalization with Giantin and a lack of ER distribution (Figure 32). This suggests that there is an increase in the Golgi residence time of KDELR-GFP, probably due to an imbalance in KDELR transport rate in WDR44 silenced cells.

We also evaluated the ER-to-Golgi anterograde transport. To this end we blocked the KDELR Golgi-to-ER retrograde transport using the mutant KDELR(D193N)-GFP, which is transported from the ER to the Golgi but does not return to the ER, thus accumulating at cis-Golgi (Townsley, Wilson et al. 1993).

We found that WDR44 KD showed a perinuclear distribution of KDELR(D193N)-GFP colocalizing with Giantin, similar to Control cells. These results suggest that WDR44 is not required for anterograde transport (Figure 33).

Interestingly, the Golgi did not suffered fragmentation when WDR44 is silenced in HeLa cells stably expressing either the normal or the mutant KDELR (Figure 33).

To confirm that the shWDR44 effect is not due to shRNA off-targets we rescued the shWDR44 phenotype by expressing the bovine WDR44 sequence tagged with HA (Bt-HA-WDR44), whose sequence is distinct to human WDR44 at the region addressed by shRNA. The shWDR44 HeLa cell line that stably expresses KDELR-GFP resulted resistant to transfection and therefore we co-transfected KDELR-GFP and Bt-HA-WDR44 in HeLa cells previously silenced for WDR44. As a negative control, we co-transfected KDELR-GFP and pCDNA3.1 empty vector. After 24 h of the transfection we analyzed KDELR-GFP and Giantin colocalization by immunofluorescence. Bt-HA-WDR44 decreased KDELR-GFP and Giantin colocalization, while pCDNA3.1 empty vector had no effect (Figure 34). The result of this complementation experiment further supports the possibility that WDR44 is required for KDELR retrograde flux.

We noticed that the complementation reestablished the flux of KDELR from the Golgi previously damped by the 48h of WDR44 silencing. However, the Golgi fragmentation seen also when WDR44 is silenced did not return to a normal Golgi morphology (Figure 34). This effect on the Golgi structure may require longer time of complementation.

Rab11a might be involved in Golgi to ER traffic accordingly with a broad analysis of silencing effects of Rabs GTPases (Galea, Bexiga et al. 2015). Considering that WDR44 is an effector of Rab11a we also analyzed KDELR-GFP distribution in shRab11a cells. We found that Rab11a silencing increases the colocalization of KDELR-GFP and Giantin, similar to WDR44 KD cells (Figure 32). This suggests that Rab11a might be involved in Golgi-to-ER retrograde trafficking, a possibility that indeed requires further support of a complementation assay.

To further explore the retrograde Golgi-to-ER transport we performed a FLIP assay that provided quantitative data on KDELR-GFP exit from the Golgi. Both shWDR44- and shRab11a-silenced cells showed decreased the exit rate of KDELR-GFP compare to shControl cells (Figure 35).

These results, together with the observation that the anterograde flux is not affected, strongly suggest that WDR44 and Rab11a somehow participate in the KDELR Golgi-to-ER retrograde transport.

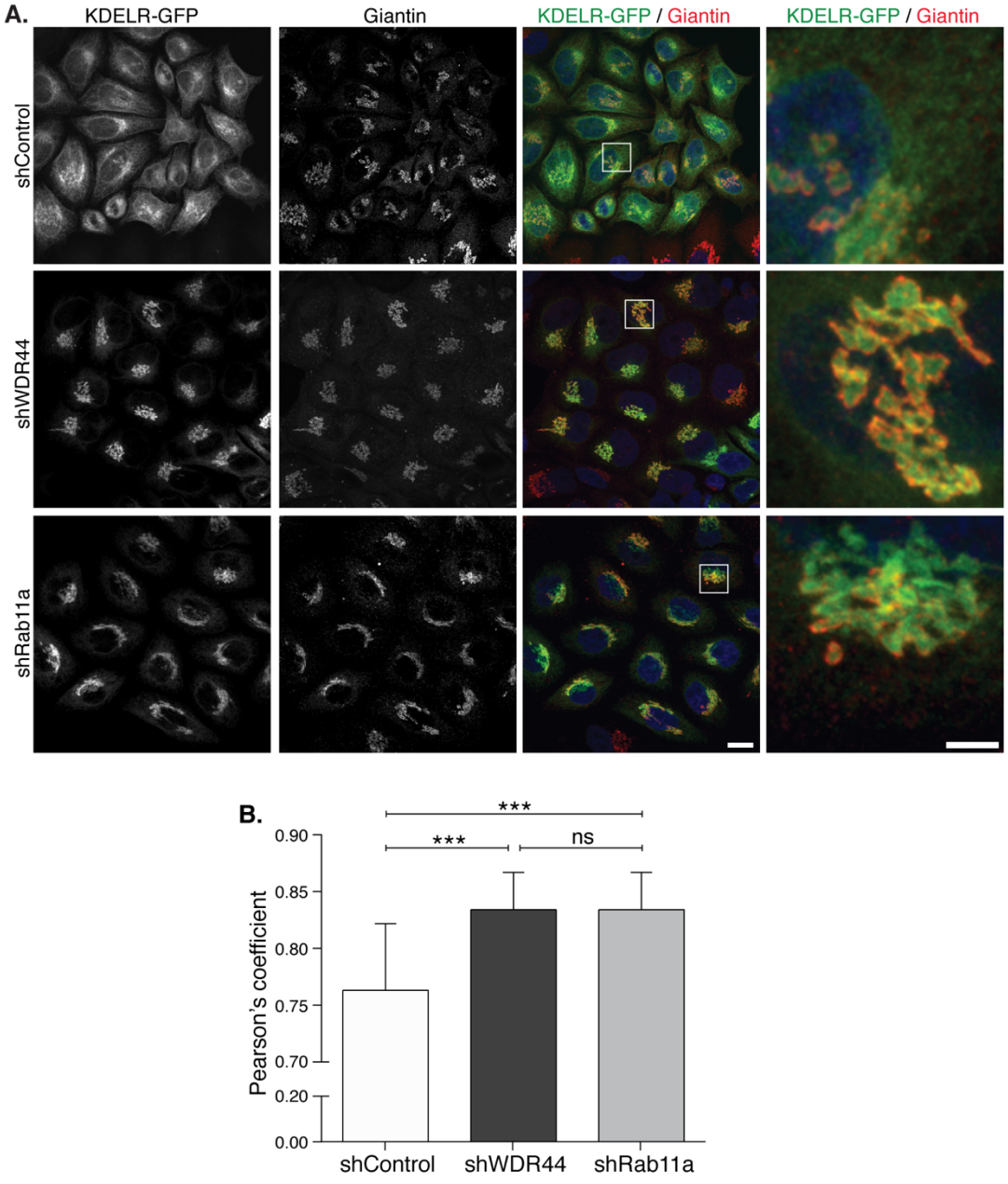

Figure 32. Analysis of KDELR distribution in WDR44 and Rab11a KD cells. A. HeLa cells stably expressing the KDELR tagged with GFP (KDELR-GFP) were silenced against to WDR44 or Rab11a. The distribution of KDELR-GFP was analyzed relative to Giantin as a cis-Golgi marker by IFI with anti-Giantin antibody and imaged by confocal microscopy. Last column show magnification of the boxed areas. Scale bar represents 20μm and 5μm in normal and magnified images, respectively. B. KDELR-GFP and Giantin colocalization was quantified by Pearson's coefficient. All data are the mean of 35-45 cells ± SEM. Asterisks denote significant differences in one-way ANOVA ***p<0.001.

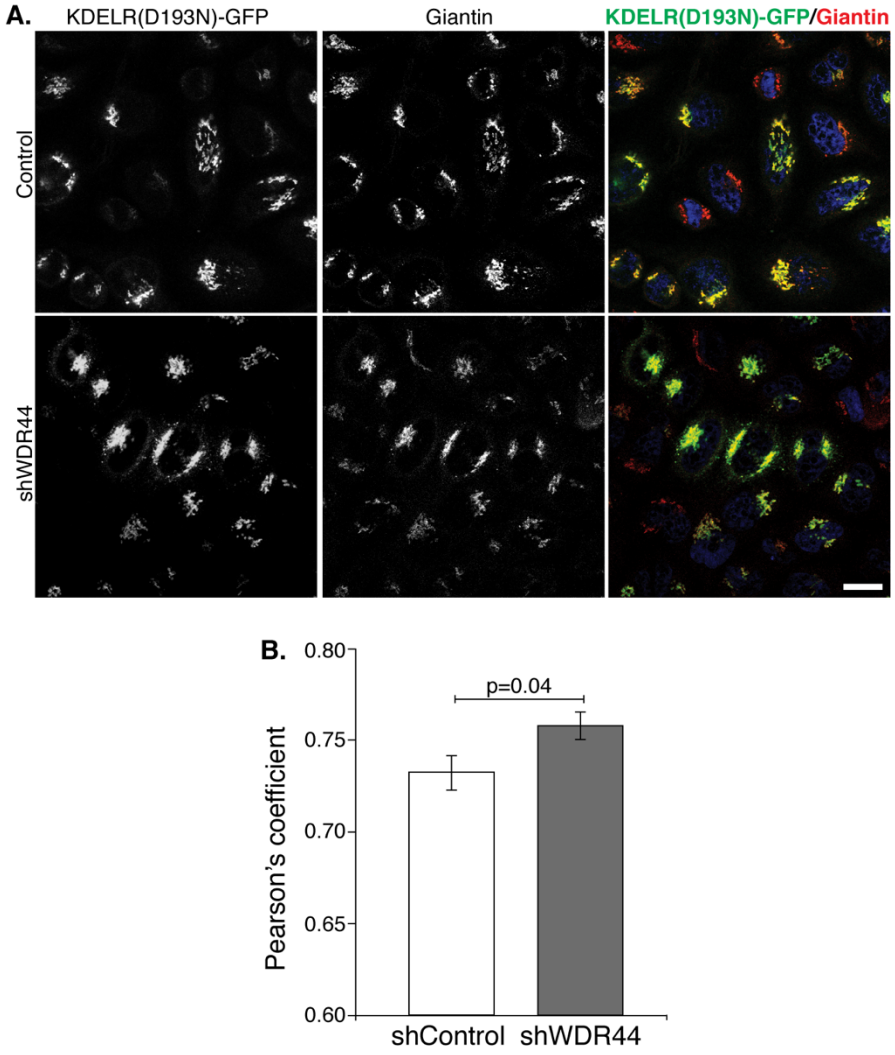

Figure 33. Effect of WDR44 silencing in KDELR(D193N) Golgi distribution. A. HeLa cells that stably express KDELR(D193N)-GFP were silenced against to WDR44. The distribution of KDELR(D193N)-GFP was analyzed relative to Giantin as a cis-Golgi marker by IFI and imaged by confocal microscopy. Scale bar represents 20um. **B.** KDELR(D193N)-GFP and Giantin colocalization was quantified by Pearson's coefficient. All data are the mean of 35-45 cells ± SEM. p-value from t-test.

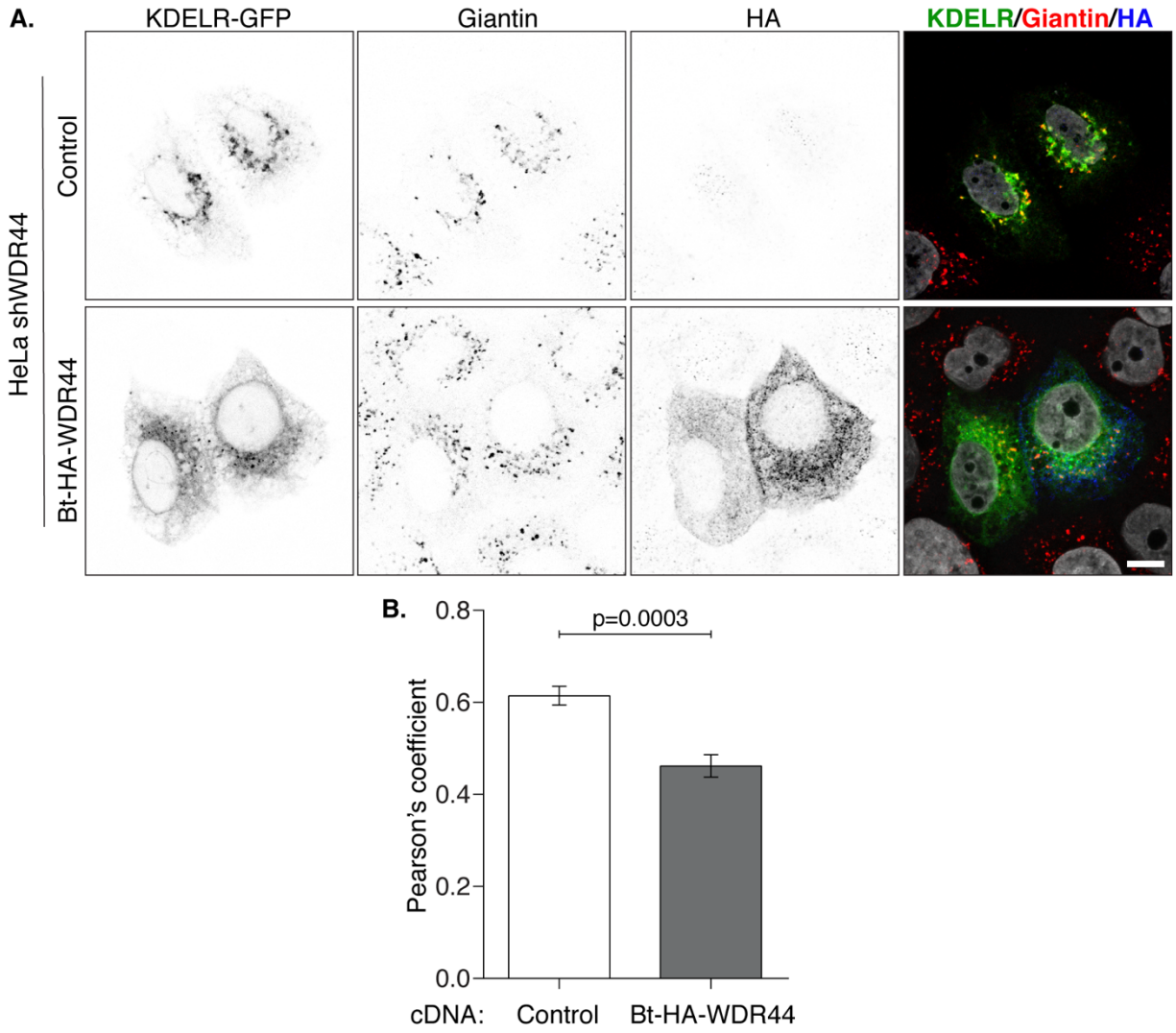

Figure 34. Rescue of KDELR Golgi accumulation phenotype in shWDR44 cells by expressing the bovine WDR44 sequence. A. HeLa cells were silenced against to WDR44 during 72 hours and then they were transfected with KDELR-GFP and pDCNA3.1 empty vector (Control) or HA tagged bovine WDR44 (Bt-HA-WDR44). After 24 hour of cDNA expression, proteins distribution was analyzed by IFI with anti-Giantin as cis-Golgi marker and anti-HA to corroborate Bt-HA-WDR44 expression. IFIs were imaged by confocal microscopy. Scale bar represents 10µm. **B.** KDELR-GFP and Giantin colocalization was quantified by Pearson's coefficient. All data represent the mean of nine cells ± SEM. p-value from t-test.

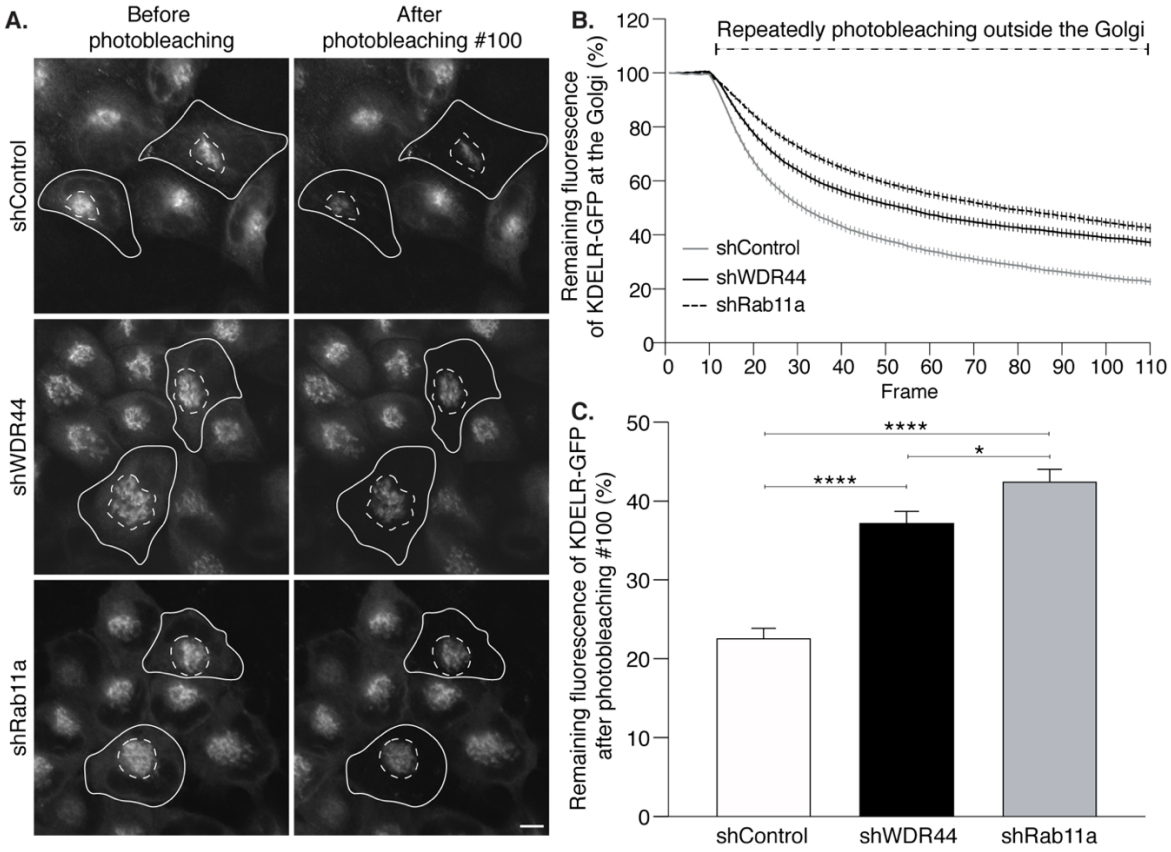

Figure 35. Analysis of KDELR exit rate from the Golgi in WDR44 and Rab11a KD cells. A. HeLa cells that stably express KDELR-GFP were silenced against to WDR44 or Rab11a. KDELR-GFP exit kinetics from Golgi was analyzed by fluorescence loss in photobleaching (FLIP) assay. The picture shows representative images of each experiment before and after 100 photobleaching events. Continuous line represents cell surface and dashed line indicates KDELR-GFP accumulated at the Golgi; The photobleaching were made continuously between the continuous and dashed line (avoiding the area contained by the dashed line). **B.** Quantification of remaining fluorescence of KDELR-GFP at Golgi (dashed line in A) after each photobleaching. **C.** Quantification of remaining fluorescence of KDELR-GFP after 100 photobleaching events. All the data represent the mean of 35-45 cells ± SEM from three independent experiments. **** $p<0.0001$, * $p<0.05$.

3.4.3.2 WDR44 depletion enhances the secretion of the KDEL-chaperone PDI

The protein disulfide isomerase (PDI) is a KDEL-containing ER enzyme that catalyzes the formation of native disulfide bonds and disulfide bond rearrangement during protein folding. PDIs, as well as other KDEL-containing chaperones, are transported to the cell surface when the KDEL signal is mutated or when the KDELR is silenced or mislocalized (Semenza, Hardwick et al. 1990). Therefore, it might be expected that WDR44 silencing should alter the retrograde trafficking of KDEL-chaperones.

We analyzed the effect of WDR44 silencing in PDI cell surface distribution by plasma membrane protein biotinylating assay. We observed an increase of PDI at the plasma membrane in WDR44 silenced cells (n=2), suggesting that this chaperone escape from the binding to KDELR that would normally retain it at the cis-Golgi until its return to the ER (Figure 36).

Rab11a silenced cells also displayed higher levels of PDI at the cell surface, though to a lower extent compared with WDR44 silencing. (Figure 36).

Altogether, these results support a lower retrieval of KDELR in WDR44 and Rab11a silenced cells.

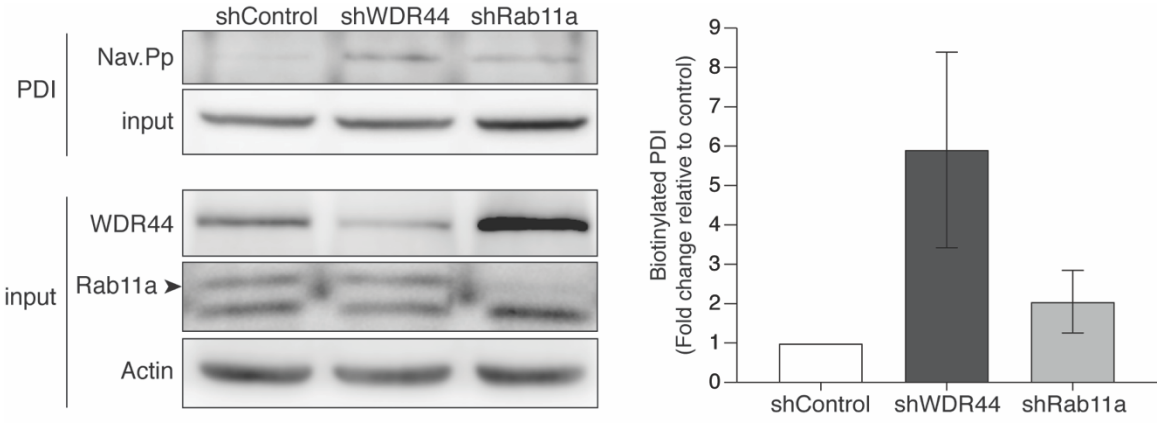

Figure 36. Analysis of PDI at the cell surface in WDR44 and Rab11a KD cells. HeLa cells were silenced against to WDR44 and Rab11a during 72h. Amount of PDI at the plasma membrane was assessed by cell-surface biotinylation, followed by neutravidin precipitation and immunoblotting. All data represent the mean of two experiments ± SEM.

3.4.4 WDR44 silencing induces the unfolded protein response (UPR) but decreases several chaperones.

A decreased KDELR transport from Golgi to ER leading to an escape of chaperones from the ER to the cell surface is expected to impact upon protein folding. Therefore, we studied whether WDR44 silencing affects the unfolded protein response (UPR) in HeLa cells.

The three main ER protein-folding sensors described, IRE1a, PERK and ATF6, are transmembrane protein sensors that transmit luminal ER information to the cytoplasm. Depending on the ER protein folding conditions, each sensor triggers a signaling cascade that induce the production of transcriptional regulators that drive the expression of UPR-related genes. Briefly, Ire1α in response to unfolded proteins, induces the unconventional XBP1 mRNA splicing (XBP1s), which is translated to a transcriptional regulator that induce the expression of chaperones, ERAD proteins and lipid synthesis-related genes (Chen and Brandizzi 2013)

PERK dimerizes in response to unfolded proteins and gets activated that induces the phosphorylation of alpha subunit of the translation initiation factor eIF2 (eIF2α) protein complex. eIF2α phosphorylation decreases the assembly of eIF2 complex, that reduces general protein translation and ER protein folding load. Despite of general attenuation of protein translation, there is an increase in translation of the transcription factor ATF4 by noncanonical initiation factors (Deepika Vasudevan, 2020). ATF4 induces CHOP transcription, as another gene expression regulator, which induces the expression of redox enzymes, cell-death related genes and GADD34. The last one recruits phosphatase PP1, which dephosphorylate eIF2α allowing to reverse the protein-synthesis shut-off, facilitating cellular recovery (McQuiston and Diehl 2017).

Finally, in response to unfolded protein accumulation the ER sensor ATF6 is transported to the Golgi where it is target of proteolytic cleavage that releases its cytosolic domain. The

cytosolic domain of ATF6 is a transcription factor that goes to the nucleus and induces ER chaperone genes expression (Hillary and FitzGerald 2018).

To study the effects of WDR44 and Rab11a silencing in UPR we analyzed the mRNA and protein levels of different UPR-related proteins by q-PCR and immunoblot, respectively, in shWDR44 and shRab11a HeLa cells. The results showed a decrease of spliced form XBP1s in shWDR44 and shRab11a cells, suggesting no activation of Ire1α UPR sensor in these conditions (Figure 37) . Consistently, WDR44 and Rab11a silenced cells showed lower Ire1α protein levels that correlates with XBP1s mRNA results (Figure 37). Even though Ire1α and XBP1s were decreased, the mRNA levels of chaperones BiP and ERdj4 were increased in shWDR44 and shRab11a cells (Figure 37), suggesting UPR activation.

We also study PERK signaling in shWDR44 and shRab11a cells. WDR44 silenced cells showed an increase of CHOP transcripts, as an ATF4 gene target, and higher GADD34 mRNA levels, which is a CHOP target gene (Figure 37). Consistently, WDR44 silenced cells showed an increase of PERK and eIF2α phosphorylation that strongly suggest activation of PERK signaling (Figure 38).

Interestingly, Rab11a silenced cells showed a different phenotype, which included a decrease of CHOP and no changes in GADD34 mRNA levels (Figure 37). Consistently, shRab11a cells showed no changes in eIF2α phosphorylation and lower levels of PERK, BiP and PDI (Figure 38).

Finally, we treated the cells with tunicamycin to compare the induced UPR-related genes in shControl, shWDR44 and shRab11a cells. shWDR44 cells showed higher mRNA levels of BiP, CHOP, ERdj4 and GADD34 compared to control cells, suggesting higher sensitivity to ER stress stimulus under WDR44 silencing (Figure 37).

It is important to note that even though WDR44 silencing induced PERK activation and higher mRNA levels of chaperones BiP and ERdj4, these cells showed a significative decrease

in protein levels of chaperones Calnexin, BiP, PDI and Ero1 compared with shControl cells (Figure 38). It is difficult to explain this lower protein level of chaperones. It might result from a sustained UPR condition.

Altogether, these results reveal that shWDR44 cells display ER stress activation suggesting a role of WDR44 in ER homeostasis.

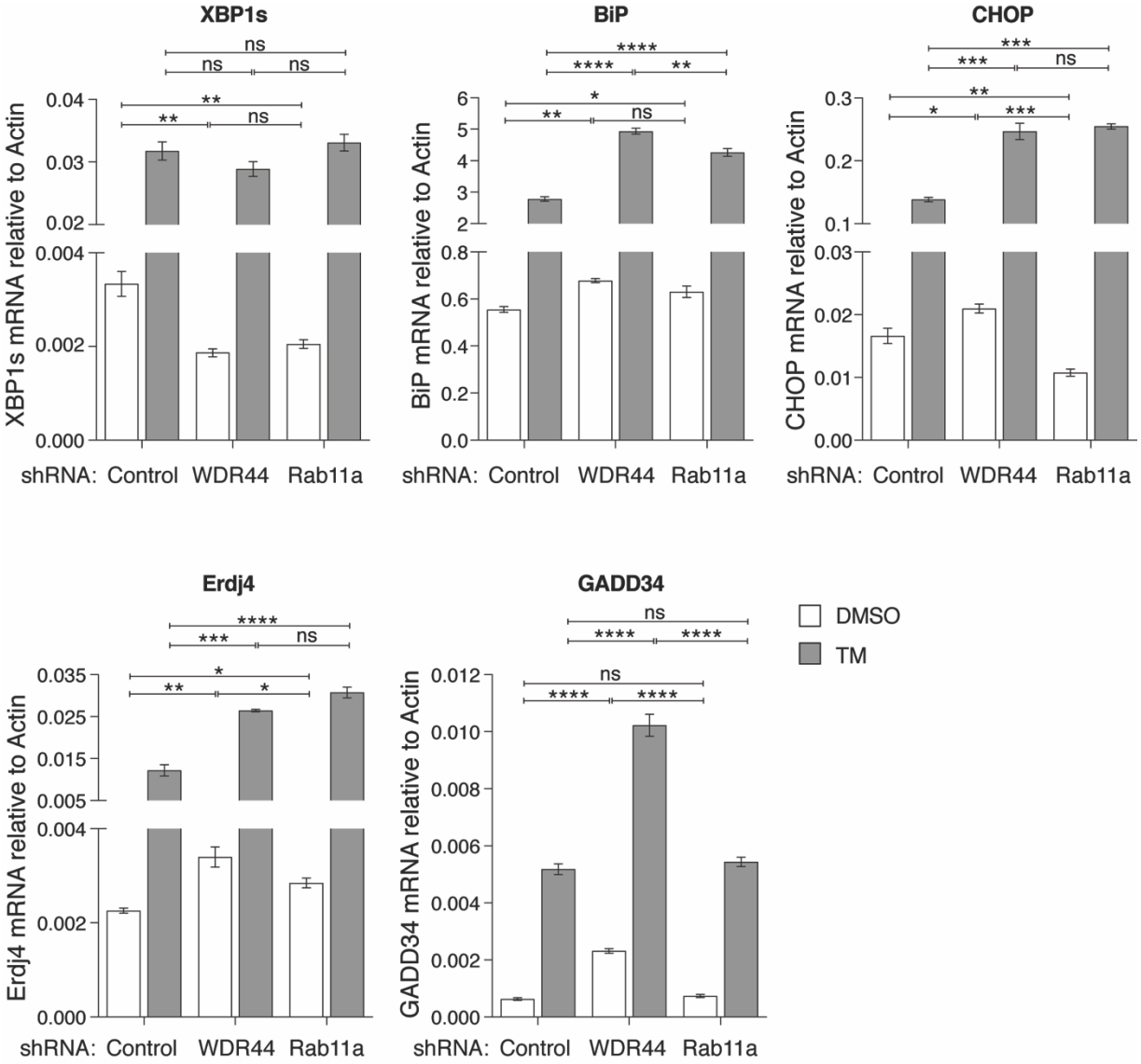

Figure 37. mRNA expression of UPR-related genes in WDR44 and Rab11a KD cells. qRT-PCR analysis of the mRNA levels of UPR-related genes normalized to actin, in Control, WDR44 and Rab11a silenced HeLa cells after DMSO and tunicamycin (10µg/mL) treatment. Data are means of n=3 ± SEM. Asterisks denote significant differences in one-way ANOVA comparing DMSO conditions * p<0.05, ** p<0.01, ***p<0.001, ****p<0.0001. *The experiments and the figure were made by Bernardita Medel during a PhD internship.*

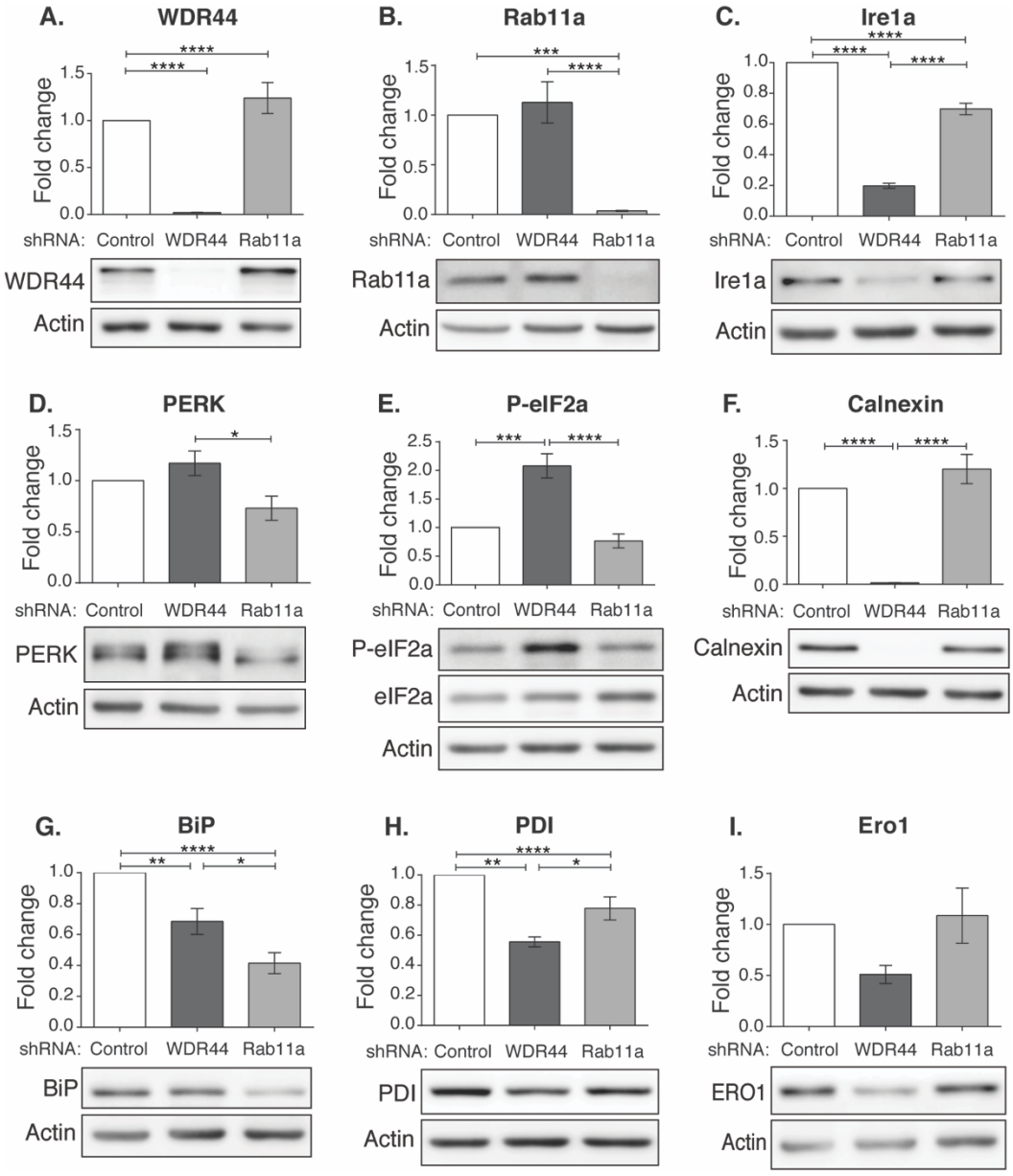

Figure 38. Analysis of UPR-related proteins in WDR44 and Rab11a KD cells. HeLa cells were silenced against to WDR44, Rab11a or Control. WDR44 **(A)** and Rab11a **(B)** silencing were confirm by immunoblot. Protein levels of different UPR markers were analyzed by immunoblot. **(C)** Ire1a, **(D)** PERK and **(E)** eIF2a were analyzed as UPR signaling markers. **(F)** Calnexin, **(G)** BiP, **(H)** PDI and **(I)** Ero1 were analyzed as ER chaperones. All data represent the mean of five independent experiments ± SEM. Asterisks denote significant differences in one-way ANOVA * $p<0.05$, ** $p<0.01$, ***$p<0.001$, ****$p<0.0001$.

3.4.4.5 Exploring mechanisms that underlay calnexin decrease in WDR44 depleted cells.

We further studied the potential mechanism that could explain the decreased level of calnexin in WDR44 depleted cells. Considering that WDR44 interacts with Rab1a and Rab1b, we analyzed the effect of Rab1a/b depletion on calnexin levels and PERK signaling. HeLa cells were silenced against Rab1a, Rab1b or both proteins using siRNA transfection, in a collaboration with Cristóbal Cerda from Patricia Burgos laboratory. Interestingly, we observed that silencing of Rab1a or Rab1b decreased the calnexin levels, and this effect was synergistical after both Rab1a and Rab1b depletion (Figure 39A, n=1). Additionally, It seems that Rab1a silencing weakly induced eIF2a activation, but this result was not as apparent as calnexin (Figure 39A). Thus, Rab1a and Rab1b silencing mimics the effect of WDR44 depletion on decreased levels of calnexin.

It has been described that silencing of Rab1b as well as the overexpression of the nucleotide empty-form mutant Rab1b-N121I decreases autophagosome formation (Zoppino, Militello et al. 2010). In order to evaluate if autophagy impairment affects calnexin levels, we analyzed calnexin in the ATG9A-deficient HeLa cell line (ATG9-KO), that lacks ATG9A, which mediates the delivery of membranes to preautophagosomal structures (Yamamoto, Kakuta et al. 2012, Mattera, Park et al. 2017). ATG9-KO cells showed similar levels of calnexin as control cells, revealing that autophagy deficiency does not decreases calnexin (Figure 39B, lanes 1 and 2, n=1).

We also evaluated whether the decrease of calnexin in WDR44 depleted cells is mediated by autophagy. We silenced WDR44 in ATG9-KO cells and we analyzed calnexin by immunoblot. We observed that depletion of WDR44 in ATG9-KO cells decreased calnexin as control cells, suggesting that silencing of WDR44 induces calnexin depletion by an autophagy-independent mechanism (Figure 39B, n=1).

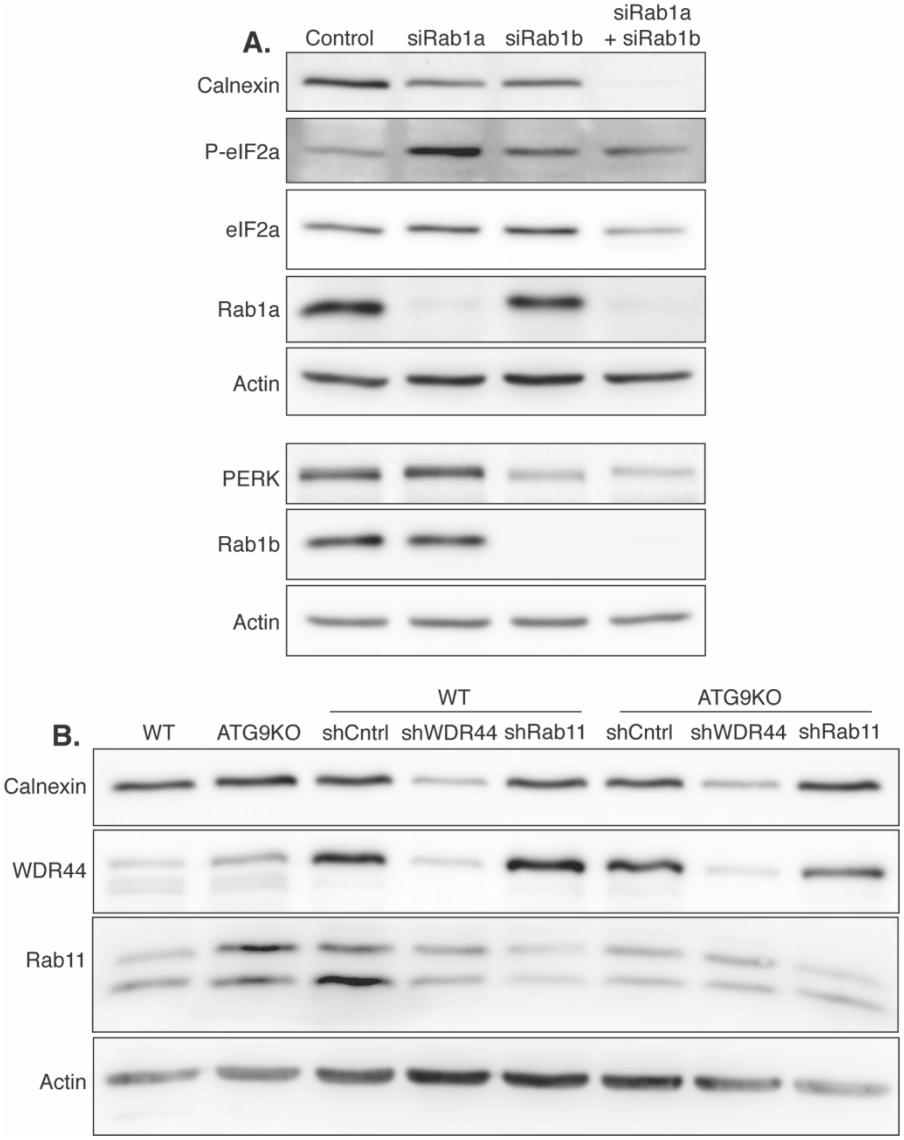

Figure 39. Analysis of Rab1 silencing and autophagy dependency on calnexin protein levels. A. HeLa cells were silenced against to Rab1a, Rab1b or both proteins by siRNA transfection, and proteins were analyzed by immunoblot (n=1). **B.** Wild-type and ATG9A Knock-out (ATG9KO)cells were silenced against to WDR44 or Rab11 using shRNA transduction and proteins were analyzed by immunoblot (n=1). *The Rab1a and Rab1b silencing were made by Cristóbal Cerda Troncoso, a PhD. student from Patricia Burgos Laboratory. All the immunoblots were made by Beatriz Vásquez.*

4. DISCUSSION

4.1 WDR44 structure and isoforms suggest unexplored protein-protein interactions.

WDR44 is the first described Rab11 binding protein but its function has been explored in just 5 reports (Zeng, Ren et al. 1999, Mammoto, Sasaki et al. 2000, Gardner, Hajjhussein et al. 2011, Walia, Cuenca et al. 2019, Lucken-Ardjomande Hasler, Vallis et al. 2020) The structure of WDR44 involves several protein-protein binding domains including a FFAT-like domain, a proline rich domain, the Rab-binding domain (RBD) and seven WD40 repeats. The FFAT-like domain is located within the residues 9-15 and binds to the ER-membrane proteins VAPA and VAPB (Baron, Pedrioli et al. 2014). The proline rich domain includes residues 210-256 and binds to GRAF-2, that is involved in membrane tubulation (Lucken-Ardjomande Hasler, Vallis et al. 2020). The RBD is located within the residues 334-504 and mediates the interaction with the membrane-bound Rab11 in a GTP-dependent manner (Zeng, Ren et al. 1999). A recent study describes that WDR44 and Rab11a interaction is regulated by Akt-mediated phosphorylation of Ser342/344 in WDR44 sequence (Walia, Cuenca et al. 2019). However, a later study revealed that the serum- and glucocorticoid-regulated kinase 3 (SGK3) but not Akt, phosphorylates to WDR44 at the Ser344 *in vitro* (Malik, Nirujogi et al. 2019). Finally, in other WD40-containing proteins, WD40 domains have been described to mediate protein-protein and protein-DNA interactions characteristic of scaffold proteins involved in a large variety of processes (Xu and Min 2011). The first and second WD40 repeats of WDR44 interact with Sec13, a subunit of COPII complex (Mammoto, Sasaki et al. 2000).

We detected by immunoblot three different forms of WDR44 with a molecular size of 143KDa, 124KDa and 108KDa. The expression of WDR44 tagged at the amino- and carboxi-terminus suggest that WDR44 is proteolytically cleaved at the amino-terminus domain within residues 175-225, losing the FFAT-like domain that interacts with VAPA/B and recruit WDR44 to the ER membranes (Lucken-Ardjomande Hasler, Vallis et al. 2020). Thus, the cleaved forms of WDR44 probably are differentially localized within the cell.

4.2 WDR44 interacts with Rab1a/b, Rab4a/b and Rab6A besides Rab11a.

Beyond the described Rab11a and VAPA/B interactions, the WDR44 structure and isoforms suggests interactions with additional proteins and still unexplored functions. Our WDR44 interactome analysis revealed 129 potential new interactions and confirmed the binding to Rab11a, VAPA and VAPB. We also evaluated the Rab11a interactome revealing 272 interacting proteins, among which only 54 are shared by the WDR44 interactome. This suggests that WDR44 has Rab11a-related and -unrelated functions.

We found cell-cell adhesion, actin filament bundle assembly, regulation of organelle assembly and translational initiation as common processes associated to WDR44 and Rab11a interactome datasets. However, among protein transport processes, Rab11a interactome displays an enrichment of proteins involved in endocytosis and exocytosis regulation. Instead, WDR44 interacting proteins are mainly related to transport from early to late endosomes, Golgi-to-ER and ER-to-Golgi.

Based on our finding that WDR44 interactome includes proteins involved in protein transport processes different from those related with the Rab11a interactome, we decided to focus on interacting proteins involved in the regulation of protein trafficking.

Rab GTPases coordinate protein trafficking at different levels, including formation, motility, tethering and fusion of vesicular and tubular carriers. They switch between an active

GTP-bound state that associates with specific membranes and inactive GDP-bound state released to cytoplasm. Interestingly, in addition to Rab11a, the WDR44 interactome suggested interactions with Rab4a, Rab4b, Rab1b, Rab6A and Rab10. We validated the interaction of WDR44 with Rab4a/b, Rab1a/b and Rab6A by GFP-trap and immunoblot assay. According with the interactome interaction scores, we also observed that each Rab co-precipitated different amounts of WDR44. Moreover, even though Rab11a co-precipitated the three forms of WDR44 (143KDa, 124KDa and 108KDa), Rab4a and Rab4b preferentially precipitated the 108KDa isoform of WDR44. Rab11a and Rab4a/b probably do not compete by WDR44 binding. Therefore, WDR44 might be able to participate simultaneously in Rab11a and Rab4a/b related processes. Rab1a, Rab1b and Rab6A interacted with the 143KDa WDR44 form but in a lesser extent than Rab11a. This may reflect differential affinities, indirect binding or regulation of their interactions through unknown mechanisms.

We then analyzed whether the coprecipitation of WDR44 with Rabs reflects a functional interaction. The incubation with GTPγS during precipitation assay increased the interaction of Rab11a with WDR44, indicating GTP-dependency (Zeng, Ren et al. 1999). In contrast, GTPγS decreased the interaction of Rab1b with WDR44, suggesting instead a GDP-dependent interaction. We cannot discard a displacement of the interaction between WDR44 and Rab1b due to an increase of WDR44 binding to other Rabs. In addition to the GTP/GDP bound state of Rabs, the differential affinities might depend on posttranslational modifications of WDR44. In fact, the interaction of WDR44 with the GTP-bound Rab11a is regulated by the Akt-mediated phosphorylation of WDR44 at Ser342/344, which under starving conditions is dephosphorylated triggering the dissociation of WDR44 from Rab11a and allowing the recruitment of FIP-3 and Rabin8 to Rab11a positive endosome and the constitution of primary cilia (Walia, Cuenca et al. 2019). This reveals that the Rab11-related functions of WDR44 are regulated and WDR44 might be displaced from recycling endosomes to other membranes in

particular cellular contexts where the interaction of WDR44 with other Rabs might occur. It would be interesting to evaluate the interaction of WDR44 with Rabs in starving or under Akt inhibitory conditions.

Altogether our results posit Rab1a/b, Rab4a/b and Rab6A as new interactors of WDR44. Those interactions depend on the WDR44 isoforms and may be regulated by the GTP/GDP state of Rab proteins. WDR44 seems to be a promiscuous Rab-binding protein that potentially participates in different protein trafficking routes, additionally to those involving Rab11a.

4.3 WDR44 localizes in sorting and recycling endosomes and Endoplasmic Reticulum.

We analyzed the distribution of endogenous WDR44 relative to RabGTPases coupled to EGFP expressed by transfection. As we previously mentioned, WDR44 has been described to distribute to perinuclear recycling endosomes and tubular endosomes associated with the ER, colocalizing in both cases with Rab11a (Zeng, Ren et al. 1999, Walia, Cuenca et al. 2019, Lucken-Ardjomande Hasler, Vallis et al. 2020). We found WDR44 colocalizing with Rab11a in vesicular structures likely corresponding to peripheral and perinuclear endosomes. We also observed partial colocalization with Rab4a and Rab4b.

Rab11a localizes to recycling endosomes and *Trans*-Golgi Network (TGN) where it functions in slow endocytic recycling and protein secretion, respectively (Ullrich, Reinsch et al. 1996, Chen, Feng et al. 1998). Recently, in Drosophila larval salivary gland, Rab11 has been described in secretory granules, regulating granule growth and secretion (Neuman, Lee et al. 2021). Rab4 has been described to regulate the rapid recycling pathway (Van Der Sluijs, Hull et al. 1991, de Renzis, Sonnichsen et al. 2002, Yudowski, Puthenveedu et al. 2009), and distributes to EEA1 early endosomes and TfR-containing endosomes (Sonnichsen, De Renzis

et al. 2000, van der Sluijs, Mohrmann et al. 2001). Consistently, WDR44 colocalizes with the recycling endosomes-related proteins TfR and the γ-Adaptin subunit of AP1 clathrin adaptor complex (Ullrich, Reinsch et al. 1996, Pagano, Crottet et al. 2004). Additionally, WDR44 seems to surround sorting endosomes labeled with EEA1, a well-known Rab5 effector (Christoforidis, McBride et al. 1999). Thus, in addition to recycling endosomes, our results show WDR44 closely related to sorting endosomes, likely due to its interaction with Rab4a and Rab4b. Considering the differential interaction of the WDR44 isoforms with Rab11a and Rab4, it seems possible that the shortest form of WDR44 is preferentially located to sorting endosomes. More experiments are needed to test this idea and evaluate how the WDR44 isoforms distribute in different populations of endosomes

Contrary to Rab11 and Rab4, we did not observe co-localization between WDR44 and Rab1a, Rab1b or Rab6A. Rab1 is described to predominantly localize to the ER-Golgi Intermediate Compartment and *cis*-Golgi membranes, though is also observed in autophagosomes (Plutner, Cox et al. 1991, Saraste, Lahtinen et al. 1995, Sannerud, Marie et al. 2006, Zoppino, Militello et al. 2010). Rab6A localizes in Golgi membranes from where it regulates intra-Golgi transport and COPI-independent Golgi-to-ER retrograde trafficking (Martinez, Schmidt et al. 1994, White, Johannes et al. 1999). Consistently, WDR44 did not colocalize with the cis-Golgi marker GM130 or the TGN protein p230 (Nakamura, Rabouille et al. 1995, Gleeson, Anderson et al. 1996), suggesting that WDR44 is not associated to Golgi membranes.

Rabs bind to specific membranes in a GTP-dependent manner. However, our functional analysis of WDR44 and Rab1b interaction suggests that both proteins interact in a GDP-dependent manner. Thus, it is probably that the interaction of WDR44 and Rab1b takes place in the cytoplasm and is not stable enough as to detect their colocalization at steady state by IFI assay. This may be supported by the potential interaction of WDR44 with the guanosine

nucleotide dissociation inhibitor 2 (GDI2) revealed by the interactome (Table I). GDI binds to several GDP-bound Rabs preventing their nucleotide exchange and their binding to the membranes (Wilson, Erdman et al. 1996, Shisheva, Chinni et al. 1999). More experiments would be required to clarify where the interactions of WDR44 with Rab1a/b and Rab6a take place and how are they regulated.

We also evaluated WDR44 localization relative to the ER. The distribution of endogenous WDR44 was similar to the localization pattern of BiP, a HSP70 chaperone localized within the lumen of the ER (Gething 1999). Both proteins show co-localization in perinuclear and peripheral regions, suggesting that WDR44 localizes to ER membranes, which has been previously described by the colocalization of WDR44 with calnexin and VAPA/B (Lucken-Ardjomande Hasler, Vallis et al. 2020). The association of WDR44 to the ER relies on its binding to VAPA/B mediated by the FFAT-like domain, that is probably cleavage in short forms of WDR44 (Lucken-Ardjomande Hasler, Vallis et al. 2020). Thus, the ER-associated WDR44 isoform should necessarily be the full-length protein.

Altogether these results show that WDR44 localizes to sorting and recycling endosomes probably mediated by the interaction with Rab11a and Rab4a/b, and also localizes to the ER, as previously described (Lucken-Ardjomande Hasler, Vallis et al. 2020).

Finally, WDR44 endosomal structures seem to decorate actin filaments close to the cell cortex and also colocalizes with the F-actin cross-linking protein actinin-4 (data not shown). Actinin-4 is suggested to be a WDR44 and Rab11a interacting protein according to the interactome datasets. WDR44 also colocalized with tubulin filaments at perinuclear and peripheral regions.

4.4 WDR44 is involved in protein transport from perinuclear recycling endosomes to the cell surface.

Although WDR44 was described more than twenty years ago as the first Rab11a-interacting protein, its function in protein transport has remaining almost completely unexplored. We address this issue by silencing WDR44 in HeLa cells by shRNA transduction and testing first endocytic recycling, based on the known role of Rab11a. We also silenced Rab11a as comparison.

For TfR recycling we preloaded the cell surface with Tf-Alexa488 (Tf-488), then Tf-488 was internalized during 30min at 37ºC; remaining Tf-488 at the plasma membrane was removed and we let to Tf-488 recycles back to the plasma membrane during different; finally, internal Tf-488 was quantified by FACS. Under this experimental setting we could not find an effect of WDR44 depletion on the endocytic recycling of transferrin receptor (TfR), even though both WDR44 and TfR colocalized in endosomal structures. Furthermore, Rab11a silencing neither affected TfR recycling in our assay. This is unexpected considering the vast literature involving Rab11a in TfR trafficking. One possibility is that Rab11b and Rab11c/Rab25, which also regulate TfR trafficking (Schlierf, Fey et al. 2000, Wang, Kumar et al. 2000), might compensate for the lack of Rab11a. It is also possible that our assay does not cover the entire recycling route of the TfR, which includes early peripheral endosomes in its fast recycling (4 min) and perinuclear recycling endosomes accounting for the low recycling pathway (20 min) (Sheff, Daro et al. 1999, Sheff, Pelletier et al. 2002). Perhaps our assay mostly analyzed the Rab4-dependent fast recycling pathway from sorting endosomes instead of the Rab11-dependent slow recycling route from the perinuclear recycling compartment.

Endocytic vesicles converge toward peripheral early endosomes (EE) decorated with Rab5, the first compartment where proteins are sorted towards degradation in lysosomes or to recycling routes towards the plasma membrane (Woodman 2000). The sorting function of EEs

relies on the presence of distinct membrane domains involved in the generation of tubular vehicles, including Rab4, retromer or retriever tubules, which sort proteins to the cell surface through a fast recycling route that has 4 min halftime. Otherwise proteins can be transported to the Rab11 perinuclear recycling endosome (RE) that mediates a more slowly recycling pathway (20 min half-life) to the plasma membrane. Tf access EEs within 2min of internalization and takes about 25 min to reach REs, times in which both compartments are maximally resolvable (Sheff, Pelletier et al. 2002). We did not evaluate the intracellular distribution of Tf after 30min of endocytosis and therefore the starting point of Tf recycling might not be synchronized between control and silenced cells. Consistently, our results show that depletion of WDR44 induces Rab11a redistribution from perinuclear to more peripheral localization, suggesting that the REs might be functionally compromised and our FACS assay is not detecting such potential compromise. Previous studies show that 76% of recycled TfR proceeds solely through EEs while 24% traversed through REs in CHO cells (Sheff, Pelletier et al. 2002). This is consistent with MDCK cells in which 65% of TfR does not traffic through RE before reaching the plasma membrane (Sheff, Daro et al. 1999). Therefore, we thought necessary to design an assay that synchronizes the TfR trafficking at the REs. We achieved this requirement using propranolol as an inhibitor of the recycling route, which can be conveniently evaluated following the epidermal growth factor receptor (EGFR) trafficking, as recently described in our laboratory (Metz, Oyanadel et al. 2021).

EGFR recycling has been described to depend on Rab11 and Rab4 (McCaffrey, Bielli et al. 2001, Cullis, Philip et al. 2002, Palmieri, Bouadis et al. 2006, Caswell, Chan et al. 2008). Propranolol, used to inhibit phosphatidic acid (PA) hydrolysis and trigger a PA pathway leading to a decrease in basal protein kinase A activity, induces ligand-independent EGFR endocytosis and accumulation in perinuclear recycling endosomes due to recycling arrest (Norambuena, Metz et al. 2010), which also compromises the recycling of TfR and LDLR, to constitutively

recycling receptors (Metz, Oyanadel et al. 2021). After propranolol removal, the EGFR recycles back to the plasma membrane from the perinuclear compartments (Norambuena, Metz et al. 2010), where Rab11 is functionally active (Campa, Margaria et al. 2018). Thus, we use propranolol as a tool for studying the effect of WDR44 silencing upon EGFR recycling from perinuclear recycling endosomes.

A cell surface biotinylation assay shows that propranolol treatment induced EGFR endocytosis in WDR44 silenced cells. However EGFR remained endocytosed after propranolol removal, revealing a decreased recycling from perinuclear RE in WDR44 KD cells. In addition, WDR44 depletion decreased total EGFR, which might be due to an imbalance of recycling and degradative transport rates. Because propranolol also inhibits recycling of TfR and LDLR (Metz, Oyanadel et al. 2021), this approach can be used in future experiments to further characterize the role of WDR44 in the perinuclear recycling endosomes extending the assessment to TfR and LDLR.

Different Rab11a effectors, including WDR44, has been involved in recycling selective cargoes. For instance, the β1-adrenergic receptor (β1-AR) traffics through Rab4a-positive sorting endosomes and then reaches perinuclear recycling endosomes colocalizing with Rab11a, which regulates β1-AR recycling from this compartment (Gardner, Hajjhussein et al. 2011). The same study shows that WDR44 or FIP3 silencing did not affect the endocytosis of β1-AR, but once endocytosed, this receptor became confined in punctate vesicles distributed throughout the cell, suggesting that WDR44 and FIP3 are involved in vesicular transport rather than fusion with the recycling compartment (Gardner, Hajjhussein et al. 2011). Silencing of Myosin Vb or FIP2, another two Rab11 effectors, also inhibit the β1-AR recycling leading to its accumulation in perinuclear endosomes. This suggests that Myosin Vb or FIP2 would work at a different levels compared with WDR44 and FIP3 in β1-AR recycling. Instead, FIP1/RCP, FIP5/Rip11 or FIP4 seemed not involved in β1-AR endocytosis or recycling (Gardner,

Hajjhussein et al. 2011). FIP5/Rip11, FIP2 and RCP have been related to the recycling of GLUT4, aquaporin2 and EGFR/α5β1 integrin, respectively (Nedvetsky, Stefan et al. 2007, Caswell, Chan et al. 2008, Schonteich, Wilson et al. 2008). All these data support the notion that Rab11 effectors can provide specificity to cargo recycling and regulate temporally and spatially distinct steps of Rab11-dependent recycling pathway. Our results indicate that WDR44 would be at least involved in recycling of EGFR.

4.5 WDR44 is involved in cell migration and invasion

Cell migration and invasion are cellular processes that require a continuous and polarized vesicular transport and protein recycling to the plasma membrane, where Rab11 and Rab4 are key regulators. Thus, we studied the effects of WDR44 silencing in cell migration and invasion by wound closure and trans-well assays. WDR44 depletion reduced cell migration both, in wound closure and trans-well experiments and it also strongly decreased cell invasion in matrigel-treated trans-wells. These results might be related with the effect of WDR44 silencing upon EGFR recycling.

Rab11 regulates integrin recycling from perinuclear recycling endosomes through its interaction with Rab11-FIP proteins, such as RCP. In tumor cells an enhanced migration/invasion capability has been associated with increased recycling of α5β1 integrin coupled to EGFR (Caswell, Chan et al. 2008). Even though Rab11 and Rab4 regulates integrin recycling, down-regulation of WDR44 was not found to affect β1 integrin recycling (Lucken-Ardjomande Hasler, Vallis et al. 2020). Therefore, the role of WDR44 in cell migration and invasion might not be related with integrin trafficking and might be more associated with cytoskeletal rearrangements, which are required for these processes (Schaks, Giannone et al. 2019).

We found in the interactome that WDR44 interacts with several proteins related with actin filament bundle assembly, including the ERM proteins Ezrin, Radixin and Moesin, Actinin-1 and Actinin-4 (ACTN1 and ACTN4), that are dimeric actin filament cross-linking proteins, and the scaffold protein IQGAP, that mediates the assembly of regulatory complexes of cytoskeletal dynamics (Hedman, Smith et al. 2015, Murphy and Young 2015, Garcia-Ortiz and Serrador 2020). All of these proteins were also present in the Rab11a interactome dataset, suggesting that they could be participating in processes involving Rab11 and WDR44. Consistently, we found WDR44 colocalization with actinin-4 and F-actin at the cell cortex. All these data suggest that WDR44 might participate in cell migration and invasion processes through its interactions with actin cytoskeleton regulators. This would be a new interesting research focus considering its relevance during cancer progression and metastasis. The role of these interactions in the involvement of WDR44 in cell migration and invasion remains to be further explored in future studies

In addition, WDR44 has also been recently related to the secretion of the neosynthesized proteins E-cadherin and metalloproteinase 14 (MMP-14) from an uncharacterized perinuclear compartment (Lucken-Ardjomande Hasler, Vallis et al. 2020). E-cadherin is a cell-cell adhesion protein that contributes to the maintenance of cell polarity. In collective cell migration, E-cadherin works as a mechanotransducer between actin assembly and Rac signaling, that induce cell cluster polarization and its forward-directed movement (Cai, Chen et al. 2014). On the other hand, MMP14 mediates extracellular matrix remodeling and cell migration during cancer metastasis (Zarrabi, Dufour et al. 2011). Thus, WDR44 might be involved in cell invasion through its function upon E-cadherin and MMP-14 secretion.

4.6 WDR44 is involved in Golgi structure maintenance

Our results unexpectedly show that WDR44 depletion induced dispersion of the Golgi complex, analyzed by GM130 and TGN46 markers. It also decreased the levels of Golgi proteins Furin and TGN46. In contrast, Rab11a depletion did not affect Golgi morphology, consistently with previous reports (Galea and Simpson 2015). Rab1b and Rab6A, which our results indicate interaction with WDR44, and known to associate with Golgi (Marie, Dale et al. 2009, Dickson, Liu et al. 2020), kept such association in WDR44 depleted cells. This suggests that Golgi fragmentation under WDR44 silencing preserves the composition of the fragments. A role of WDR44 in Golgi morphology and homeostasis has not been described and might be related with the role of Rab1, which depletion also induces Golgi fragmentation in different cell lines (Slavin, Garcia et al. 2011, Galea and Simpson 2015). It would be interesting to test whether overexpression of Rab1 restores the Golgi fragmentation in WDR44 depleted cells.

4.7 WDR44 functions in Golgi-to-ER retrograde transport of KDELR.

Golgi architecture maintenance also depends on the balance of protein transport at the ER-Golgi interface. The interactome of WDR44 suggested interactions with proteins related with the Golgi-to-ER retrograde transport, including Rab1a/b, Rab6A and three subunits of COPI coat complex αCOP, βCOP and δCOP (ARCN1). Rab11a and Rab4b have also been related with Golgi-to-ER retrograde transport (Galea, Bexiga et al. 2015). Furthermore, WDR44 localizes at the ER due to its interaction with the ER membrane proteins VAPA and VAPB (Baron, Pedrioli et al. 2014, Lucken-Ardjomande Hasler, Vallis et al. 2020). Therefore, we analyzed the WDR44 function in protein transport at the ER-Golgi interface using KDELR as protein model.

Our results revealed that WDR44 silencing decreased Golgi-to-ER retrograde transport of KDELR-GFP, increasing its accumulation at the Golgi. Bovine BtWDR44-HA rescued the

Golgi accumulation of KDELR-GFP in WDR44 depleted cells, thus indicating a specific effect of WDR44 silencing on this process rather than an off-target effect. However, BtWDR44-HA expression during 16h did not rescue Golgi fragmentation in WDR44 silenced cells, probably because this phenotype requires a more complex machinery rearrangement. We also observed that WDR44 silencing does not affect the localization of KDELR(D193N) in the Golgi, indicating that it does not affect the ER-to-Golgi anterograde transport. Thus, our results reveal that WDR44 is involved in Golgi-to-ER retrograde transport of KDELR.

The mechanism by which WDR44 depletion inhibits Golgi-to-ER retrograde transport remains unknown. It is possible to be related with its interaction with Rab1 and COPI. Rab1 regulates the Golgi-to-ER retrograde transport by its interaction with GBF1 that is the GEF of Arf1 (Garcia-Mata, Szul et al. 2003, Monetta, Slavin et al. 2007), which induces the recruitment of COPI coat to Golgi membranes (Alvarez, Garcia-Mata et al. 2003). On the other hand, COPI-coated vesicles are one of the main Golgi-to-ER retrograde transport carriers (Haase and Rabouille 2015, Custer, Foster et al. 2019). The Golgi-to-ER transport of the KDELR depends on COPI-coated vesicles (Cabrera, Muniz et al. 2003). Thus, WDR44 might be involved in the retrieval of KDELR towards the ER through its interaction with Rab1 and the COPI coat subunits. It would be interesting to evaluate if WDR44 is also involved in the transport of another COPI-dependent cargoes.

Even though Rab11a is localized in endosome membranes, it has also been observed in a minor fraction (<5%) of BFA-induced Golgi-derived carriers in HeLa cells (Galea, Bexiga et al. 2015). Depletion of Rab11a has been described to inhibit the Golgi-to-ER transport of N-Acetylgalactosamine under BFA treatment. Accordingly, our results also revealed that Rab11a silencing decreased the Golgi-to-ER transport of KDELR. These results suggest a little explored role of Rab11a at the ER-Golgi interface and opens the possibility that Rab11 is

involved in the mechanism by which WDR44 plays a role in the Golgi-to-ER transport of KDELR.

Several studies reveal that the inhibition of Golgi-to-ER transport induces Golgi fragmentation, as we observed in WDR44 depleted cells. Rab1a or Rab1b silencing induce Golgi fragmentation in HeLa cells (Galea and Simpson 2015). The down-regulation βCOP also induce Golgi fragmentation in HeLa (Saitoh, Shin et al. 2009) and *in vitro* incubation of Golgi stacks in the absence of COPI coatomer induces cisternal fenestration (Misteli and Warren 1994). Thus, the inhibition of Golgi-to-ER retrograde transport, induces Golgi fragmentation, that might be the case in the WDR44 depleted cells. It would be interesting to evaluate whether WDR44 depletion affects the availability of Rab1 and COPI or their recruitment to the *cis*-Golgi and the ERGIC.

4.8 KDEL-containing Protein disulfide isomerase is miss-transported to the plasma membrane under WDR44 deletion

KDELR recognizes KDEL-containing ER resident proteins within the Golgi (Lewis, Sweet et al. 1990, Semenza, Hardwick et al. 1990, Vaux, Tooze et al. 1990) and mediates their retrieval to the ER in COPI coated vesicles (Majoul, Straub et al. 2001). Therefore, an expected consequence of a failure in its trafficking back to the ER is its saturation with KDEL-bearing chaperones. As a consequence, KDEL-bearing chaperones would follow the exocytic pathway towards the cell surface instead of recycling to the ER.

Pelham H. et al. (1988), first showed that deletion of the KDELR ortholog in yeast leads to the secretion of HDEL-containing proteins, equivalent to the KDEL-containing proteins in mammals (Pelham 1988, Pelham, Hardwick et al. 1988). KDELR saturation occurs under ER stress conditions resulting in the secretion of KDEL-bearing (Yamamoto, Hamada et al. 2003). These data prompted us to test whether WDR44 depletion reproduces these effects, as an

independent evidence of KDELR trafficking alteration. To this end, we chose protein disulfide isomerase (PDI) as a well-known ligand of KDELR, known to become secreted when its KDEL sequence is removed (Mazzarella, Srinivasan et al. 1990). Furthermore, PDI has been detected at the cell surface under certain conditions (Zai, Rudd et al. 1999)

We found higher levels of PDI at the cell surface when WDR44 or Rab11a are silenced, thus suggesting that its recycling to the ER became impaired under these conditions. The higher levels of PDI surface levels seen under WDR44 relative to Rab11a silencing might be due to a compensatory effect of the enhanced WDR44 expression observed in Rab11a silenced cells.

4.9 Analysis of the unfolded protein response triggered under WDR44 silencing

ER-resident chaperones, oxidoreductases, and glycosylation enzymes mediate protein folding as crucial constituents of the ER quality control system. An imbalance in the availability of these proteins might be expected to trigger the unfolded protein response (UPR). The UPR can be evaluated through the three ER transmembrane proteins known to work as unfolded protein sensors: Ire1α, PERK and ATF6. These sensors are normally interacting with the chaperone BiP in the lumen of the ER and this interaction is displaced when the levels of unfolded proteins increase and capture BiP. Dissociation from BiP activates these UPR sensors, which in turn increases the expression of chaperones and decreases protein translation as a mechanism designed to compensate protein folding demands (Read and Schroder 2021). Therefore, UPR offered an additional way of analyzing the consequence of WDR44 silencing related with the KDELR trafficking alteration eventually leading to an impaired ER chaperone function in the ER.

We show that WDR44 silenced cells have an increased levels of PERK and increased phosphorylation of the translation initiation factor 2 (eIF2α), indicating activation of the PERK

signaling cascade that downregulates protein translation (Hamanaka, Bennett et al. 2005). Also in the same pathway, WDR44 KD cells showed higher mRNA levels of PERK signaling target genes such as the transcription factor CHOP and the growth arrest and DNA damage-inducible protein GADD34. In addition, WDR44 silencing strongly decreases the levels of Ire1α and its mediated XBP1 splicing product. PERK activation and Ire1α signaling decrease reflect late stages of UPR and a failed ER-stress adaptation (Chang, Lawrence et al. 2018).

A persistent activity of PERK is known to induce the transcription of pro-apoptotic genes and promotes cell death (Iurlaro and Munoz-Pinedo 2016). The signs of prolonged UPR found in WDR44 silenced cells might explain why we could not obtain stably WDR44 silenced HeLa cells and we have to do all the functional experiments under acute WDR44 depletion conditions. WDR44 depletion seems to promote an irresolvable ER stress.

Interestingly, we did not observe similar UPR characteristics under Rab11a depletion. Neither eIF2α phosphorylation nor the mRNA levels of CHOP and GADD34 became altered when Rab11a is silenced. Rab11a silencing did not induce PERK- or Ire1α -mediated UPR under our conditions, thus differing from the WD44R silencing.

We also analyzed several chaperones well-known to increase upon UPR activation. WDR44 silencing increased the mRNA levels of BiP and its co-factor ERdj4, as expected for the activation of UPR (Sato, Urano et al. 2000, Dong, Bridges et al. 2008). However, we found decreased the protein levels of BiP, as well as PDI, two KDELR-bearing chaperones whose retention within the Golgi-to-ER recycling pathway would be impaired under WDR44 silencing. A similar observation of the decreased levels of PDI oxidase Ero1, which is also retained by the KDELR system (Anelli, Alessio et al. 2003, Otsu, Bertoli et al. 2006), further suggest loss of proteins levels due to missorting in the exocytic route.

An interesting observation, though difficult to explain, is the sharp decrease observed in the levels of the ER transmembrane chaperone calnexin when WDR44, Rab1a or Rab1b are

depleted. Calnexin is not a KDELR dependent chaperone and it is retained at the ER by different mechanisms. Calnexin phosphorylation within the cytosolic domain enhances its association with membrane-bound ribosomes, which contributes to its retention in the ER (Chevet, Wong et al. 1999). An interaction with the sorting protein PACS-2, involving COPI in a ternary complex, also retains calnexin within the ER (Myhill, Lynes et al. 2008). It is tempting to speculate that an impaired COPI-mediated trafficking from Golgi-to-ER might be the common alteration impinged by the silencing of WDR44 and Rab1 proteins leading to calnexin instability.

Calnexin seems to be synthesized in excess (5 fold) than needed and most of it is degraded (Dallavilla, Abrami et al. 2016). Calnexin has a half-life of 5h, which increases to 46h after dual palmitoylation in its cytoplasmic domain (Dallavilla, Abrami et al. 2016). Calnexin palmitoylation can be inhibited by its phosphorylation leading to its increased turnover (Dallavilla, Abrami et al. 2016). The steady state levels of calnexin are regulated by the transmembrane ubiquitin ligase Nixin/ZNRF4 that mediates its proteasome-dependent degradation (Neutzner, Neutzner et al. 2011). Additionally, calnexin is a FAM134 co-receptor for misfolded procollagen and together, calnexin and FAM134, mediates LC3-dependent autophagic degradation of procollagen in a process that also might include degradation of calnexin itself (Forrester, De Leonibus et al. 2019). We show that WDR44 depletion decreases calnexin even in the autophagy deficient cells ATG9-KO. Therefore, WDR44 seems to be involved in calnexin stability through a mechanism independent of autophagy. Further experiments are required to evaluate the different mechanisms that might be involved in the decreased levels of calnexin of WDR44 depleted cells.

4.10 Emerging role of WDR44 in Golgi-to-ER retrograde transport

Our results involve for the first time WDR44 in the Golgi-to-ER retrograde transport of the KDELR. KDEL-containing proteins are recognized at the Golgi lumen by the KDELR, which in turn interacts with COPI through its cytosolic tail. Rab1a and Rab1b at the Golgi recruit Arf-GEF GBF1 that activates the small GTPase Arf1, enhancing its Golgi localization (Dumaresq-Doiron, Savard et al. 2010). GTP-bound Arf1 interacts with coatomer subunits β and γCOP allowing coat stabilization (Zhao, Helms et al. 1997). The accumulation of GTP-bound Arf1 together BARS and endophilinB proteins, as well as phosphatidic acid and diacylglycerol, at the neck of the emerging vesicle triggers vesicle scission (Yang, Lee et al. 2005, Park, Yang et al. 2019). After vesicle release, ArfGAP1 induces GTP hydrolysis of GTP-bound Arf1, leading to partial coat dissociation. Some COPI components are retained during vesicle movement, which are then required for vesicle docking at the ER (Travis, Kokona et al. 2019). This docking process involves the heterotrimeric B-subcomplex of COPI coat (αCOP, βCOP and εCOP) particularly αCOPI and εCOPI subunits that bind to the NRZ-tethering complex (NAG, RINT1 and ZW10) (Hirose, Arasaki et al. 2004, Hsia and Hoelz 2010) . Finally, the fusion of COPI vesicles with the ER membrane relies in the v-SNARE, ERS24 and the t-SNAREs Sec22b, Use1, BNIP1 and syntaxin 18 (STX18) (Tagaya, Arasaki et al. 2014). Based on this data and our results we can propose a model of WDR44 function in the Golgi-to-ER transport of the KDELR, whereby WDR44 would participate in the docking of COPI-coated vesicles to the ER.

The following set of results suggest a role of WDR44 in the docking of COPI vesicles to the ER: 1. We did not find WDR44 in Golgi but instead colocalizing with BiP, indicating an ER distribution that corroborates previous observations (Baron, Pedrioli et al. 2014, Lucken-Ardjomande Hasler, Vallis et al. 2020); 2. Our interactome show potential interactions of WDR44 with Rab1a/b and the COPI subunits αCOP, βCOP and δCOP. At least we corroborated the interaction with Rab1a/b in coimmunoprecipitation experiments. The

interaction with COPI should be addressed in future experiments; 3. GTPγS decreased WDR44 and Rab1b interaction, suggesting that WDR44 preferentially binds to Rab1b-GDP, which is still present in vesicles arriving to the ER, as vesicle uncoating by GTP hydrolysis started before; 4. Our interactome and published data show that WDR44 binds to VAPA/B, which are ER-resident tethers for many organelles (Rocha, Kuijl et al. 2009, De Vos, Morotz et al. 2012, Zhao, Liu et al. 2018, Lucken-Ardjomande Hasler, Vallis et al. 2020). VAPA/B is involved in ER-to-Golgi interface transport; overexpression of VAPA inhibits the ER-to-Golgi transport of VSGV (Prosser, Tran et al. 2008) and VAPB inhibition leads to accumulation of COPI-coated vesicles due decreased vesicle consumption (Soussan, Burakov et al. 1999). Additionally, depletion of VAPA and VAPB induces Golgi fragmentation and inhibition of Golgi-mediated transport (Peretti, Dahan et al. 2008), similar to WDR44 silencing. A recent analysis of VAPA/B interactomes suggest that VAPA and VAPB interacts with the tethering factors RINT1 and ZW10, and the SNAREs Sec22b and STX18 (Weir, Xie et al. 2001, Cabukusta, Berlin et al. 2020). Therefore, WDR44 might contribute together with VAPA/B to the ER tethering of COPI vesicles through its interaction with COPI and Rab1 (Figure 40).

Since Rab11a depletion decreases KDELR Golgi-to-ER transport, we cannot discard that Rab11a could also be involved in protein transport at the ER-Golgi interface. In fact, Rab11a silencing decreases the Golgi-to-ER retrograde transport of the Golgi protein GalNAc-T2 under BFA treatment without affecting Golgi morphology (Galea and Simpson 2015). WDR44 interacts with Rab11a by a Rab Binding Domain (RBD) which differs from the FFAT-like domain that mediates the WDR44 and VAPA/B interaction. Considering this, the binding of WDR44 with Rab11a or VAPA/B are not exclusive and could occur at the same time. Consistently, same as WDR44, Rab11a interactome revealed a potential interaction with αCOP, but with a lower binding score than WDR44. Thus, our results reveals a potential and

unexplored role of Rab11a in Golgi-to-ER retrograde transport that could be related to WDR44 function.

The Golgi structure also relies on its membrane lipid composition. There is much evidence supporting the role of the ER transmembrane proteins VAPA and VAPB (VAPA/B) in regulating the lipid composition of the Golgi membrane. VAPA/B interact with the FFYT motif of the lipid-transfer/binding proteins Nir2, the oxysterol-binding protein (OSBP) and the ceramide-transfer protein (CERT), that also bind to phosphatidylinositols in the Golgi membranes, allowing the nonvesicular lipid transport from the ER (Amarilio, Ramachandran et al. 2005, Kawano, Kumagai et al. 2006, Peretti, Dahan et al. 2008, Mesmin, Bigay et al. 2013). Consistently, VAPA/B depletion reduces phosphatidylinositol-4-phosphate (PI4P), diacylglycerol (DAG) and sphingomyelin (SM) in Golgi membranes, and induces unstacked Golgi structure (Peretti, Dahan et al. 2008). VAPA/B depletion does not affect the ER-to-Golgi transport of VSV-G, but it decreases its TGN-to-PM trafficking, inducing long VSV-G tubules at the TGN and suggesting an impaired fission of the TGN-derived carriers (Peretti, Dahan et al. 2008). VAPA/B silencing decreases the TGN-to-lysosomes transport of cathepsin D, that is consistent with the decrease of the AP1 subunit γ-adaptin at Golgi and redistributes the KDELR to the ER, that normally cycles between the ER and the cis-Golgi (Peretti, Dahan et al. 2008). Since VAPA/B silencing does not affect ER-to-Golgi transport of VSV-G, it seems that the Golgi-to-ER retrograde transport is perturbed in VAPA/B depleted cells (Peretti, Dahan et al. 2008). Thus, depletion of WDR44 might affect the function of VAPA/B in nonvesicular lipid transport at the ER-Golgi contacts sites affecting vesicular protein transport and Golgi structure.

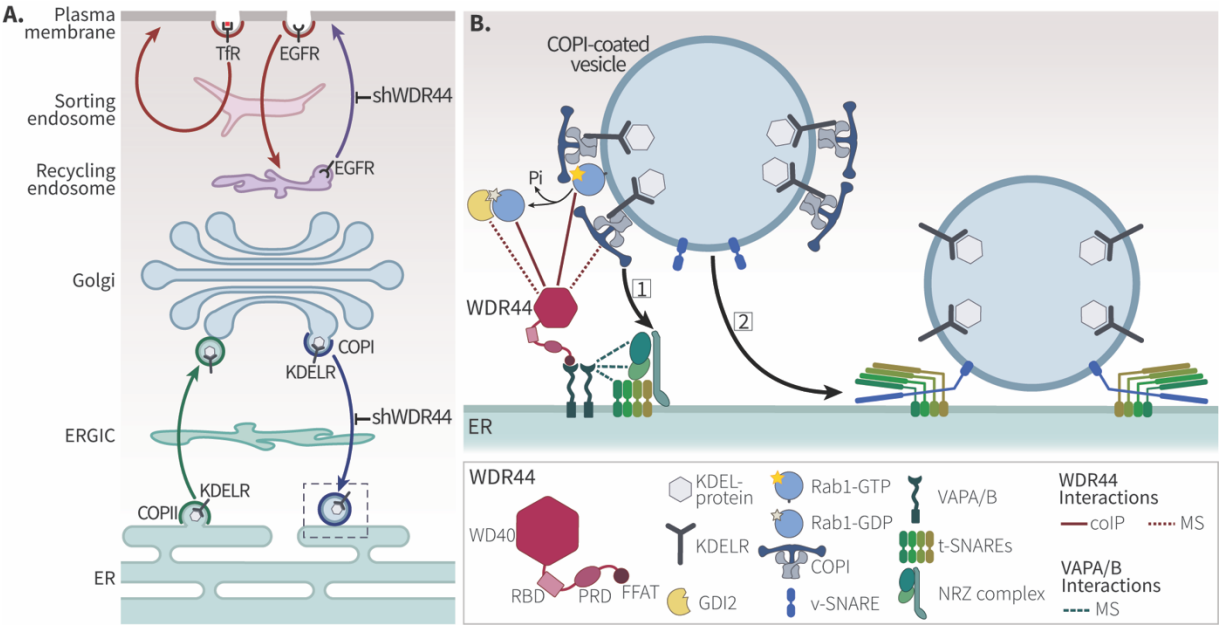

Figure 40. Graphical abstract of WDR44 functions in vesicular protein transport evaluated in this thesis. A. WDR44 depletion impairs the endocytic recycling of EGFR from the perinuclear recycling endosomes (purple arrow) and seems do not affect the fast recycling of TfR through the sorting/early endosomes. Silencing of WDR44 decreases the Golgi to-ER retrograde transport of KDELR without affecting its anterograde ER-to-Golgi trafficking. **B.** Suggested mechanism that underlay the role of WDR44 in Golgi-to-ER transport (dashed line box in A) **(1)** The KDELR is transported from the Golgi to the ER in COPI-coated vesicles (Cabrera, Muniz et al. 2003). COPI-vesicles partially retain the coat and Rab1 during the arrival to the ER. Remaining coat is recognized by the tethering complex NRZ (RINT1, ZW10 and NAG) which is associated to t-SNAREs (Sec22b, STX18, BNIP1, Use1) (Hirose, Arasaki et al. 2004, Hsia and Hoelz 2010, Tagaya, Arasaki et al. 2014) . **(2)** After the docking, the fusion of the vesicle takes place through the interaction of t-SNAREs and the v-SNARE ERS24 (Tagaya, Arasaki et al. 2014). Recent evidence has suggested that the ER tethering proteins VAPA and VAPB interact with the ER tethering complex NRZ and the t-SNARES Sec22b and STX18 (1, green dashed lines) (Cabukusta, Berlin et al. 2020). WDR44 interacts with VAPA/B and it localizes to the ER (Lucken-Ardjomande Hasler, Vallis et al. 2020). Our results reveal that WDR44 interacts with Rab1 (red lines) probably in a GDP-dependent manner and their also suggest the interaction with three subunits of COPI complex and GDI (dashed red lines). In this scenario, WDR44 might participate in the docking of COPI-coated vesicles at the ER, through its interaction with VAPA/B, Rab1 and COPI.

5. CONCLUSIONS

Our results suggest that WDR44 participates in endocytic recycling from the perinuclear recycling endosome and for the first time involve to WDR44 in the Golgi-to-ER retrograde transport.

Our WDR44 interactome suggests the interaction with proteins related with endocytic recycling as Rab4a and Rab4b and protein trafficking at the ER-Golgi interface as Rab1b, Rab6A, subunits of COPI coat complex and VAPA/B. We validated the interaction with Rab1a/b, Rab6A and Rab4a/b.

Our functional assays reveal that WDR44 is involved in the endocytic recycling of EGFR from the perinuclear recycling endosome towards the plasma membrane and cell migration and invasion.

WDR44 is involved in the Golgi-to-ER retrograde transport of the KDELR having an impact upon the localization of KDEL-containing chaperones, Golgi morphology and the unfolded protein response.

BIBLIOGRAPHY

Allan, B. B., B. D. Moyer and W. E. Balch (2000). "Rab1 recruitment of p115 into a cis-SNARE complex: programming budding COPII vesicles for fusion." Science **289**(5478): 444-448.

Alvarez, C., R. Garcia-Mata, E. Brandon and E. Sztul (2003). "COPI recruitment is modulated by a Rab1b-dependent mechanism." Mol Biol Cell **14**(5): 2116-2127.

Amarilio, R., S. Ramachandran, H. Sabanay and S. Lev (2005). "Differential regulation of endoplasmic reticulum structure through VAP-Nir protein interaction." J Biol Chem **280**(7): 5934-5944.

Anelli, T., M. Alessio, A. Bachi, L. Bergamelli, G. Bertoli, S. Camerini, A. Mezghrani, E. Ruffato, T. Simmen and R. Sitia (2003). "Thiol-mediated protein retention in the endoplasmic reticulum: the role of ERp44." EMBO J **22**(19): 5015-5022.

Arakel, E. C. and B. Schwappach (2018). "Formation of COPI-coated vesicles at a glance." J Cell Sci **131**(5).

Barbero, P., L. Bittova and S. R. Pfeffer (2002). "Visualization of Rab9-mediated vesicle transport from endosomes to the trans-Golgi in living cells." J Cell Biol **156**(3): 511-518.

Barlowe, C. K. and E. A. Miller (2013). "Secretory protein biogenesis and traffic in the early secretory pathway." Genetics **193**(2): 383-410.

Baron, Y., P. G. Pedrioli, K. Tyagi, C. Johnson, N. T. Wood, D. Fountaine, M. Wightman and G. Alexandru (2014). "VAPB/ALS8 interacts with FFAT-like proteins including the p97 cofactor FAF1 and the ASNA1 ATPase." BMC Biol **12**: 39.

Barra, J., J. Cerda-Infante, L. Sandoval, P. Gajardo-Meneses, J. F. Henriquez, M. Labarca, C. Metz, J. Venegas, C. Retamal, C. Oyanadel, J. Cancino, A. Soza, M. A. Cuello, J. C. Roa, V. P. Montecinos and A. Gonzalez (2021). "D-Propranolol Impairs EGFR Trafficking and Destabilizes Mutant p53 Counteracting AKT Signaling and Tumor Malignancy." Cancers (Basel) **13**(14).

Bonifacino, J. S. and B. S. Glick (2004). "The mechanisms of vesicle budding and fusion." Cell **116**(2): 153-166.

Bouchet, J., I. Del Rio-Iniguez, R. Lasserre, S. Aguera-Gonzalez, C. Cuche, A. Danckaert, M. W. McCaffrey, V. Di Bartolo and A. Alcover (2016). "Rac1-Rab11-FIP3 regulatory hub coordinates vesicle traffic with actin remodeling and T-cell activation." EMBO J **35**(11): 1160-1174.

Boucrot, E., S. Saffarian, R. Zhang and T. Kirchhausen (2010). "Roles of AP-2 in clathrin-mediated endocytosis." PLoS One **5**(5): e10597.

Burd, C. and P. J. Cullen (2014). "Retromer: a master conductor of endosome sorting." Cold Spring Harb Perspect Biol **6**(2).

Cabrera, M., M. Muniz, J. Hidalgo, L. Vega, M. E. Martin and A. Velasco (2003). "The retrieval function of the KDEL receptor requires PKA phosphorylation of its C-terminus." Mol Biol Cell **14**(10): 4114-4125.

Cabukusta, B., I. Berlin, D. M. van Elsland, I. Forkink, M. Spits, A. W. M. de Jong, J. Akkermans, R. H. M. Wijdeven, G. M. C. Janssen, P. A. van Veelen and J. Neefjes (2020). "Human VAPome Analysis Reveals MOSPD1 and MOSPD3 as Membrane Contact Site Proteins Interacting with FFAT-Related FFNT Motifs." Cell Rep **33**(10): 108475.

Cai, D., S. C. Chen, M. Prasad, L. He, X. Wang, V. Choesmel-Cadamuro, J. K. Sawyer, G. Danuser and D. J. Montell (2014). "Mechanical feedback through E-cadherin promotes direction sensing during collective cell migration." Cell **157**(5): 1146-1159.

Campa, C. C., J. P. Margaria, A. Derle, M. Del Giudice, M. C. De Santis, L. Gozzelino, F. Copperi, C. Bosia and E. Hirsch (2018). "Rab11 activity and PtdIns(3)P turnover removes recycling cargo from endosomes." Nat Chem Biol **14**(8): 801-810.

Castle, A. M., L. E. Stahl and J. D. Castle (1992). "A 13-amino acid n-terminal domain of a basic proline-rich protein is necessary for storage in secretory granules and facilitates exit from the endoplasmic reticulum." J Biol Chem **267**(18): 13093-13100.

Caswell, P. T., M. Chan, A. J. Lindsay, M. W. McCaffrey, D. Boettiger and J. C. Norman (2008). "Rab-coupling protein coordinates recycling of alpha5beta1 integrin and EGFR1 to promote cell migration in 3D microenvironments." J Cell Biol **183**(1): 143-155.

Caswell, P. T. and J. C. Norman (2006). "Integrin trafficking and the control of cell migration." Traffic **7**(1): 14-21.

Chang, T. K., D. A. Lawrence, M. Lu, J. Tan, J. M. Harnoss, S. A. Marsters, P. Liu, W. Sandoval, S. E. Martin and A. Ashkenazi (2018). "Coordination between Two Branches of the Unfolded Protein Response Determines Apoptotic Cell Fate." Mol Cell **71**(4): 629-636 e625.

Chavrier, P., R. G. Parton, H. P. Hauri, K. Simons and M. Zerial (1990). "Localization of low molecular weight GTP binding proteins to exocytic and endocytic compartments." Cell **62**(2): 317-329.

Chavrier, P., P. van der Sluijs, Z. Mishal, B. Nagelkerken and J. P. Gorvel (1997). "Early endosome membrane dynamics characterized by flow cytometry." Cytometry **29**(1): 41-49.

Chen, H. Y., R. A. Kelley, T. Li and A. Swaroop (2021). "Primary cilia biogenesis and associated retinal ciliopathies." Semin Cell Dev Biol **110**: 70-88.

Chen, W., Y. Feng, D. Chen and A. Wandinger-Ness (1998). "Rab11 is required for trans-golgi network-to-plasma membrane transport and a preferential target for GDP dissociation inhibitor." Mol Biol Cell **9**(11): 3241-3257.

Chen, Y. and F. Brandizzi (2013). "IRE1: ER stress sensor and cell fate executor." Trends Cell Biol **23**(11): 547-555.

Chevet, E., H. N. Wong, D. Gerber, C. Cochet, A. Fazel, P. H. Cameron, J. N. Gushue, D. Y. Thomas and J. J. Bergeron (1999). "Phosphorylation by CK2 and MAPK enhances calnexin association with ribosomes." EMBO J **18**(13): 3655-3666.

Christoforidis, S., H. M. McBride, R. D. Burgoyne and M. Zerial (1999). "The Rab5 effector EEA1 is a core component of endosome docking." Nature **397**(6720): 621-625.

Collawn, J. F., M. Stangel, L. A. Kuhn, V. Esekogwu, S. Q. Jing, I. S. Trowbridge and J. A. Tainer (1990). "Transferrin receptor internalization sequence YXRF implicates a tight turn as the structural recognition motif for endocytosis." Cell **63**(5): 1061-1072.

Conti, F., S. Sertic, A. Reversi and B. Chini (2009). "Intracellular trafficking of the human oxytocin receptor: evidence of receptor recycling via a Rab4/Rab5 "short cycle"." Am J Physiol Endocrinol Metab **296**(3): E532-542.

Cullis, D. N., B. Philip, J. D. Baleja and L. A. Feig (2002). "Rab11-FIP2, an adaptor protein connecting cellular components involved in internalization and recycling of epidermal growth factor receptors." J Biol Chem **277**(51): 49158-49166.

Custer, S. K., J. N. Foster, J. W. Astroski and E. J. Androphy (2019). "Abnormal Golgi morphology and decreased COPI function in cells with low levels of SMN." Brain Res **1706**: 135-146.

D'Souza, R. S., R. Semus, E. A. Billings, C. B. Meyer, K. Conger and J. E. Casanova (2014). "Rab4 orchestrates a small GTPase cascade for recruitment of adaptor proteins to early endosomes." Curr Biol **24**(11): 1187-1198.

Dallavilla, T., L. Abrami, P. A. Sandoz, G. Savoglidis, V. Hatzimanikatis and F. G. van der Goot (2016). "Model-Driven Understanding of Palmitoylation Dynamics: Regulated Acylation of the Endoplasmic Reticulum Chaperone Calnexin." PLoS Comput Biol **12**(2): e1004774.

de Renzis, S., B. Sonnichsen and M. Zerial (2002). "Divalent Rab effectors regulate the sub-compartmental organization and sorting of early endosomes." Nat Cell Biol **4**(2): 124-133.

De Vos, K. J., G. M. Morotz, R. Stoica, E. L. Tudor, K. F. Lau, S. Ackerley, A. Warley, C. E. Shaw and C. C. Miller (2012). "VAPB interacts with the mitochondrial protein PTPIP51 to regulate calcium homeostasis." Hum Mol Genet **21**(6): 1299-1311.

de Wit, H., Y. Lichtenstein, R. B. Kelly, H. J. Geuze, J. Klumperman and P. van der Sluijs (2001). "Rab4 regulates formation of synaptic-like microvesicles from early endosomes in PC12 cells." Mol Biol Cell **12**(11): 3703-3715.

Dickson, L. J., S. Liu and B. Storrie (2020). "Rab6 is required for rapid, cisternal-specific, intra-Golgi cargo transport." Sci Rep **10**(1): 16604.

Dong, M., J. P. Bridges, K. Apsley, Y. Xu and T. E. Weaver (2008). "ERdj4 and ERdj5 are required for endoplasmic reticulum-associated protein degradation of misfolded surfactant protein C." Mol Biol Cell **19**(6): 2620-2630.

Dong, R., Y. Saheki, S. Swarup, L. Lucast, J. W. Harper and P. De Camilli (2016). "Endosome-ER Contacts Control Actin Nucleation and Retromer Function through VAP-Dependent Regulation of PI4P." Cell **166**(2): 408-423.

Dumaresq-Doiron, K., M. F. Savard, S. Akam, S. Costantino and S. Lefrancois (2010). "The phosphatidylinositol 4-kinase PI4KIIIalpha is required for the recruitment of GBF1 to Golgi membranes." J Cell Sci **123**(Pt 13): 2273-2280.

Eggers, C. T., J. C. Schafer, J. R. Goldenring and S. S. Taylor (2009). "D-AKAP2 interacts with Rab4 and Rab11 through its RGS domains and regulates transferrin receptor recycling." J Biol Chem **284**(47): 32869-32880.

Elkin, S. R., A. M. Lakoduk and S. L. Schmid (2016). "Endocytic pathways and endosomal trafficking: a primer." Wien Med Wochenschr **166**(7-8): 196-204.

Escrevente, C., L. Bento-Lopes, J. S. Ramalho and D. C. Barral (2021). "Rab11 is required for lysosome exocytosis through the interaction with Rab3a, Sec15 and GRAB." J Cell Sci **134**(11).

Faini, M., R. Beck, F. T. Wieland and J. A. Briggs (2013). "Vesicle coats: structure, function, and general principles of assembly." Trends Cell Biol **23**(6): 279-288.

Ferro, E., C. Bosia and C. C. Campa (2021). "RAB11-Mediated Trafficking and Human Cancers: An Updated Review." Biology (Basel) **10**(1).

Forrester, A., C. De Leonibus, P. Grumati, E. Fasana, M. Piemontese, L. Staiano, I. Fregno, A. Raimondi, A. Marazza, G. Bruno, M. Iavazzo, D. Intartaglia, M. Seczynska, E. van Anken, I. Conte, M. A. De Matteis, I. Dikic, M. Molinari and C. Settembre (2019). "A selective ER-phagy exerts procollagen quality control via a Calnexin-FAM134B complex." EMBO J **38**(2).

Galea, G., M. G. Bexiga, A. Panarella, E. D. O'Neill and J. C. Simpson (2015). "A high-content screening microscopy approach to dissect the role of Rab proteins in Golgi-to-ER retrograde trafficking." J Cell Sci **128**(13): 2339-2349.

Galea, G. and J. C. Simpson (2015). "High-content analysis of Rab protein function at the ER-Golgi interface." Bioarchitecture **5**(3-4): 44-53.

Garcia-Mata, R., T. Szul, C. Alvarez and E. Sztul (2003). "ADP-ribosylation factor/COPI-dependent events at the endoplasmic reticulum-Golgi interface are regulated by the guanine nucleotide exchange factor GBF1." Mol Biol Cell **14**(6): 2250-2261.

Garcia-Ortiz, A. and J. M. Serrador (2020). "ERM Proteins at the Crossroad of Leukocyte Polarization, Migration and Intercellular Adhesion." Int J Mol Sci **21**(4).

Gardner, L. A., H. Hajjhussein, K. C. Frederick-Dyer and S. W. Bahouth (2011). "Rab11a and its binding partners regulate the recycling of the ss1-adrenergic receptor." Cell Signal **23**(1): 46-57.

Gething, M. J. (1999). "Role and regulation of the ER chaperone BiP." Semin Cell Dev Biol **10**(5): 465-472.

Gidon, A., S. Bardin, B. Cinquin, J. Boulanger, F. Waharte, L. Heliot, H. de la Salle, D. Hanau, C. Kervrann, B. Goud and J. Salamero (2012). "A Rab11A/myosin Vb/Rab11-FIP2 complex frames two late recycling steps of langerin from the ERC to the plasma membrane." Traffic **13**(6): 815-833.

Gleeson, P. A., T. J. Anderson, J. L. Stow, G. Griffiths, B. H. Toh and F. Matheson (1996). "p230 is associated with vesicles budding from the trans-Golgi network." J Cell Sci **109 (Pt 12)**: 2811-2821.

Gravotta, D., A. Deora, E. Perret, C. Oyanadel, A. Soza, R. Schreiner, A. Gonzalez and E. Rodriguez-Boulan (2007). "AP1B sorts basolateral proteins in recycling and biosynthetic routes of MDCK cells." Proc Natl Acad Sci U S A **104**(5): 1564-1569.

Greenfield, J. P., L. W. Leung, D. Cai, K. Kaasik, R. S. Gross, E. Rodriguez-Boulan, P. Greengard and H. Xu (2002). "Estrogen lowers Alzheimer beta-amyloid generation by stimulating trans-Golgi network vesicle biogenesis." J Biol Chem **277**(14): 12128-12136.

Guo, Y., D. W. Sirkis and R. Schekman (2014). "Protein sorting at the trans-Golgi network." Annu Rev Cell Dev Biol **30**: 169-206.

Haase, G. and C. Rabouille (2015). "Golgi Fragmentation in ALS Motor Neurons. New Mechanisms Targeting Microtubules, Tethers, and Transport Vesicles." Front Neurosci **9**: 448.

Hales, C. M., R. Griner, K. C. Hobdy-Henderson, M. C. Dorn, D. Hardy, R. Kumar, J. Navarre, E. K. Chan, L. A. Lapierre and J. R. Goldenring (2001). "Identification and characterization of a family of Rab11-interacting proteins." J Biol Chem **276**(42): 39067-39075.

Hamanaka, R. B., B. S. Bennett, S. B. Cullinan and J. A. Diehl (2005). "PERK and GCN2 contribute to eIF2alpha phosphorylation and cell cycle arrest after activation of the unfolded protein response pathway." Mol Biol Cell **16**(12): 5493-5501.

Han, J., K. Pluhackova and R. A. Bockmann (2017). "The Multifaceted Role of SNARE Proteins in Membrane Fusion." Front Physiol **8**: 5.

Hay, J. C., H. Hirling and R. H. Scheller (1996). "Mammalian vesicle trafficking proteins of the endoplasmic reticulum and Golgi apparatus." J Biol Chem **271**(10): 5671-5679.

Hedman, A. C., J. M. Smith and D. B. Sacks (2015). "The biology of IQGAP proteins: beyond the cytoskeleton." EMBO Rep **16**(4): 427-446.

Heffernan, L. F. and J. C. Simpson (2014). "The trials and tubule-ations of Rab6 involvement in Golgi-to-ER retrograde transport." Biochem Soc Trans **42**(5): 1453-1459.

Hillary, R. F. and U. FitzGerald (2018). "A lifetime of stress: ATF6 in development and homeostasis." J Biomed Sci **25**(1): 48.

Hirose, H., K. Arasaki, N. Dohmae, K. Takio, K. Hatsuzawa, M. Nagahama, K. Tani, A. Yamamoto, M. Tohyama and M. Tagaya (2004). "Implication of ZW10 in membrane trafficking between the endoplasmic reticulum and Golgi." EMBO J **23**(6): 1267-1278.

Horgan, C. P., S. R. Hanscom, R. S. Jolly, C. E. Futter and M. W. McCaffrey (2010). "Rab11-FIP3 binds dynein light intermediate chain 2 and its overexpression fragments the Golgi complex." Biochem Biophys Res Commun **394**(2): 387-392.

Horgan, C. P., S. R. Hanscom, R. S. Jolly, C. E. Futter and M. W. McCaffrey (2010). "Rab11-FIP3 links the Rab11 GTPase and cytoplasmic dynein to mediate transport to the endosomal-recycling compartment." J Cell Sci **123**(Pt 2): 181-191.

Hsia, K. C. and A. Hoelz (2010). "Crystal structure of alpha-COP in complex with epsilon-COP provides insight into the architecture of the COPI vesicular coat." Proc Natl Acad Sci U S A **107**(25): 11271-11276.

Imamura, T., J. Huang, I. Usui, H. Satoh, J. Bever and J. M. Olefsky (2003). "Insulin-induced GLUT4 translocation involves protein kinase C-lambda-mediated functional coupling between Rab4 and the motor protein kinesin." Mol Cell Biol **23**(14): 4892-4900.

Iurlaro, R. and C. Munoz-Pinedo (2016). "Cell death induced by endoplasmic reticulum stress." FEBS J **283**(14): 2640-2652.

Jagoe, W. N., A. J. Lindsay, R. J. Read, A. J. McCoy, M. W. McCaffrey and A. R. Khan (2006). "Crystal structure of rab11 in complex with rab11 family interacting protein 2." Structure **14**(8): 1273-1283.

Jarvela, T. and A. D. Linstedt (2012). "Irradiation-induced protein inactivation reveals Golgi enzyme cycling to cell periphery." J Cell Sci **125**(Pt 4): 973-980.

Ji, H. H., L. L. Yao, C. Liu and X. D. Li (2019). "Regulation of Myosin-5b by Rab11a and the Rab11 family interacting protein 2." Biosci Rep **39**(1).

Jin, M. and J. R. Goldenring (2006). "The Rab11-FIP1/RCP gene codes for multiple protein transcripts related to the plasma membrane recycling system." Biochim Biophys Acta **1759**(6): 281-295.

Johannes, L. and V. Popoff (2008). "Tracing the retrograde route in protein trafficking." Cell **135**(7): 1175-1187.

Kampf, L. L., R. Schneider, L. Gerstner, R. Thunauer, M. Chen, M. Helmstadter, A. Amar, A. C. Onuchic-Whitford, R. Loza Munarriz, A. Berdeli, D. Muller, E. Schrezenmeier, K. Budde, S. Mane, K. M. Laricchia, H. L. Rehm, D. G. MacArthur, R. P. Lifton, G. Walz, W. Romer, C. Bergmann, F. Hildebrandt and T. Hermle (2019). "TBC1D8B Mutations Implicate RAB11-Dependent Vesicular Trafficking in the Pathogenesis of Nephrotic Syndrome." J Am Soc Nephrol **30**(12): 2338-2353.

Karcher, R. L., S. W. Deacon and V. I. Gelfand (2002). "Motor-cargo interactions: the key to transport specificity." Trends Cell Biol **12**(1): 21-27.

Kawano, M., K. Kumagai, M. Nishijima and K. Hanada (2006). "Efficient trafficking of ceramide from the endoplasmic reticulum to the Golgi apparatus requires a VAMP-associated protein-interacting FFAT motif of CERT." J Biol Chem **281**(40): 30279-30288.

Kelly, E. E., C. P. Horgan and M. W. McCaffrey (2012). "Rab11 proteins in health and disease." Biochem Soc Trans **40**(6): 1360-1367.

Klinger, S. C., P. Siupka and M. S. Nielsen (2015). "Retromer-Mediated Trafficking of Transmembrane Receptors and Transporters." Membranes (Basel) **5**(3): 288-306.

Knodler, A., S. Feng, J. Zhang, X. Zhang, A. Das, J. Peranen and W. Guo (2010). "Coordination of Rab8 and Rab11 in primary ciliogenesis." Proc Natl Acad Sci U S A **107**(14): 6346-6351.

Kuijpers, M., K. L. Yu, E. Teuling, A. Akhmanova, D. Jaarsma and C. C. Hoogenraad (2013). "The ALS8 protein VAPB interacts with the ER-Golgi recycling protein YIF1A and regulates membrane delivery into dendrites." EMBO J **32**(14): 2056-2072.

Lewis, M. J. and H. R. Pelham (1992). "Ligand-induced redistribution of a human KDEL receptor from the Golgi complex to the endoplasmic reticulum." Cell **68**(2): 353-364.

Lewis, M. J., D. J. Sweet and H. R. Pelham (1990). "The ERD2 gene determines the specificity of the luminal ER protein retention system." Cell **61**(7): 1359-1363.

Li, J., E. Ahat and Y. Wang (2019). "Golgi Structure and Function in Health, Stress, and Diseases." Results Probl Cell Differ **67**: 441-485.

Li, L., W. Omata, I. Kojima and H. Shibata (2001). "Direct interaction of Rab4 with syntaxin 4." J Biol Chem **276**(7): 5265-5273.

Lindsay, A. J., F. Jollivet, C. P. Horgan, A. R. Khan, G. Raposo, M. W. McCaffrey and B. Goud (2013). "Identification and characterization of multiple novel Rab-myosin Va interactions." Mol Biol Cell **24**(21): 3420-3434.

Lock, J. G. and J. L. Stow (2005). "Rab11 in recycling endosomes regulates the sorting and basolateral transport of E-cadherin." Mol Biol Cell **16**(4): 1744-1755.

Lucken-Ardjomande Hasler, S., Y. Vallis, M. Pasche and H. T. McMahon (2020). "GRAF2, WDR44, and MICAL1 mediate Rab8/10/11-dependent export of E-cadherin, MMP14, and CFTR DeltaF508." J Cell Biol **219**(5).

Ma, M. and C. G. Burd (2020). "Retrograde trafficking and plasma membrane recycling pathways of the budding yeast Saccharomyces cerevisiae." Traffic **21**(1): 45-59.

Majoul, I., K. Sohn, F. T. Wieland, R. Pepperkok, M. Pizza, J. Hillemann and H. D. Soling (1998). "KDEL receptor (Erd2p)-mediated retrograde transport of the cholera toxin A subunit from the Golgi involves COPI, p23, and the COOH terminus of Erd2p." J Cell Biol **143**(3): 601-612.

Majoul, I., M. Straub, S. W. Hell, R. Duden and H. D. Soling (2001). "KDEL-cargo regulates interactions between proteins involved in COPI vesicle traffic: measurements in living cells using FRET." Dev Cell **1**(1): 139-153.

Malik, N., R. S. Nirujogi, J. Peltier, T. Macartney, M. Wightman, A. R. Prescott, R. Gourlay, M. Trost, D. R. Alessi and A. Karapetsas (2019). "Phosphoproteomics reveals that the hVPS34 regulated SGK3 kinase specifically phosphorylates endosomal proteins including Syntaxin-7, Syntaxin-12, RFIP4 and WDR44." Biochem J **476**(20): 3081-3107.

Mallard, F., B. L. Tang, T. Galli, D. Tenza, A. Saint-Pol, X. Yue, C. Antony, W. Hong, B. Goud and L. Johannes (2002). "Early/recycling endosomes-to-TGN transport involves two SNARE complexes and a Rab6 isoform." J Cell Biol **156**(4): 653-664.

Mammoto, A., T. Sasaki, Y. Kim and Y. Takai (2000). "Physical and functional interaction of rabphilin-11 with mammalian Sec13 protein. Implication in vesicle trafficking." J Biol Chem **275**(18): 13167-13170.

Mani, S. and M. Thattai (2016). "Stacking the odds for Golgi cisternal maturation." Elife **5**.

Marie, M., H. A. Dale, R. Sannerud and J. Saraste (2009). "The function of the intermediate compartment in pre-Golgi trafficking involves its stable connection with the centrosome." Mol Biol Cell **20**(20): 4458-4470.

Marra, P., L. Salvatore, A. Mironov, Jr., A. Di Campli, G. Di Tullio, A. Trucco, G. Beznoussenko, A. Mironov and M. A. De Matteis (2007). "The biogenesis of the Golgi ribbon: the roles of membrane input from the ER and of GM130." Mol Biol Cell **18**(5): 1595-1608.

Martinez, O., C. Antony, G. Pehau-Arnaudet, E. G. Berger, J. Salamero and B. Goud (1997). "GTP-bound forms of rab6 induce the redistribution of Golgi proteins into the endoplasmic reticulum." Proc Natl Acad Sci U S A **94**(5): 1828-1833.

Martinez, O., A. Schmidt, J. Salamero, B. Hoflack, M. Roa and B. Goud (1994). "The small GTP-binding protein rab6 functions in intra-Golgi transport." J Cell Biol **127**(6 Pt 1): 1575-1588.

Matanis, T., A. Akhmanova, P. Wulf, E. Del Nery, T. Weide, T. Stepanova, N. Galjart, F. Grosveld, B. Goud, C. I. De Zeeuw, A. Barnekow and C. C. Hoogenraad (2002). "Bicaudal-D regulates COPI-independent Golgi-ER transport by recruiting the dynein-dynactin motor complex." Nat Cell Biol **4**(12): 986-992.

Mattera, R., S. Y. Park, R. De Pace, C. M. Guardia and J. S. Bonifacino (2017). "AP-4 mediates export of ATG9A from the trans-Golgi network to promote autophagosome formation." Proc Natl Acad Sci U S A **114**(50): E10697-E10706.

Mazzarella, R. A., M. Srinivasan, S. M. Haugejorden and M. Green (1990). "ERp72, an abundant luminal endoplasmic reticulum protein, contains three copies of the active site sequences of protein disulfide isomerase." J Biol Chem **265**(2): 1094-1101.

McCaffrey, M. W., A. Bielli, G. Cantalupo, S. Mora, V. Roberti, M. Santillo, F. Drummond and C. Bucci (2001). "Rab4 affects both recycling and degradative endosomal trafficking." FEBS Lett **495**(1-2): 21-30.

McQuiston, A. and J. A. Diehl (2017). "Recent insights into PERK-dependent signaling from the stressed endoplasmic reticulum." F1000Res **6**: 1897.

Mellman, I. and W. J. Nelson (2008). "Coordinated protein sorting, targeting and distribution in polarized cells." Nat Rev Mol Cell Biol **9**(11): 833-845.

Merithew, E., S. Hatherly, J. J. Dumas, D. C. Lawe, R. Heller-Harrison and D. G. Lambright (2001). "Structural plasticity of an invariant hydrophobic triad in the switch regions of Rab GTPases is a determinant of effector recognition." J Biol Chem **276**(17): 13982-13988.

Mesaki, K., K. Tanabe, M. Obayashi, N. Oe and K. Takei (2011). "Fission of tubular endosomes triggers endosomal acidification and movement." PLoS One **6**(5): e19764.

Mesmin, B., J. Bigay, J. Moser von Filseck, S. Lacas-Gervais, G. Drin and B. Antonny (2013). "A four-step cycle driven by PI(4)P hydrolysis directs sterol/PI(4)P exchange by the ER-Golgi tether OSBP." Cell **155**(4): 830-843.

Metz, C., C. Oyanadel, J. Jung, C. Retamal, J. Cancino, J. Barra, G. Du, A. Soza and A. Gonzalez (2021). "Phosphatidic acid-PKA signaling regulates p38 and ERK1/2 function in ligandindependent EGFR endocytosis." Traffic.

Meyers, J. M. and R. Prekeris (2002). "Formation of mutually exclusive Rab11 complexes with members of the family of Rab11-interacting proteins regulates Rab11 endocytic targeting and function." J Biol Chem **277**(50): 49003-49010.

Mironov, A. A., G. V. Beznoussenko, R. S. Polishchuk and A. Trucco (2005). "Intra-Golgi transport: a way to a new paradigm?" Biochim Biophys Acta **1744**(3): 340-350.

Miserey-Lenkei, S., H. Bousquet, O. Pylypenko, S. Bardin, A. Dimitrov, G. Bressanelli, R. Bonifay, V. Fraisier, C. Guillou, C. Bougeret, A. Houdusse, A. Echard and B. Goud (2017). "Coupling fission and exit of RAB6 vesicles at Golgi hotspots through kinesin-myosin interactions." Nat Commun **8**(1): 1254.

Misteli, T. and G. Warren (1994). "COP-coated vesicles are involved in the mitotic fragmentation of Golgi stacks in a cell-free system." J Cell Biol **125**(2): 269-282.

Monetta, P., I. Slavin, N. Romero and C. Alvarez (2007). "Rab1b interacts with GBF1 and modulates both ARF1 dynamics and COPI association." Mol Biol Cell **18**(7): 2400-2410.

Moyer, B. D., B. B. Allan and W. E. Balch (2001). "Rab1 interaction with a GM130 effector complex regulates COPII vesicle cis--Golgi tethering." Traffic **2**(4): 268-276.

Mu, F. T., J. M. Callaghan, O. Steele-Mortimer, H. Stenmark, R. G. Parton, P. L. Campbell, J. McCluskey, J. P. Yeo, E. P. Tock and B. H. Toh (1995). "EEA1, an early endosome-associated protein. EEA1 is a conserved alpha-helical peripheral membrane protein flanked by cysteine "fingers" and contains a calmodulin-binding IQ motif." J Biol Chem **270**(22): 13503-13511.

Murphy, A. C. and P. W. Young (2015). "The actinin family of actin cross-linking proteins - a genetic perspective." Cell Biosci **5**: 49.

Myhill, N., E. M. Lynes, J. A. Nanji, A. D. Blagoveshchenskaya, H. Fei, K. Carmine Simmen, T. J. Cooper, G. Thomas and T. Simmen (2008). "The subcellular distribution of calnexin is mediated by PACS-2." Mol Biol Cell **19**(7): 2777-2788.

Nakamura, N., C. Rabouille, R. Watson, T. Nilsson, N. Hui, P. Slusarewicz, T. E. Kreis and G. Warren (1995). "Characterization of a cis-Golgi matrix protein, GM130." J Cell Biol **131**(6 Pt 2): 1715-1726.

Nedvetsky, P. I., E. Stefan, S. Frische, K. Santamaria, B. Wiesner, G. Valenti, J. A. Hammer, 3rd, S. Nielsen, J. R. Goldenring, W. Rosenthal and E. Klussmann (2007). "A Role of myosin Vb and Rab11-FIP2 in the aquaporin-2 shuttle." Traffic **8**(2): 110-123.

Neefjes, J. and B. Cabukusta (2021). "What the VAP: The Expanded VAP Family of Proteins Interacting With FFAT and FFAT-Related Motifs for Interorganellar Contact." Contact (Thousand Oaks) **4**: 25152564211012246.

Neuman, S. D., A. R. Lee, J. E. Selegue, A. T. Cavanagh and A. Bashirullah (2021). "A novel function for Rab1 and Rab11 during secretory granule maturation." J Cell Sci **134**(15).

Neutzner, A., M. Neutzner, A. S. Benischke, S. W. Ryu, S. Frank, R. J. Youle and M. Karbowski (2011). "A systematic search for endoplasmic reticulum (ER) membrane-associated RING finger proteins identifies Nixin/ZNRF4 as a regulator of calnexin stability and ER homeostasis." J Biol Chem **286**(10): 8633-8643.

Norambuena, A., C. Metz, J. E. Jung, A. Silva, C. Otero, J. Cancino, C. Retamal, J. C. Valenzuela, A. Soza and A. Gonzalez (2010). "Phosphatidic acid induces ligand-independent epidermal growth factor receptor endocytic traffic through PDE4 activation." Mol Biol Cell **21**(16): 2916-2929.

Odorizzi, G. and I. S. Trowbridge (1997). "Structural requirements for basolateral sorting of the human transferrin receptor in the biosynthetic and endocytic pathways of Madin-Darby canine kidney cells." J Cell Biol **137**(6): 1255-1264.

Opdam, F. J., A. Echard, H. J. Croes, J. A. van den Hurk, R. A. van de Vorstenbosch, L. A. Ginsel, B. Goud and J. A. Fransen (2000). "The small GTPase Rab6B, a novel Rab6 subfamily member, is cell-type specifically expressed and localised to the Golgi apparatus." J Cell Sci **113 (Pt 15)**: 2725-2735.

Otsu, M., G. Bertoli, C. Fagioli, E. Guerini-Rocco, S. Nerini-Molteni, E. Ruffato and R. Sitia (2006). "Dynamic retention of Ero1alpha and Ero1beta in the endoplasmic reticulum by interactions with PDI and ERp44." Antioxid Redox Signal **8**(3-4): 274-282.

Pagano, A., P. Crottet, C. Prescianotto-Baschong and M. Spiess (2004). "In vitro formation of recycling vesicles from endosomes requires adaptor protein-1/clathrin and is regulated by rab4 and the connector rabaptin-5." Mol Biol Cell **15**(11): 4990-5000.

Palmieri, D., A. Bouadis, R. Ronchetti, M. J. Merino and P. S. Steeg (2006). "Rab11a differentially modulates epidermal growth factor-induced proliferation and motility in immortal breast cells." Breast Cancer Res Treat **100**(2): 127-137.

Park, S. Y., J. S. Yang, Z. Li, P. Deng, X. Zhu, D. Young, M. Ericsson, R. L. H. Andringa, A. J. Minnaard, C. Zhu, F. Sun, D. B. Moody, A. J. Morris, J. Fan and V. W. Hsu (2019). "The late stage of COPI vesicle fission requires shorter forms of phosphatidic acid and diacylglycerol." Nat Commun **10**(1): 3409.

Pavelka, M., J. Neumuller and A. Ellinger (2008). "Retrograde traffic in the biosynthetic-secretory route." Histochem Cell Biol **129**(3): 277-288.

Peden, A. A., E. Schonteich, J. Chun, J. R. Junutula, R. H. Scheller and R. Prekeris (2004). "The RCP-Rab11 complex regulates endocytic protein sorting." Mol Biol Cell **15**(8): 3530-3541.

Pelham, H. R. (1988). "Evidence that luminal ER proteins are sorted from secreted proteins in a post-ER compartment." EMBO J **7**(4): 913-918.

Pelham, H. R., K. G. Hardwick and M. J. Lewis (1988). "Sorting of soluble ER proteins in yeast." EMBO J **7**(6): 1757-1762.

Peretti, D., N. Dahan, E. Shimoni, K. Hirschberg and S. Lev (2008). "Coordinated lipid transfer between the endoplasmic reticulum and the Golgi complex requires the VAP proteins and is essential for Golgi-mediated transport." Mol Biol Cell **19**(9): 3871-3884.

Pfeffer, S. R. (2013). "Rab GTPase regulation of membrane identity." Curr Opin Cell Biol **25**(4): 414-419.

Pfeffer, S. R. (2017). "Rab GTPases: master regulators that establish the secretory and endocytic pathways." Mol Biol Cell **28**(6): 712-715.

Plutner, H., A. D. Cox, S. Pind, R. Khosravi-Far, J. R. Bourne, R. Schwaninger, C. J. Der and W. E. Balch (1991). "Rab1b regulates vesicular transport between the endoplasmic reticulum and successive Golgi compartments." J Cell Biol **115**(1): 31-43.

Prosser, D. C., D. Tran, P. Y. Gougeon, C. Verly and J. K. Ngsee (2008). "FFAT rescues VAPA-mediated inhibition of ER-to-Golgi transport and VAPB-mediated ER aggregation." J Cell Sci **121**(Pt 18): 3052-3061.

Puri, C., M. Vicinanza, A. Ashkenazi, M. J. Gratian, Q. Zhang, C. F. Bento, M. Renna, F. M. Menzies and D. C. Rubinsztein (2018). "The RAB11A-Positive Compartment Is a Primary Platform for Autophagosome Assembly Mediated by WIPI2 Recognition of PI3P-RAB11A." Dev Cell **45**(1): 114-131 e118.

Read, A. and M. Schroder (2021). "The Unfolded Protein Response: An Overview." Biology (Basel) **10**(5).

Renard, H. F., L. Johannes and P. Morsomme (2018). "Increasing Diversity of Biological Membrane Fission Mechanisms." Trends Cell Biol **28**(4): 274-286.

Rink, J., E. Ghigo, Y. Kalaidzidis and M. Zerial (2005). "Rab conversion as a mechanism of progression from early to late endosomes." Cell **122**(5): 735-749.

Roberts, M., S. Barry, A. Woods, P. van der Sluijs and J. Norman (2001). "PDGF-regulated rab4-dependent recycling of alphavbeta3 integrin from early endosomes is necessary for cell adhesion and spreading." Curr Biol **11**(18): 1392-1402.

Rocha, N., C. Kuijl, R. van der Kant, L. Janssen, D. Houben, H. Janssen, W. Zwart and J. Neefjes (2009). "Cholesterol sensor ORP1L contacts the ER protein VAP to control Rab7-RILP-p150 Glued and late endosome positioning." J Cell Biol **185**(7): 1209-1225.

Saitoh, A., H. W. Shin, A. Yamada, S. Waguri and K. Nakayama (2009). "Three homologous ArfGAPs participate in coat protein I-mediated transport." J Biol Chem **284**(20): 13948-13957.

Salazar, G. and A. Gonzalez (2002). "Novel mechanism for regulation of epidermal growth factor receptor endocytosis revealed by protein kinase A inhibition." Mol Biol Cell **13**(5): 1677-1693.

Sannerud, R., M. Marie, C. Nizak, H. A. Dale, K. Pernet-Gallay, F. Perez, B. Goud and J. Saraste (2006). "Rab1 defines a novel pathway connecting the pre-Golgi intermediate compartment with the cell periphery." Mol Biol Cell **17**(4): 1514-1526.

Saraste, J., U. Lahtinen and B. Goud (1995). "Localization of the small GTP-binding protein rab1p to early compartments of the secretory pathway." J Cell Sci **108 (Pt 4)**: 1541-1552.

Sato, K. and A. Nakano (2007). "Mechanisms of COPII vesicle formation and protein sorting." FEBS Lett **581**(11): 2076-2082.

Sato, N., F. Urano, J. Yoon Leem, S. H. Kim, M. Li, D. Donoviel, A. Bernstein, A. S. Lee, D. Ron, M. L. Veselits, S. S. Sisodia and G. Thinakaran (2000). "Upregulation of BiP and CHOP by the unfolded-protein response is independent of presenilin expression." Nat Cell Biol **2**(12): 863-870.

Schafer, J. C., R. E. McRae, E. H. Manning, L. A. Lapierre and J. R. Goldenring (2016). "Rab11-FIP1A regulates early trafficking into the recycling endosomes." Exp Cell Res **340**(2): 259-273.

Schaks, M., G. Giannone and K. Rottner (2019). "Actin dynamics in cell migration." Essays Biochem **63**(5): 483-495.

Schlierf, B., G. H. Fey, J. Hauber, G. M. Hocke and O. Rosorius (2000). "Rab11b is essential for recycling of transferrin to the plasma membrane." Exp Cell Res **259**(1): 257-265.

Schonteich, E., G. M. Wilson, J. Burden, C. R. Hopkins, K. Anderson, J. R. Goldenring and R. Prekeris (2008). "The Rip11/Rab11-FIP5 and kinesin II complex regulates endocytic protein recycling." J Cell Sci **121**(Pt 22): 3824-3833.

Semenza, J. C., K. G. Hardwick, N. Dean and H. R. Pelham (1990). "ERD2, a yeast gene required for the receptor-mediated retrieval of luminal ER proteins from the secretory pathway." Cell **61**(7): 1349-1357.

Shaughnessy, R., C. Retamal, C. Oyanadel, A. Norambuena, A. Lopez, M. Bravo-Zehnder, F. J. Montecino, C. Metz, A. Soza and A. Gonzalez (2014). "Epidermal growth factor receptor endocytic traffic perturbation by phosphatidate phosphohydrolase inhibition: new strategy against cancer." FEBS J **281**(9): 2172-2189.

Sheff, D., L. Pelletier, C. B. O'Connell, G. Warren and I. Mellman (2002). "Transferrin receptor recycling in the absence of perinuclear recycling endosomes." J Cell Biol **156**(5): 797-804.

Sheff, D. R., E. A. Daro, M. Hull and I. Mellman (1999). "The receptor recycling pathway contains two distinct populations of early endosomes with different sorting functions." J Cell Biol **145**(1): 123-139.

Shiba, T., H. Koga, H. W. Shin, M. Kawasaki, R. Kato, K. Nakayama and S. Wakatsuki (2006). "Structural basis for Rab11-dependent membrane recruitment of a family of Rab11-interacting protein 3 (FIP3)/Arfophilin-1." Proc Natl Acad Sci U S A **103**(42): 15416-15421.

Shisheva, A., S. R. Chinni and C. DeMarco (1999). "General role of GDP dissociation inhibitor 2 in membrane release of Rab proteins: modulations of its functional interactions by in vitro and in vivo structural modifications." Biochemistry **38**(36): 11711-11721.

Sievers, F. and D. G. Higgins (2018). "Clustal Omega for making accurate alignments of many protein sequences." Protein Sci **27**(1): 135-145.

Slavin, I., I. A. Garcia, P. Monetta, H. Martinez, N. Romero and C. Alvarez (2011). "Role of Rab1b in COPII dynamics and function." Eur J Cell Biol **90**(4): 301-311.

Song, S., W. Cong, S. Zhou, Y. Shi, W. Dai, H. Zhang, X. Wang, B. He and Q. Zhang (2019). "Small GTPases: Structure, biological function and its interaction with nanoparticles." Asian J Pharm Sci **14**(1): 30-39.

Sonnichsen, B., S. De Renzis, E. Nielsen, J. Rietdorf and M. Zerial (2000). "Distinct membrane domains on endosomes in the recycling pathway visualized by multicolor imaging of Rab4, Rab5, and Rab11." J Cell Biol **149**(4): 901-914.

Soussan, L., D. Burakov, M. P. Daniels, M. Toister-Achituv, A. Porat, Y. Yarden and Z. Elazar (1999). "ERG30, a VAP-33-related protein, functions in protein transport mediated by COPI vesicles." J Cell Biol **146**(2): 301-311.

Spang, A. (2013). "Retrograde traffic from the Golgi to the endoplasmic reticulum." Cold Spring Harb Perspect Biol **5**(6).

Tagaya, M., K. Arasaki, H. Inoue and H. Kimura (2014). "Moonlighting functions of the NRZ (mammalian Dsl1) complex." Front Cell Dev Biol **2**: 25.

Telot, L., E. Rousseau, E. Lesuisse, C. Garcia, B. Morlet, T. Leger, J. M. Camadro and V. Serre (2018). "Quantitative proteomics in Friedreich's ataxia B-lymphocytes: A valuable approach to decipher the biochemical events responsible for pathogenesis." Biochim Biophys Acta Mol Basis Dis **1864**(4 Pt A): 997-1009.

Townsley, F. M., D. W. Wilson and H. R. Pelham (1993). "Mutational analysis of the human KDEL receptor: distinct structural requirements for Golgi retention, ligand binding and retrograde transport." EMBO J **12**(7): 2821-2829.

Trahey, M. and J. C. Hay (2010). "Transport vesicle uncoating: it's later than you think." F1000 Biol Rep **2**: 47.

Travis, S. M., B. Kokona, R. Fairman and F. M. Hughson (2019). "Roles of singleton tryptophan motifs in COPI coat stability and vesicle tethering." Proc Natl Acad Sci U S A **116**(48): 24031-24040.

Ullrich, O., S. Reinsch, S. Urbe, M. Zerial and R. G. Parton (1996). "Rab11 regulates recycling through the pericentriolar recycling endosome." J Cell Biol **135**(4): 913-924.

Urbe, S., L. A. Huber, M. Zerial, S. A. Tooze and R. G. Parton (1993). "Rab11, a small GTPase associated with both constitutive and regulated secretory pathways in PC12 cells." FEBS Lett **334**(2): 175-182.

Van Der Sluijs, P., M. Hull, A. Zahraoui, A. Tavitian, B. Goud and I. Mellman (1991). "The small GTP-binding protein rab4 is associated with early endosomes." Proc Natl Acad Sci U S A **88**(14): 6313-6317.

van der Sluijs, P., K. Mohrmann, M. Deneka and M. Jongeneelen (2001). "Expression and properties of Rab4 and its effector rabaptin-4 in endocytic recycling." Methods Enzymol **329**: 111-119.

van Galen, P., A. Kreso, N. Mbong, D. G. Kent, T. Fitzmaurice, J. E. Chambers, S. Xie, E. Laurenti, K. Hermans, K. Eppert, S. J. Marciniak, J. C. Goodall, A. R. Green, B. G. Wouters, E. Wienholds and J. E. Dick (2014). "The unfolded protein response governs integrity of the haematopoietic stem-cell pool during stress." Nature **510**(7504): 268-272.

Vaux, D., J. Tooze and S. Fuller (1990). "Identification by anti-idiotype antibodies of an intracellular membrane protein that recognizes a mammalian endoplasmic reticulum retention signal." Nature **345**(6275): 495-502.

Viotti, C. (2016). "ER to Golgi-Dependent Protein Secretion: The Conventional Pathway." Methods Mol Biol **1459**: 3-29.

Walia, V., A. Cuenca, M. Vetter, C. Insinna, S. Perera, Q. Lu, D. A. Ritt, E. Semler, S. Specht, J. Stauffer, D. K. Morrison, E. Lorentzen and C. J. Westlake (2019). "Akt Regulates a Rab11-Effector Switch Required for Ciliogenesis." Dev Cell **50**(2): 229-246 e227.

Wallace, D. M., A. J. Lindsay, A. G. Hendrick and M. W. McCaffrey (2002). "The novel Rab11-FIP/Rip/RCP family of proteins displays extensive homo- and hetero-interacting abilities." Biochem Biophys Res Commun **292**(4): 909-915.

Wallace, D. M., A. J. Lindsay, A. G. Hendrick and M. W. McCaffrey (2002). "Rab11-FIP4 interacts with Rab11 in a GTP-dependent manner and its overexpression condenses the Rab11 positive compartment in HeLa cells." Biochem Biophys Res Commun **299**(5): 770-779.

Wang, X., R. Kumar, J. Navarre, J. E. Casanova and J. R. Goldenring (2000). "Regulation of vesicle trafficking in madin-darby canine kidney cells by Rab11a and Rab25." J Biol Chem **275**(37): 29138-29146.

Wang, Z., J. G. Edwards, N. Riley, D. W. Provance, Jr., R. Karcher, X. D. Li, I. G. Davison, M. Ikebe, J. A. Mercer, J. A. Kauer and M. D. Ehlers (2008). "Myosin Vb mobilizes recycling endosomes and AMPA receptors for postsynaptic plasticity." Cell **135**(3): 535-548.

Wei, J. H. and J. Seemann (2010). "Unraveling the Golgi ribbon." Traffic **11**(11): 1391-1400.

Weide, T., M. Bayer, M. Koster, J. P. Siebrasse, R. Peters and A. Barnekow (2001). "The Golgi matrix protein GM130: a specific interacting partner of the small GTPase rab1b." EMBO Rep **2**(4): 336-341.

Weir, M. L., H. Xie, A. Klip and W. S. Trimble (2001). "VAP-A binds promiscuously to both v- and tSNAREs." Biochem Biophys Res Commun **286**(3): 616-621.

Welz, T., J. Wellbourne-Wood and E. Kerkhoff (2014). "Orchestration of cell surface proteins by Rab11." Trends Cell Biol **24**(7): 407-415.

Westlake, C. J., L. M. Baye, M. V. Nachury, K. J. Wright, K. E. Ervin, L. Phu, C. Chalouni, J. S. Beck, D. S. Kirkpatrick, D. C. Slusarski, V. C. Sheffield, R. H. Scheller and P. K. Jackson (2011). "Primary cilia membrane assembly is initiated by Rab11 and transport protein particle II (TRAPPII) complex-dependent trafficking of Rabin8 to the centrosome." Proc Natl Acad Sci U S A **108**(7): 2759-2764.

White, J., L. Johannes, F. Mallard, A. Girod, S. Grill, S. Reinsch, P. Keller, B. Tzschaschel, A. Echard, B. Goud and E. H. Stelzer (1999). "Rab6 coordinates a novel Golgi to ER retrograde transport pathway in live cells." J Cell Biol **147**(4): 743-760.

Wieland, T. (1976). "Interaction of phallotoxins with actin." Adv Enzyme Regul **15**: 285-300.

Wilson, A. L., R. A. Erdman and W. A. Maltese (1996). "Association of Rab1B with GDP-dissociation inhibitor (GDI) is required for recycling but not initial membrane targeting of the Rab protein." J Biol Chem **271**(18): 10932-10940.

Woodman, P. G. (2000). "Biogenesis of the sorting endosome: the role of Rab5." Traffic **1**(9): 695-701.

Wu, H., P. Carvalho and G. K. Voeltz (2018). "Here, there, and everywhere: The importance of ER membrane contact sites." Science **361**(6401).

Xu, C. and J. Min (2011). "Structure and function of WD40 domain proteins." Protein Cell **2**(3): 202-214.

Yamamoto, H., S. Kakuta, T. M. Watanabe, A. Kitamura, T. Sekito, C. Kondo-Kakuta, R. Ichikawa, M. Kinjo and Y. Ohsumi (2012). "Atg9 vesicles are an important membrane source during early steps of autophagosome formation." J Cell Biol **198**(2): 219-233.

Yamamoto, H., H. Koga, Y. Katoh, S. Takahashi, K. Nakayama and H. W. Shin (2010). "Functional cross-talk between Rab14 and Rab4 through a dual effector, RUFY1/Rabip4." Mol Biol Cell **21**(15): 2746-2755.

Yamamoto, K., H. Hamada, H. Shinkai, Y. Kohno, H. Koseki and T. Aoe (2003). "The KDEL receptor modulates the endoplasmic reticulum stress response through mitogen-activated protein kinase signaling cascades." J Biol Chem **278**(36): 34525-34532.

Yang, J. S., S. Y. Lee, S. Spano, H. Gad, L. Zhang, Z. Nie, M. Bonazzi, D. Corda, A. Luini and V. W. Hsu (2005). "A role for BARS at the fission step of COPI vesicle formation from Golgi membrane." EMBO J **24**(23): 4133-4143.

Yu, I. M. and F. M. Hughson (2010). "Tethering factors as organizers of intracellular vesicular traffic." Annu Rev Cell Dev Biol **26**: 137-156.

Yu, S., G. Yehia, J. Wang, E. Stypulkowski, R. Sakamori, P. Jiang, B. Hernandez-Enriquez, T. S. Tran, E. M. Bonder, W. Guo and N. Gao (2014). "Global ablation of the mouse Rab11a gene impairs early embryogenesis and matrix metalloproteinase secretion." J Biol Chem **289**(46): 32030-32043.

Yudowski, G. A., M. A. Puthenveedu, A. G. Henry and M. von Zastrow (2009). "Cargo-mediated regulation of a rapid Rab4-dependent recycling pathway." Mol Biol Cell **20**(11): 2774-2784.

Zai, A., M. A. Rudd, A. W. Scribner and J. Loscalzo (1999). "Cell-surface protein disulfide isomerase catalyzes transnitrosation and regulates intracellular transfer of nitric oxide." J Clin Invest **103**(3): 393-399.

Zarrabi, K., A. Dufour, J. Li, C. Kuscu, A. Pulkoski-Gross, J. Zhi, Y. Hu, N. S. Sampson, S. Zucker and J. Cao (2011). "Inhibition of matrix metalloproteinase 14 (MMP-14)-mediated cancer cell migration." J Biol Chem **286**(38): 33167-33177.

Zeng, J., M. Ren, D. Gravotta, C. De Lemos-Chiarandini, M. Lui, H. Erdjument-Bromage, P. Tempst, G. Xu, T. H. Shen, T. Morimoto, M. Adesnik and D. D. Sabatini (1999). "Identification of a putative effector protein for rab11 that participates in transferrin recycling." Proc Natl Acad Sci U S A **96**(6): 2840-2845.

Zhang, X. and Y. Wang (2016). "Glycosylation Quality Control by the Golgi Structure." J Mol Biol **428**(16): 3183-3193.

Zhao, L., J. B. Helms, B. Brugger, C. Harter, B. Martoglio, R. Graf, J. Brunner and F. T. Wieland (1997). "Direct and GTP-dependent interaction of ADP ribosylation factor 1 with coatomer subunit beta." Proc Natl Acad Sci U S A **94**(9): 4418-4423.

Zhao, Y. G., N. Liu, G. Miao, Y. Chen, H. Zhao and H. Zhang (2018). "The ER Contact Proteins VAPA/B Interact with Multiple Autophagy Proteins to Modulate Autophagosome Biogenesis." Curr Biol **28**(8): 1234-1245 e1234.

Zhen, Y. and H. Stenmark (2015). "Cellular functions of Rab GTPases at a glance." J Cell Sci **128**(17): 3171-3176.

Zhukovsky, M. A., A. Filograna, A. Luini, D. Corda and C. Valente (2019). "Phosphatidic acid in membrane rearrangements." FEBS Lett **593**(17): 2428-2451.

Ziemer, M. A., A. Mason and D. M. Carlson (1982). "Cell-free translations of proline-rich protein mRNAs." J Biol Chem **257**(18): 11176-11180.

Zoppino, F. C., R. D. Militello, I. Slavin, C. Alvarez and M. I. Colombo (2010). "Autophagosome formation depends on the small GTPase Rab1 and functional ER exit sites." Traffic **11**(9): 1246-1261.

Zulkefli, K. L., F. J. Houghton, P. Gosavi and P. A. Gleeson (2019). "A role for Rab11 in the homeostasis of the endosome-lysosomal pathway." Exp Cell Res **380**(1): 55-68.